Spatial and temporal heterogeneity in life history and productivity trends of Atlantic Weakfish (*Cynoscion regalis*) and implications for fisheries management

Allison L. White

Thesis submitted to the faculty of the Virginia Polytechnic Institute and State University in partial fulfillment of the requirements for the degree of

Master of Science

In

Fisheries and Wildlife Conservation

Yan Jiao, Committee Chair

Eric Hallerman

Donald J. Orth

06/26/2017

Blacksburg, Virginia

Keywords: Atlantic Weakfish, fisheries stock assessment, spatial heterogeneity, temporal heterogeneity, non-linear mixed-effects models, generalized linear mixed-effects models

Spatial and temporal heterogeneity in life history and productivity trends of Atlantic Weakfish (*Cynoscion regalis*) and implications for fisheries management

Allison L. White

ABSTRACT

Stock assessment scientists largely ignore the spatial and temporal heterogeneity inherent in fish populations when they assess stock status. This thesis addresses the effects of spatial and temporal heterogeneity on stock assessment models using Atlantic Weakfish (*Cynoscion regalis*) as a case study. First, spatial and temporal variation were incorporated into length-, weight-, and maturity-at-age estimates using mixed-effects models (Chapter Two). The resulting heterogeneous weight and maturity parameters then were applied to per-recruit analyses to examine the sensitivity of biological reference points to spatial and temporal variation in life-history attributes (Chapter Three). Mixed-effects life-history models incorporating spatial and temporal variation revealed distinct regional and annual trends. In several instances, the homogeneous modelling approach produced life-history parameter estimates that varied significantly from means produced by the heterogeneous models. In some cases, this difference was so great that the homogeneous means were much higher or lower than the heterogeneous means for all regions or years. Minimized AIC statistics revealed that spatially and temporally integrated mixed-effects models were more robust and descriptive of Atlantic Weakfish life history than the standard homogeneous models. Per-recruit and biological reference points derived from these life-history estimates in Chapter Three were highly sensitive to spatial and temporal variations in weight parameters. Ignoring this spatial and temporal heterogeneity in

Atlantic Weakfish life history could cause overfishing or underfishing of Weakfish in certain regions and years.

Spatial and temporal heterogeneity in life history and productivity trends of Atlantic Weakfish (*Cynoscion regalis*) and implications for fisheries management

Allison L. White

GENERAL AUDIENCE ABSTRACT

Many stocks of commercially and recreationally harvested marine fish have displayed a declining trend in recent years. Marine fisheries are a vital component of the global economy, and, as such, sophisticated management measures have been developed to reduce and reverse this trend. These management strategies are based on regular reports from fisheries stock assessment scientists, who evaluate the status of fish stocks by modelling life history and productivity trends. One of the greatest challenges to stock assessments is the identification and incorporation of variability in fish populations. There is an inherent variation in fish growth, maturity, and productivity among geographical locations and over time. To produce the most effective management strategies, stock assessments must incorporate this spatial (regional) and temporal (annual) variation. In this thesis, I used mixed effects models to integrate spatial and temporal variation in life history and productivity using Atlantic Weakfish (*Cynoscion regalis*) as a case study. Distinct trends were observed in fishery-independent data for this species that were reflected in spatially and temporally incorporated models. However, these trends were masked in the standard models which incorporated neither spatial nor temporal variation. This oversight could cause weakfish to be overfished in certain regions and years and underfished in others. To maximize the effectiveness of management and the sustainable fisheries yield in all regions and years for Atlantic Weakfish and other harvested species, I highly recommend using

spatially and temporally incorporated life history and productivity models such as the ones developed in this thesis.

ACKNOWLEDGEMENTS

First and foremost, I would like to extend my deepest thanks and appreciation to my advisor, Dr. Yan Jiao, for giving me the opportunity to work with and learn from her. Dr. Jiao has greatly expanded my knowledge and perception of population dynamics models and how they are applied to real fish populations for consideration in management. She has always been willing to answer and discuss my questions and shown great patience in doing so. Most importantly, she has always pushed me to do my best, whether it be in class, on my thesis, and even for my career. Without Dr. Jiao's extensive knowledge and insight into the quantitative methods of fisheries stock assessment, this thesis would not have been possible. I would also like to thank my other advisory committee members for their support and guidance. Dr. Don Orth always offered a unique perspective on fisheries populations, often led him to ask me questions about my models that I would otherwise never have thought to consider. Dr. Eric Hallerman provided insight into population genetics that caused me to rethink my definition of fisheries stocks and consider the potential impacts on my models of interest.

In addition to my committee, several of my peers contributed to the completion of this thesis. Former laboratory members Dan Hua and Yafei Zhang were very welcoming and always eager to offer any advice to help me get started when I first came to Virginia Tech. Erica Brown also helped me through much of my first year of graduate school, even as I helped her. Dr. Can Zhou was always willing to help me with coding problems and review my work, for which I am extremely grateful. I would also like to extend my thanks to my other lab-mates, Corbin Hilling, Qiuyun Ma, Baochao Liao, and Rujia Bi, for their companionship and insight.

TABLE OF CONTENTS

LIST OF TABLES

CHAPTER THREE: Sensitivity of productivity to spatial and temporal variations in life history of Atlantic Weakfish (*Cynoscion regalis*)

LIST OF FIGURES

CHAPTER TWO: Spatial and Temporal Heterogeneity in Growth and Maturity of Atlantic Weakfish (*Cynoscion regalis*)

Chapter One

INTRODUCTION

1.1 Spatial Heterogeneity in Marine Fisheries

Spatial heterogeneity is of increasing concern to marine fisheries managers and stock assessment scientists. Spatial variations within stock populations have largely been ignored in assessments due to the complexity that they add to fisheries models, and ignoring spatial variation may be one of the primary causes of management failures (Tyler and Rose 1994; Booth 2000; Cianelli et al. 2008; Pascoe et al. 2009; Lorenzen et al. 2010). Patterns of fish species abundance have been observed to change notably over time (Cianelli et al. 2008). Thus, emphasis has frequently been placed on the temporal trends of fisheries, while spatially heterogeneous factors such as environmental conditions and fishing pressures are averaged over large geographic distributions of fish stocks (Cianelli et al. 2008). However, the observed temporal variations in catch and abundance may well be driven by such spatial heterogeneity in fish stocks. For this reason, it is crucial to understand the spatial structure of stocks for assessments and management considerations.

The spatial structure of fish population dynamics can be viewed in several ways. Some stocks may be geographically isolated, while others are considered to be more mobile and are demographically denser in some areas within their range (Hilborn and Walters 1987). Population stability may be increased among spatially heterogeneous stocks by the diffusion of fishes from areas with higher abundance into habitats in which the population has become extinct (Huffaker 1958; Tyler and Rose 1994). Disregarding local extinctions and recolonization, spatial heterogeneity also may increase population stability by allowing emigration of individuals that

are unable to survive or reproduce in their natal habitats (Łomnicki 1980; Tyler and Rose 1994). Such low fitness may occur in a natal habitat as a result of density-dependent demographic processes, regime shifts, or anthropogenic causes such as overfishing and pollution.

Spatial structure of fish populations can further be described by two common models used to incorporate spatial heterogeneity into population dynamics (Tyler and Rose 1994). Reaction-diffusion models treat a population as a single entity that grows and diffuses throughout a habitat. Within this habitat, areas which have more of the resources necessary for the population have faster growth rates and lower emigration than areas with less capacity to support the population. Metapopulation models treat a population as a collective of spatially separated subpopulations, each with its own dynamics, between which individuals move.

1.1a Sources of Spatial Variation in Fish

Sources of spatial variation within fish stocks can be assigned to two distinct groups: environmental and anthropogenic. Environmental sources of spatial heterogeneity include physiochemical gradients that may occur throughout a species' geographic range. Environmental conditions directly affect the behavior and physiology of fish, thereby influencing their distribution, growth, mortality, and ability to reproduce (Brander 2010). Environmental conditions also indirectly affect fish stocks through their impacts on the productivity, structure, and composition of the ecosystems on which fish rely for sustenance (Brander 2010).

Global climate change has become a primary concern in fisheries research (Roessig et al. 2004; Perry et al. 2005; Brander 2010; Cheung et al. 2010). This concern stems from the heavy reliance of fisheries productivity on environmental conditions such as temperature, currents, and ocean upwelling (Cheung et al. 2010). Sarmiento et al. (2004) predicted that global primary

productivity may increase anywhere from 0.7-8.1% by the year 2050. A study of plankton samples collected between 1958 and 2002 showed that phytoplankton abundance has already increased in the cooler Northeast Atlantic and decreased in warmer regions south of 50°N (Richardson and Schoeman 2004).

Spatial shifts in primary productivity are expected to instigate redistribution of fishes as well (Perry et al. 2005; Cheung et al. 2010). Perry et al. (2005) examined 36 species of demersal North Sea fishes for significant distribution shifts between 1977 and 2001. The authors found that the mean latitudes of centers of distribution for 15 of these species did change in relation to rising sea temperatures, with 13 of these changes being northward. Further evidence supporting the observed pole-ward migration of marine fisheries was provided by Cheung et al. (2010), who projected an average of 30-70% increase of catch potential in high-latitude regions and a decrease in catch potential of up to 40% in the tropics.

Alternate impacts of climate change on the spatial heterogeneity of fish stocks may involve trophic interactions and local extinctions. Some species may be slower to disperse or less responsive to changes in environmental conditions than others (Perry et al. 2005). Differential rates of response to climate change potentially could cause trophic mismatch in space or time and disrupt species interactions (Perry et al. 2005; Hsieh et al. 2008). Climate change also could increase the probability of local extinctions by reducing the availability of suitable habitats (Thomas et al. 2004).

Spatial heterogeneity of fish stocks is also influenced by anthropogenic forces such as fishing pressure. Evidence has shown that fishing pressure reduces spatial heterogeneity by forcing fish populations to congregate in smaller spatial patches, or “put all their eggs in a smaller spatial basket” (Hsieh et al. 2008). Spatial variation also may be reduced by age

truncations caused by size-targeting of fisheries, thus limiting a population's ability to move throughout its entire distribution (Hsieh et al. 2006). Hsieh et al. (2008) found that exploited species are more sensitive to climatic changes, and that they show a much clearer distributional shift in response to such changes than unexploited species. The authors attributed these observations to the reduction in spatial heterogeneity of fish stocks by fisheries effort.

Berkes et al. (2006) described the effect of fishing on the spatial variation of stocks as exhibiting a "frontier exploitation pattern," in which fishermen move from location to location, depleting fish stocks beyond profitability and then moving on to fish the next spot. Fishermen understand and take advantage of the spatial structure of abundance in fish stocks (Norse 2010). Why, then, do stock assessments ignore the spatial structure of fish populations? The mismatch of resource use and assessment sets management up for failure. In order to fully understand and effectively manage the relationship between abundance and catch rate in a fishery, scientists must shift towards incorporating spatial as well as temporal variation of fish stocks in their assessments.

1.2. Atlantic Weakfish

1.2a Distribution

Atlantic Weakfish (*Cynoscion regalis*; family Sciaenidae) inhabit the North American Atlantic coast from Massachusetts to Florida (Bulloch 1986). Although they are occasionally reported from as far north as Nova Scotia, they are primarily abundant from New York to North Carolina (Bigelow and Schroeder 1953; Mercer 1985). Atlantic Weakfish participate in seasonal inshore migration into northern bays and estuaries to spawn (Hildebrand and Schroeder 1928). This migration occurs in the spring, with spawning activity peaking in late May and early June

(Graves et al. 1992). In the fall, Atlantic Weakfish move south to overwinter in warmer offshore waters (Bigelow and Schroeder 1953).

1.2b Life History

Atlantic Weakfish can grow to be 1,000 mm or more and live up to 17 years (Tringali et al. 2011). These fish reach sexual maturity at a young age, usually around a year and no later than two years old (Bulloch 1986). Lowerre-Barbieri et al. (1996) studied Atlantic Weakfish spawning patterns in Chesapeake Bay and concluded that these fish also reach maturity at a small size, with females having a mean total length of 170 mm at first maturity and males a mean total length of 164 mm. Genetic analyses of Atlantic Weakfish revealed no significant heterogeneity and concluded that the fish are genetically indistinguishable throughout their geographic range (Crawford et al. 1988; Graves et al. 1992). From this, one might assume that other biological factors, such as growth, maturity, and natural mortality rates, are also spatially indistinct. However, several recent studies have found significant spatial heterogeneity of Atlantic Weakfish life history.

1.2c Spatial Variation of Life History

Previous research indicates that Atlantic Weakfish life-history characteristics do exhibit spatial variation. Shepherd and Grimes (1983) found distinct differences in Atlantic Weakfish growth among six geographic subdivisions spanning from Cape Cod, Massachusetts to Cape Fear, North Carolina. The authors observed a general trend of larger (older) fish in the northern subdivisions, with a discrepancy of 49 cm and seven years between the largest northern and southern fishes. In a similar study of juvenile Atlantic Weakfish in Delaware Bay, Paperno et al.

(2000) found that growth rates consistently followed the spatial pattern of highest in the middle bay, lowest in the upper bay, and intermediate in the lower bay. The results of Shepherd and Grimes (1983) imply that growth varies more drastically on a coast-wide spatial scale. The observations of Paperno et al. (2000) suggest that life-history characteristics also vary within the smaller spatial dimension of a bay or estuary, although these variations may be less pronounced.

Many aspects of Atlantic Weakfish life history likely contribute to the spatial variation observed in these studies. Variations in fish growth often have been attributed to spatially and temporally sensitive factors such as temperature, energetic costs of migration and spawning, and prey availability (Nikolsky 1963; Jones and Johnston 1977; Glebe and Leggett 1981). Young-of-the-year Atlantic Weakfish remain in the shallow bays and estuaries during their first summer (Graves et al. 1992). Fish are the most vulnerable to their environments at this stage of their life. Thus, the wide range of environmental conditions, locations, and ecosystems found in bays and estuaries along the U.S. Atlantic coast should be reflected in the life-history characteristics of their local Atlantic Weakfish populations.

1.2d Productivity Heterogeneity

Productivity analyses are crucial to the stock assessment and management of fisheries. Yield per-recruit (YPR) and spawning stock biomass per-recruit (SPR) analyses are used to estimate biological reference points, which in turn are used as management targets and thresholds (Haddon 2001). The most recent Atlantic Weakfish stock assessment reported significant decreases in spawning stock biomass per-recruit in recent years and hypothesized that the likely cause is temporal heterogeneity in Weakfish natural mortality (Sullivan et al. 2016). Both YPR and SPR are calculated from rates of natural mortality, maturity, and growth, which

often exhibit spatial as well as temporal variation (Beverton and Holt 1957; Quinn and Deriso 1999). In addition, these productivity estimates are calculated from fishing effort data (such as fishing mortality, selectivity, and discards) that also exhibit spatial and temporal heterogeneity.

Given the apparent space- and time-varying nature of the components upon which YPR and SPR analyses are dependent, it is reasonable to assume that the subsequent productivity and biological reference points also must be spatially and temporally heterogeneous. Therefore, the most realistic management targets can be determined only by incorporating the spatial and temporal heterogeneity of the Atlantic Weakfish stock into the productivity models developed in its assessment.

1.3 Objectives

The overall objective of this thesis was to compare spatial and temporal trends in Atlantic Weakfish and evaluate the influence of this heterogeneity on models commonly utilized in stock assessment. In Chapter Two, I investigated spatial and temporal variation of growth and maturity using mixed-effects models incorporating the random effects of region and year on life-history parameters. I then compared parameters estimated from these heterogeneous mixed-effects models with those estimated from standard homogeneous models to determine which provide more robust life-history estimates. In Chapter Three, I evaluated the influence of spatially and temporally integrated growth parameters on Atlantic Weakfish productivity by comparing yield and spawning stock biomass per-recruit derived from homogeneous and heterogeneous weight estimates. My main objective in this chapter was to determine the sensitivity of biological reference points to these different weight parameters. I hope that the resulting spatial and temporal effects upon biological reference points frequently used as

management targets will indicate the appropriate spatial and temporal units for use in management, and thereby increase the effectiveness of management strategies for Atlantic Weakfish.

1.4 Literature Cited

Berkes, F., Hughes, T. P., Steneck, R. S., Wilson, J. A., Belwood, D. R., Crona, B., Folke, C., Gunderson, L. H., Leslie, H. M., Norberg, J., Nyström, M., Olsson, P., Österblom, H., Scheffer, M., and Worm, B. 2006. Globalization, roving bandits, and marine resources. Science 311:1557-1558.

Beverton, R. H. J., and Holt, S. J. 1957.On the dynamics of exploited fish populations. Fisheries Investigations, Ser. 2, Vol. 19. UK Ministry of Agriculture and Fisheries, London.

Bigelow, H. and Schroeder, W. 1953. Fishes of the Gulf of Maine. U.S. Fisheries and Wildlife Service, Fisheries Bulletin 53:577p.

Booth, A. J. 2000. Incorporating the spatial component of fisheries data into stock assessment models. ICES Journal of Marine Science 57:858-865.

Brander, K. 2010. Impacts of climate change on fisheries. Journal of Marine Systems 79:389 402.

Bulloch, D. K. 1996. Marine gamefish of the middle Atlantic: Weakfish. American Littoral Society 14(3):21-23.

Cheung, W. W. L., Lam, V. W. Y., Sarmiento, J. L., Kearney, K., Watson, R., Zeller, K., and Pauly, D. 2010. Large-scale redistribution of maximum fisheries catch potential in the global ocean under climate change. Global Change Biology 16:24-35.

Cianelli, L., Fauchald, P., Chan, K. S., Agostini, V. N., and Dingsør, G. E. 2008. Spatial fisheries ecology: Recent progress and future prospects. Journal of Marine Systems 71:223-236.

Crawford, M. K., Grimes, C. B., and Buroker, N. E. 1988. Stock identification of Weakfish, *Cynoscion regalis*, in the middle Atlantic region. Fishery Bulletin 87:205-211.

Glebe, B. D. and Leggett, W. C. 1981. Latitudinal differences in energy allocation and use during the freshwater migrations of American shad (*Alosa sapidissimia*) and their life history consequences. Canadian Journal of Fisheries and Aquatic Science 38:806-820.

Graves, J. E., McDowell, J. R., and Jones, M. L. 1992. A genetic analysis of Weakfish *Cynoscion regalis* stock structure along the mid-Atlantic Coast. Fishery Bulletin 90:469-475.

Hastie, T. J. and Tibshirani, J. R. 1986. Generalized additive models. Stat. Sci. 1:297-318.

Hilborn, R. and Walters, C. J. 1987. A general model for simulation of stock and fleet dynamics in spatially heterogeneous fisheries. Canadian Journal of Fisheries and Aquatic Sciences 44:1366-1369.

Hildebrand, S. F. and Schroeder, W. C. 1928. Fishes of Chesapeake Bay. Bulletin of the United States Bureau of Fisheries 43(1):366p.

Hsieh, C., Reiss, C. S., Hunter, J. R., Beddington, J. R., May, R. M., and Sugihara, G. 2006. Fishing elevates variability in the abundance of exploited species. Nature (London) 443:859-962.

Hsieh, C., Reiss, C. S., Hewitt, R. P., and Sugihara, G. 2008. Spatial analysis shows that fishing enhances the climatic sensitivity of marine fishes. Canadian Journal of Fisheries and Aquatic Sciences 65:947-961.

Huffaker, C. B. 1958. Experimental studies on predation: dispersion factors and predator-prey oscillations. Hilgardia 27:343-383.

Johnston, R. 2012. NEFSC multispecies bottom trawl survey. Ecosystems Survey Branch, NOAA, Woods Hole, Massachusetts: 17 p.

Jones, R. and Johnston, C. 1977. Growth, reproduction, and mortality in gadoid fish species. Pages 37-62 *in* J. H. Steele, editor. Fisheries Mathematics, Academic Press, New York.

Łomnicki, A. 1980. Regulation of population density due to individual differences and patchy environment. Oikos 35:185-193.

Lorenzen, K., Steneck, R. S., Warner, R. R., Parma, A. M., Coleman, F. C., and Leber, K. M. 2010. The spatial dimensions of fisheries: Putting it all in place. Bulletin of Marine Science 86(2):169-177.

Lowerre-Barbieri, S. K., Chittenden, M. E., and Barbieri, L. R. The multiple spawning pattern of Weakfish in the Chesapeake Bay and Middle Atlantic Bight. Journal of Fish Biology 48:1139-1163.

McCullagh, P. and Nelder, J. A.1983. General Linear Models: Monographs on Statistics and Applied Probability. Chapman and Hall, London.

Mercer, L. P. 1985. Fishery Management Plan for the weakfish, (*Cynoscion regalis*) fishery. Fisheries Management Report No. 7 Atlantic States Marine Fisheries Commission. North Carolina Department of Natural Resources and Community Development, Division of Marine Fisheries Special Scientific Report No. 46, 129 p.

Nikolsky, G. V. 1963. The Ecology of Fishes. Academic Press, New York.

Norse, E. A. 2010. Ecosystem-based spatial planning and management of marine fisheries: Why and how? Bulletin of Marine Science 86(2):179-195.

Paperno, R., Targett, T. E., and Grecay, P. A. 2000. Spatial and temporal variation in recent growth, overall growth, and mortality of juvenile Weakfish (*Cynoscion regalis*) in Delaware Bay. Estuaries 23(1):10-20.

Pascoe, S., Bustamante, R., Wilcox, C., and Gibbs, M. 2009. Spatial fisheries management: A framework for multi-objective qualitative assessment. Ocean and Coastal Management 52:130-138.

Perry, A. L., Low, P. J., Ellis, J. R., and Reynolds, J. D. 2005. Climate change and distribution shifts in marine fishes. Science 308:1912-1915.

Quinn, T. J., and Deriso, R. B. 1999. Quantitative Fish Dynamics. Oxford University Press, New York.

Richardson, A. J. and Schoeman, D. S. 2004. Climate impact on plankton ecosystems in the Northeast Atlantic. Science 305:1609-1612.

Roessig, J. M., Woodley, C. M., Cech, J. J., Jr., and Hansen, L. J. 2004. Effects of global climate change on marine and estuarine fishes and fisheries. Reviews in Fish Biology and Fisheries 14:251-275.

Sarmiento, J. L., Slater, R., Barber, R., Bopp, L., Doney, S. C., Hirst, A. C., Kleypas, J., Matear, R., Mikolajewicz, U., Monfray, P., Soldatov, V., Spall, S. A., and Stouffer, R. 2004. Response of ocean ecosystems to climate warming. Global Biogeochemical Cycles 18:*GB3003, doi:10.1029/2003GB002134.*

Shepherd, G. and Grimes, C. B. 1983. Geographic and historic variations in growth of Weakfish, *Cynoscion regalis*, in the Middle Atlantic Bight. Fishery Bulletin 81(4):803-813.

Sullivan, P., Buckel, J., and Deroba, J. 2016. Weakfish Benchmark Stock Assessment and Peer Review. Atlantic States Marine Fisheries Commission, Arlington, Virginia; 270 p.

Thomas, C. D., Cameron, A., Green, R. E., Bakkenes, M., Beaumont, L. J., Collingham, Y. C., Erasmus, B. F. N., Ferreira de Siqueira, M., Grainger, A., Hannah, L., Hughes, L., Huntley, B., Van Jaarsveld, A. S., Midgley, G. F., Miles, L., Ortega-Huerta, M. A., Peterson, A. T., Phillips, O. L., and Williams, S. E. 2004. Extinction risk from climate change. Nature (London) 427:145-148.

Tringali, M. D., Seyoum, S., Higham, M., and Wallace, E. M. 2011. A dispersal-dependent zone of introgressive hybridization between Weakfish, *Cynoscion regalis*, and sand seatrout, *C. arenarius*, (Sciaenidae) in Florida Atlantic. Journal of Heredity 102(4):416-432.

Tyler, J. A., and Rose, K. A. 1994. Individual variability and spatial heterogeneity in fish population models. Reviews in Fish Biology and Fisheries 4:91-123.

CHAPTER TWO: Spatial and temporal heterogeneity in growth and maturity of Atlantic Weakfish (*Cynoscion regalis*)

2.1 Abstract

Individual variability in life-history characteristics is frequently overlooked in fisheries stock assessment models. In favor of simplicity, these models often assume "average" growth or maturity across all scales of space and time for a given fish stock. In the present study, mixed-effects models were used to explore the effects of spatial and temporal variation on growth and maturity models of Atlantic Weakfish (*Cynoscion regalis*). Standard homogeneous life-history models and heterogeneous models incorporating regional and temporal variation were compared among four separate datasets representing varying scales of space and time. For each dataset, results of the standard model approach assuming neither spatial nor temporal heterogeneity were compared to those of three mixed-effects models which incorporated region, year, and both region and year as the grouping variables for the random effects. The results of this study indicate that standard homogeneous models that assume no spatial or temporal heterogeneity mask regional and annual trends in length, weight, and maturity of Atlantic Weakfish that are much more predictive and insightful for management of the stock. These trends were apparent in all mixed-effects models, which better fit all datasets than homogeneous models for both growth and maturity. Models incorporating both spatial and temporal heterogeneity were the most robust. These models also provided the advantage of comparing the scaled random effects of regional and annual variation within each dataset.

Keywords: Mixed-effects models, individual variability, spatial heterogeneity, temporal heterogeneity, fish growth, maturity, Atlantic Weakfish

2.2 Introduction

In fisheries science, estimates of life-history characteristics are the basis of population dynamics models that are used to determine sustainable harvests for managing stocks (Beverton and Holt 1957; Ricker 1975). Conservation-oriented management objectives often are derived from analyses of size-at-age and age- or length-at-maturity. These analyses provide scaled yield calculations and biological reference points such as $F_{0.1}$, $F_{\max}$, and $F_{\%}$ that are used as fisheries management thresholds (Beverton and Holt 1957; Gulland 1983; Quinn and Deriso 1999; Haddon 2001). Growth and maturity are also related to other important life-history traits such as natural mortality, reproductive success, and likelihood of survival (Healey 1991; Charnov 1993; McGurk 1996; Jensen 1998; Heath et al. 1999; Quinn et al. 2004).

Fisheries population dynamics models usually assume that population growth can be adequately described through mean growth parameters (Sainsbury 1980; Pilling et al. 2002). However, this "average" growth approach ignores the considerable variation often seen in individual growth trajectories around the mean population growth, commonly referred to as "individual variability" (Pilling et al. 2002). Individual variability is frequently hypothesized to result from spatial and temporal heterogeneity driven by variations in ocean conditions, resource availability, genetic structure, and fishing intensity (Beacham 1983; Hutchings and Myers 1994; Trippel 1995; Krohn et al. 1997; Jiao et al. 2010; Hua et al. 2015). Ignoring individual variability in fish life-history models can lead to unrealistic or biased estimates of productivity analyses and biological reference points, which could greatly reduce the effectiveness of fisheries management strategies.

In recent decades, many different methods have been applied to examine individual variability in fish populations. The standard approach commonly used in stock assessment

models involves examining life-history traits "averaged" for individuals separated into groups based on the source of variation under scrutiny (e.g., Shepherd and Grimes 1983; Isaac 1990; Paperno et al. 2000). As an example, when considering spatial and temporal variation, it would be prudent to divide individuals into groups based on units of space and time, such as region and year. This standard approach assumes that all life-history parameters are fixed, that a common variance exists for the residuals across all populations within a given group, and that there is no variation among populations. Models are fit separately to data divided into the desired groups and then related using various multiple comparison tests. This method has been favored in the past due to the simplicity of the models involved. In practice, models must be fitted repeatedly for numerous subsets of data that are likely to vary in size and scope. Furthermore, the error associated with individual parameter estimates is incorporated into the estimates of the mean parameters and of their variability.

Further studies have attempted to negate some of these drawbacks in growth models by allowing individual fish growth to include a nonrandom component dependent on sampling covariates (such as depth or latitude) or more detailed population partitions (such as year classes; Weisberg 1993; Kimura 2008). This fixed-effects approach summarizes information by functionally relating population parameters to covariates. However, this approach still requires adequate sampling of the population of interest with minimal intrinsic error such as sampling or ageing error. In addition, the fixed-effects approach ignores correlations between fish in the same group. Finally, the fixed effects can only be estimated up to an arbitrary additive constant. This makes comparisons between different surveys, areas, or time periods complicated.

With the advent of efficient parameter estimation software, the use of mixed-effects, or hierarchical, models has become increasingly popular (Pinheiro and Bates 2000; Fitzmaurice et

al. 2004; McCulloch et al. 2008). This is especially true for fisheries models, in which the mixed-effect approach offers many benefits over the standard and fixed-effects approaches. Primarily, the use of both fixed effects associated with population means and random effects associated with individual variability includes the impact of among-group variation. This approach assumes that the life-history parameters for each individual fish represent samples from a multivariate population of growth parameters characteristic of the population or group in question. Mixed-effects methods combine population average with individual data, improving estimates by a process of shrinkage using pooled data rather than working with individual subsets of data.

Several recent studies have applied nonlinear mixed-effects methods to the von Bertalanffy growth model in order to analyze individual variability in fish growth (Pilling et al. 2002; Helser et al. 2004; Hart and Chute 2009; Zhang et al. 2009; Alós et al. 2010; Weisberg et al. 2010; Hua et al. 2015). Other studies have used mixed-effects models to further explore and incorporate the random effects of spatial heterogeneity in fish populations. Helser and Lai (2004) used nonlinear mixed-effects models to examine the random effects of geographic location of various populations of largemouth bass (*Micropterus salmoides*), and Escati-Peñaloza et al. (2010) used these methods to analyze spatial variation in growth patterns of striped clams (*Ameghinomya antiqua*). Jiao et al. (2010) used Bayesian hierarchical methods to explore temporal variation of red abalone (*Haliotis rufescens*) related to El Niño.

Mixed-effects models also have been applied in analyses of individual variability in fish maturity. Punt et al. (2006) used mixed-effects models to estimate relationships between maturity and length for rock lobsters (*Jasus edwardsii*) in which the random effects of parameters depended on region and year in order to account for spatial and temporal heterogeneity. Jonsson et al. (2012) investigated these effects more directly by raising Atlantic salmon (*Salmo salar*) in

tanks with various temperatures and food qualities and incorporating tank as a random effect in their mixed-effects models for age- and size-at-maturity.

In this thesis, mixed-effects methods were applied to examine the individual variability present in Atlantic Weakfish (*Cynoscion regalis*) due to spatial and temporal heterogeneity in life history. As Atlantic Weakfish have a large geographic distribution ranging from Nova Scotia to Florida, spatial variation is expected to have a significant impact on expression of their life-history traits. Like all populations, Weakfish are also subject to variations over time. Temporal trends in life history are responses to variations in environmental conditions and fishing pressure caused by weather events, changes in economy, etc.

Previous research has examined the spatial variation of Weakfish growth by comparing models individually fitted to length data among subdivided regions in the Middle Atlantic Bight and Delaware Bay (Shepherd and Grimes 1983; Paperno et al. 2000). However, these studies focused on very small segments of the entire Weakfish distribution. In addition, there has been little research into the spatial heterogeneity of other Weakfish life-history attributes (such as maturity) or into temporal heterogeneity of any Weakfish life-history characteristics.

This thesis aims to improve our understanding of the effects of spatial and temporal heterogeneity in life-history attributes of Atlantic Weakfish. Spatial and temporal variation was incorporated into growth and maturity analyses using mixed-effects models. These models then were applied to examine trends in growth and maturity across various regions and years. Furthermore, results of the heterogeneous mixed-effects models were compared to those of homogeneous models in order to determine which provide more robust life-history estimates. In this approach, I hoped to develop a model that could be applied to life-history data for any species and used to determine spatial and temporal trends in growth and maturity. Identifying

these trends will contribute to the improvement of spatially and temporally explicit fisheries management efforts.

2.3 Methodology

In this study, mixed-effects models were used to explore the effects of spatial and temporal variation on growth and maturity of Atlantic Weakfish (*Cynoscion regalis*) using four datasets that collectively cover the entire known geographic distribution of this species. The results of the mixed-effects approach were compared to those of the standard approach in which no individual variability was assumed. Mixed-effects models for size- and maturity-at-age examined the influence of spatial and temporal variation by grouping the random effects on parameters by region, year, and both region and year.

2.3a Data Sources

Data were taken from four fishery-independent surveys that sampled various regions and years. These surveys were the Northeast Fisheries Science Center (NEFSC) Bottom Trawl Survey, the Northeast Area Monitoring and Assessment Program (NEAMAP), the Southeast Area Monitoring and Assessment Program for the South Atlantic (SEAMAP-SA or SEAMAP), and the Chesapeake Bay Multispecies Monitoring and Assessment Program (ChesMMAP). Collectively, these surveys sampled the approximate equivalent of the entire Atlantic Weakfish geographic distribution and spanned a period of 16 years (Table 1, Figure 1).

The NEFSC bottom trawl survey has been sampling along the Atlantic coast from the Scotian Shelf southwest of Nova Scotia to the Cape Lookout National Seashore, NC since 1963 (Johnston 2012). The survey has sampled from September to October since its inception. In

1968, NEFSC added a spring survey from February through April. The NEAMAP bottom trawl survey has been operating in the spring and fall of each year since 2007 (Bonzek et al. 2009). This survey samples fishes and invertebrates from Montauk, NY to Cape Hatteras, NC. The NEFSC and NEAMAP surveys were chosen for this study because they both sample the area of highest abundance of Atlantic Weakfish.

The SEAMAP-SA shallow-water trawl survey has sampled the South Atlantic Bight from Cape Hatteras, NC to Cape Canaveral, FL during the spring, summer, and fall since 1983 (Eldridge 1988). The data from this survey represent the geographic area in which Weakfish occur that is not sampled by either the NEFSC or NEAMAP surveys. The ChesMMAP large-mesh bottom trawl survey has been sampling in the Chesapeake Bay since 2002 (Bonzek et al. 2011). The survey runs every March through November and targets late juvenile and adult fishes. This survey samples from a much smaller area than the others used in this study, but offers data from a wider seasonal scale and covers a crucial nursery habitat used by Atlantic Weakfish.

Each data set was divided into regions and years in order to examine effects across spatial and temporal scales. Data from the NEFSC, NEAMAP, and SEAMAP surveys were divided into regions by latitude in 1° increments (Figure 2). The NEFSC data set was divided into seven regions, while the NEAMAP and SEAMAP data sets were each divided into six regions. The ChesMMAP data set was divided into 6 regions by 0.38° increments (Figure 2). Data collected from the two northern surveys was normally distributed, with most of the data being sampled from the middle regions (Figure 3). The data distribution from the southern survey, however, was strongly skewed spatially, with the majority of the sampling occurring in the northern range of the survey area. The Chesapeake Bay survey data distribution was also strongly skewed

spatially, with the majority of the data being collected from the southern range of the survey area near the mouth of the bay.

The NEFSC and SEAMAP datasets covered the longest time frames, each representing 12 years of sampling (Figure 4). The ChesMMAP dataset represented the next largest amount of time surveyed at ten years of sampling, followed by the NEAMAP dataset that only included six years. The NEFSC data distribution was roughly normal in a temporal sense, with the majority of the sampling effort occurring in the middle of the time series between 2002 and 2008. The NEAMAP survey showed a more skewed annual distribution, as sampling efforts have increased over time since the survey's inception in 2007. SEAMAP sampling effort decreased between 2001 and 2007, followed by an increase in data collection from 2008 to 2014. The ChesMMAP survey displayed a bimodal distribution of annual sampling effort, with peaks in 2005 and 2010. However, there is a generally decreasing trend over the entire time series sampled by this survey. Due to the high variation in regions and years sampled by the four surveys, each dataset was considered separately when modeling spatial and temporal heterogeneity.

2.3b Growth

Spatial and temporal heterogeneity in Atlantic Weakfish growth was examined by fitting three different nonlinear mixed-effects models to length- and weight-at-age data. These mixed-effects models were compared to a less complex non-mixed model similar to those commonly used in fish growth analyses. Models were fitted using the growth equations developed by von Bertalanffy (1938). All of the models and analyses included in this study were developed using R statistical software (R Core Team 2014).

Model 1

The base model used here as a contrast to mixed-effects methods mirrors the standard approach presented by Isaac (1990). In this approach, the von Bertalanffy growth model is fit separately to back-calculated length-at-age measurements of fish within a given population. Then the least-squares estimates of the growth parameters are summarized by their means and variances. This standard modeling approach assumes that all growth parameters are fixed, that a common variance exists for the residuals across all groups, and that there is no relationship among groups.

In this study, the simplified non-mixed nonlinear growth models were fitted to length and weight data from the four surveys using least-squares regressions. Mean length L_i at age t_i for $i = 1, 2,\ldots, N$ fish was fit using the model

$$L_i = L_\infty(1-e^{-k(t_i-t_0)}) + \varepsilon_i; \quad (1)$$

where L_∞ is the average maximum length, k is the growth rate parameter toward the maximum, t_0 is the hypothetical age at length zero, and ε_i is assumed to be an independent error with mean zero and common variance σ^2. Mean weight W_i was fitted using the log-transformed model

$$\ln(W_i) = \ln(W_\infty) + b\ln(1-e^{-k(t_i-t_0)}) + \varepsilon_i; \quad (2)$$

in which b is the allometric growth parameter and all other parameters are the same as those used in Equation 1.

The b parameter was calculated from the weight-length relationship as seen in Haddon (2001). Weight is related to length by:

$$W_t = aL_t^{\,b}10^{\varepsilon_i}; \quad (3)$$

in which a and b are parameters and ε_i is the multiplicative error term for the ith fish. This relationship is easily transformed to a linear model by taking the natural logarithm of both sides, as seen in Equation 4:

$$\ln(W_t) = \ln(a) + b\ln(L_t) + \varepsilon_i \,. \quad (4)$$

In this simplified model, *a* is the intercept and *b* the slope of the weight-length regression equation. These parameters were estimated for each survey by fitting this linear model to weight and length data using the LM function from the stats package in R (R Core Team 2014). The nonlinear least-squares (NLS) function from the same package then was used to fit the simplified non-mixed nonlinear growth models shown in Equations 1 and 2.

Model 2

This model incorporates spatial heterogeneity in growth by assuming a random effect δ_j on the growth parameters grouped by region *j*. The model was run twice, first with a random effect on $L_{\infty j}$ ($\delta_j^{L_\infty}$, Equation 5), and then with random effects on both $L_{\infty j}$ and k_j ($\delta_j^{L_\infty}$, δ_j^{k} , Equation 6).

$$L_{ij} = (L_\infty + \delta_j^{L_\infty})(1 - e^{-(k)(t_i - t_0)}) + \varepsilon_{ij}\,; \quad (5)$$

$$L_{ij} = (L_\infty + \delta_j^{L_\infty})(1 - e^{-(k+\delta_j^{k})(t_i - t_0)}) + \varepsilon_{ij} \quad (6)$$

The parameter t_0 was considered to be without mixed-effect, as it seems unlikely that the age at length zero is impacted by environmental conditions that vary over space or time.

The additional structure of the $\delta_j^{L_\infty}$ and δ_j^{k} mixed-effects model on the growth parameters ($L_\infty + \delta_j^{L_\infty}$) and ($k + \delta_j^{k}$) imposes the assumption that each $L_{\infty i}$ and k_i pair is a random sample from the population of growth parameters within each region. This population can be characterized by a multivariate normal distribution (MVN) with mean $\mu = 0$ and variance-covariance matrix Σ, or

$$\begin{pmatrix} \delta_j^{L_\infty} \\ \delta_j^{k} \end{pmatrix} \sim MVN(\mu, \Sigma) \quad (7)$$

for each region *j*, where

$$\Sigma = \begin{bmatrix} V_{L_\infty}^2 & V_{L_\infty k} \\ V_{L_\infty k} & V_k^2 \end{bmatrix} \quad (8)$$

The nonlinear mixed-effect model for weight-at-age is similar to the length-at-age mixed-effect model. Again, the average maximum size and growth rate parameters are assumed to have a random effect due to spatial variation. The $\delta_j^{W_\infty}$ weight-at-age equation therefore becomes:

$$\ln(W_{ij}) = \ln(W_\infty + \delta_j^{W_\infty}) + b\ln(1 - e^{-(k)(t_i - t_0)}) + \varepsilon_{ij}; \quad (9)$$

and the $\delta_j^{W_\infty}$ and δ_j^k weight-at-age equation is:

$$\ln(W_{ij}) = \ln(W_\infty + \delta_j^{W_\infty}) + b\ln(1 - e^{-(k+\delta_j^k)(t_i - t_0)}) + \varepsilon_{ij}; \quad (10)$$

in which $\varepsilon_{ij} \sim N(0, \sigma^2)$ and

$$\begin{pmatrix} \delta_j^{W_\infty} \\ \delta_j^k \end{pmatrix} \sim MVN(\mu, \Sigma) \quad (11)$$

for each region *j*, where

$$\Sigma = \begin{bmatrix} V_{W_\infty^2} & V_{W_\infty k} \\ V_{W_\infty k} & V_{k^2} \end{bmatrix} \quad (12)$$

The allometric growth parameter *b* was taken from the weight-length relationship (Equation 4). Nonlinear mixed-effects growth models were fitted to length and weight data from the four surveys using the NLMER function from the lme4 package (Bates et al. 2015).

Model 3

This model incorporates temporal heterogeneity in growth by assuming a random effect on the growth parameters grouped by year. Length-at-age was modeled using Equations 5-8 and

weight-at-age was modeled using Equations 9-12. Growth parameters L_∞, W_∞, and k were randomly sampled from the population of growth parameters within each year.

Model 4

This model incorporates both spatial and temporal heterogeneity in growth by assuming uncorrelated random effects on the growth parameters grouped by region and year. Length- and weight-at-age were modeled as previously described with parameters being sampled randomly from the populations of growth parameters within each region and year. The nonlinear mixed-effects models described in Models 3 and 4 were fit to growth data using the NLMER function from the lme4 package (Bates et al. 2015).

Model Comparison

The first comparison among the results of the four models was made using the Akaike Information Criteria (AIC) test (Akaike 1974):

$$AIC = -2LL + 2p; \tag{13}$$

where the AIC statistic is calculated using the negative log-likelihood (LL) and number of parameters (p) in each model. This test provides a measure of goodness-of-fit that can be used to compare different models in a set of candidate models. Models fit with the smallest AIC values provide the best tradeoff between fit and number of parameters within the model.

The mixed-effects models were further compared with the likelihood-ratio test (LRT) using the ANOVA function from the stats package (R Core Team 2014). The likelihood ratio (λ) applied here is simply defined as the ratio of the likelihood (L) of a null set of parameters from a reduced model (θ_0) to the likelihood of an alternative set of parameters from a full model (θ_A):

$$\lambda = \frac{L(\theta_0)}{L(\theta_A)}; \quad (14)$$

Likelihood-ratio tests were used to examine the influence of the additional random effect (e.g., year) on growth parameters in mixed-effects models integrating both spatial and temporal variation (θ_A = M4) compared to reduced models that only considered one random effect (θ_0 = M2 and M3). This test also was used to observe the impact of random effects on additional growth parameters (i.e., *k*) in full models that incorporated random effects on two growth parameters (e.g., $\theta_A = \delta_j^{W_\infty}$ and δ_j^k) in contrast to reduced models that only incorporated random effects on one growth parameter (e.g., $\delta_j^{W_\infty}$). In addition to comparing AIC values and LRT statistics, mixed-effects models of growth were compared by looking at the variances of their random effects as well as the combined fixed and random effects of their estimated growth parameters.

2.3c Maturity

Spatial and temporal heterogeneity in Atlantic Weakfish maturity-at-age was analyzed using methods much the same as those used for growth. The results from a non-mixed generalized linear maturity model (Model 1) were compared to those from generalized linear mixed-effects models incorporating spatial variation (Model 2), temporal variation (Model 3), and both spatial and temporal variation (Model 4) in maturity. Only data from the ChesMMAP survey were used to examine maturity-at-age. While the NEFSC, NEAMAP, and SEAMAP surveys all collected maturity data for Weakfish, none of them sampled during their respective spawning seasons. This prevents in-depth analyses of Weakfish maturity in most of its geographic distribution and leads to increased bias in existing maturity analyses for this species.

The ChesMMAP survey provides the most comprehensive maturity data for Atlantic Weakfish by far, and therefore was used to evaluate the spatial and temporal heterogeneity of female and male maturity-at-age.

Model 1

A base model was fit to categorical maturity data (i.e., mature or not mature) using the logit link function

$$\ln\left(\frac{P_t}{1-P_t}\right) = \alpha + \beta t + \varepsilon_t \ ; \tag{15}$$

with intercept α and explanatory variable βt, in which t is age and the slope β is equivalent to the age at which 50% of the fish are mature ($P_t = 0.5$) and has an assumed independent error defined as $\varepsilon_t \sim N(0,\sigma^2)$. Maturity data were assumed to have a binomial distribution

$$M_t \sim binomial(N_t, P_t); \tag{16}$$

where M_t is the maturity observation and P_t represents the proportion of female or male mature fish in each age class. This model, which assumes no spatial or temporal heterogeneity, was fit using the generalized linear model (GLM) function in the stats package (R Core Team 2014).

Model 2

Spatial heterogeneity was incorporated into the maturity model by entering region as a random effect into a generalized linear mixed-effects model. Doing so changed the logit link function to:

$$\ln\left(\frac{P_{tj}}{1-P_{tj}}\right) = (\alpha + \delta_j^{\alpha}) + (\beta t + \delta_j^{\beta}) + \varepsilon_{tj}; \tag{17}$$

in which δ_j^{α} represents the effect caused by randomly selecting intercepts from each region *j*, δ_j^{β} is the random slope, and the random error not explained by spatial variation is defined as $\varepsilon_{tj} \sim N(0,\sigma^2)$. As in the nonlinear mixed-effects models used in the growth analyses, the additional structure of the δ_j^{α} and δ_j^{β} mixed-effects model on the maturity parameters ($\alpha + \delta_j^{\alpha}$) and ($\beta + \delta_j^{\beta}$) imposes the assumption that each α and β pair is a random sample from the population of maturity parameters within each region. This population is characterized by:

$$\begin{pmatrix} \delta_j^{\alpha} \\ \delta_j^{\beta} \end{pmatrix} \sim MVN(\mu, \Sigma) \tag{18}$$

for each region *j* where $\mu = 0$ and the variance-covariance matrix Σ is:

$$\Sigma = \begin{bmatrix} V_{\alpha}^2 & V_{\alpha\beta} \\ V_{\alpha\beta} & V_{\beta}^2 \end{bmatrix} \tag{19}$$

Generalized linear mixed-effects models were fit to maturity data using the GLMER function from the lme4 package (Bates et al. 2015).

Model 3

Temporal heterogeneity was incorporated into the maturity-at-age model by replacing region with year as a random effect in Equation 17. Maturity parameters α and β were randomly sampled from the population of intercepts and slopes within each year *j* using the GLMER function.

Model 4

This model incorporated both spatial and temporal heterogeneity into the maturity model by entering both region and year as random effects into Equation 17. In this model, δ_j^{α} and δ_j^{β}

represent the uncorrelated effects caused by randomly selecting intercepts and slopes from each region and year. As in Models 2 and 3, this was done using the GLMER function to apply a generalized linear mixed-effects model.

Model Comparison

As in the growth analyses, the four maturity models were compared using the AIC test (Equation 13). Models with lower AIC values were considered to have better goodness-of-fit. The mixed-effects models were further compared using the likelihood-ratio test (LRT; Equation 14). To determine the relative significance of spatial versus temporal heterogeneity, two LRTs were performed. Significance of spatial variation was examined by running a LRT with Model 3 (year effect) as the null model and Model 4 (region and year effect) as the alternative model to determine the additional random effect of region on maturity. Vice versa, temporal significance was examined via a LRT in which Model 2 (region effect) served as the null model and Model 4 (region and year effect) again was the alternative model so that the additional random effect of year on maturity could be observed.

2.4 Results

The results of this study strongly support the importance of integrating spatial and temporal heterogeneity into Atlantic Weakfish life-history models. Mixed-effects models revealed a strong influence of both spatial and temporal variation on Weakfish growth and maturity. Distinct trends were observed in all life-history parameter estimates produced by heterogeneous models. In all analyses, these spatially and temporally integrated estimates varied from the averaged estimates produced by the standard homogeneous model. Furthermore, mixed-

effects models incorporating spatial and temporal heterogeneity were more robust than the homogeneous model for both growth and maturity analyses of all datasets, meaning that they provided life history estimates which better fit the data and that their performance was less susceptible to alterations in variables such as starting parameter estimates.

Length-at-Age

Length-at-age models were significantly impacted by the incorporation of spatial and temporal heterogeneity. Mixed-effects models that incorporated regional and annual variation fit the data better than the standard homogeneous model (M1) in all four surveys (Table 2). In three of the four surveys, spatially and temporally integrated models (M4) were the most robust. The only exception was the SEAMAP survey, in which a one-parameter, spatially integrated model ($M2_{L\infty}$) produced the lowest AIC statistic (Table 3).

The Atlantic Weakfish length-at-age curve produced by the standard homogeneous model (M1) exhibited a different shape than those produced by the regional and temporal effects from spatially and temporally integrated models (M4) for all four datasets (Figure 5; Figure 7). The homogeneous model curve appeared to cross all regional and annual curves in the NEFSC survey. In the NEAMAP and ChesMMAP surveys, the length-at-age curve produced by the homogeneous model appeared to be a rough average of the region- and year-specific curves produced by the heterogeneous model. The length-at-age curve from the homogeneous model was lower than all region- and year-specific curves in the SEAMAP survey.

The standard approach assumes that the homogeneous model produces a length-at-age relationship that should be "averaged" across all regions and years sampled for the population. However, a comparison of homogeneous length parameter estimates to mean heterogeneous

parameter estimates incorporating both spatial and temporal heterogeneity showed that this modeling approach does not yield accurate results. Mean length estimates produced by the standard homogeneous model (M1) differed from those produced by the spatially and temporally heterogeneous model (M4) in every dataset. In the NEFSC survey, L_∞ and t_0 estimates produced by the heterogeneous model were nearly half those produced by the homogeneous model, while k was more than doubled (Table 5).

The standard approach assumption of "averaged" length-at-age is further discredited when comparing homogeneous parameter estimates to region- and year-specific parameter estimates produced by the heterogeneous model. In the NEFSC dataset, the L_∞ estimate produced by the homogeneous model (M1) was higher than all of the region-specific L_∞ estimates produced by the heterogeneous model (M4) and really only described the northern-most region (Figure 6). The homogeneous L_∞ estimate in the SEAMAP dataset, on the other hand, was lower than any of the region-specific L_∞ estimates. The corresponding k estimates produced by the homogeneous model were lower (NEFSC) and higher (SEAMAP) than all region-specific estimates. The homogeneous L_∞ estimates in the NEAMAP and ChesMMAP surveys appeared to be much closer to an average of the region-specific L_∞ estimates. However, the k estimates produced by the homogeneous model were lower than any of the spatial estimates produced by the heterogeneous model for both surveys. This disparity in parameters estimated by the standard homogeneous model (M1) and heterogeneous model (M4) present in all four surveys suggests that in none of them does the standard model describe any of the regions sampled in each survey.

This discrepancy in parameter estimates produced by homogeneous and heterogeneous models is mirrored in the temporal effects of length-at-age parameters (Figure 8). As in the region-specific L_∞ estimates, year-specific estimates of the L_∞ parameter are all lower than the

homogeneous estimate in the NEFSC survey and higher in the SEAMAP survey. Correlated *k* estimates are lower than all year-specific estimates for NEFSC and higher for SEAMAP. Also like the regional trends, homogeneous L_∞ estimates produced by the standard model (M1) appear to be approximate averages of the annual estimates produced by the heterogeneous model (M4) for the NEAMAP and ChesMMAP surveys. However, the homogeneous *k* estimates in these surveys were still lower than the year-specific estimates. Thus, the standard homogeneous model does not accurately describe the Atlantic Weakfish population in any of the regions or years sampled in the four surveys.

The surveys that sampled from larger geographical areas (NEFSC, NEAMAP, and SEAMAP) displayed stronger spatial trends than temporal trends in Atlantic Weakfish length-at-age. Length-at-age showed the most spatial variation in the two northern surveys (Figure 5). Models that incorporated spatial heterogeneity in length-at-age (i.e., M2 and M4) had the lowest AIC values of the seven competing models for both the NEFSC and NEAMAP datasets (Table 2). Likelihood-ratio tests treating regional heterogeneity as the additional component in the full model compared to the null models (i.e., θ_A = M4 and θ_0 = M3) revealed a significant difference in parameters estimated by the two competing models at a significant level of $\alpha = 0.0001$ (Table 3).

Furthermore, standard deviations of the three most robust spatially heterogeneous models were much higher for the random effects of region than those for year (Table 4). This indicates that the random effect of region on parameters explained more of the variance in length-at-age than the random effect of year.

Among the two northern surveys, heterogeneous models that integrated random effects on two length parameters (i.e., L_∞ and *k*) were more robust than those that considered only the

random effects on one (i.e., L_∞; Table 2). Two-parameter models had lower Akaike differences (Δ_i, Table 3) from the best-fitting model (i.e., M4 $_{L\infty,k}$) than did one-parameter mixed-effects models fit to data from the NEFSC and NEAMAP surveys. In addition, LRTs considering the parameter *k* as the extra factor in the full versus reduced model (e.g., θ_A = M2 $_{L\infty,k}$ and θ_0 = M2 $_{L\infty}$) showed significant variation in parameter estimates produced by the two models in both spatially and temporally integrated length-at-age models (Table 3). One exception to the AIC and LRT statistics supporting two-parameter over one-parameter mixed-effects models was Model 3 for the NEFSC dataset. In this instance, the one-parameter model fit the data better than the two-parameter model, and the LRT comparing the two models failed to reject the null hypothesis that there is no significant difference in parameter estimates between the two (Table 3). This result is likely due to very little temporal variation observed for the growth rate parameter (*k*) in length-at-age for this survey.

In both the NEFSC and NEAMAP surveys, temporal as well as spatial variation was prominent in length-at-age models. Models incorporating both spatial and temporal heterogeneity (M4) produced the lowest AIC values for both datasets (Table 2). Furthermore, all heterogeneous mixed-effects models fit the data better than the standard homogeneous model (M1; Table 2). However, in comparison to the regional variation in length-at-age seen in the spatially and temporally incorporated model (M4; Figure 5), variation among years was much less pronounced in the northern datasets (Figure 7). This outcome is reflected in the regional and annual trends observed among L_∞ and *k* parameter estimates produced by Model 4. For both surveys, maximum length parameter estimates (L_∞) produced by models incorporating both spatial and temporal heterogeneity increased among regions from south to north (Figure 6). Corresponding growth rate parameter estimates (*k*) decreased proportionally. In contrast, annual

estimates displayed much less variation within each survey and appeared to change randomly from year to year (Figure 8).

Like the northern surveys, the southern SEAMAP survey also displayed stronger spatial than temporal variation. In this survey, spatially explicit length-at-age models were more robust than mixed-effects models that integrated temporal heterogeneity, as well as those that integrated both spatial and temporal heterogeneity, as based on AIC statistics (Table 2). Additionally, standard deviations of the random effect of region on parameters from the three most robust models were higher when grouped by region than by year (Table 4). This outcome suggests that a higher amount of variation in length estimates is explained by spatial rather than temporal variation.

Unlike the northern surveys, however, the LRTs treating regional heterogeneity as the additional component in the full model compared to the null (i.e., θ_A = M4 and θ_0 = M3) did not reveal a significant difference in parameters estimated by the two competing models (Table 3). The same outcome held true when considering the LRTs treating the additional parameter (*k*) and annual heterogeneity as the extra components in the full models (e.g., θ_A = M2 $_{L\infty,k}$ and θ_0 = M2 $_{L\infty}$; θ_A = M4 and θ_0 = M2). The only significant difference in model parameters was seen in the added components of parameter *k* in the temporally integrated model (i.e., θ_A = M3 $_{L\infty,k}$ and θ_0 = M3 $_{L\infty}$) and annual variation in the two-parameter model (e.g., θ_A = M4 $_{L\infty,k}$ and θ_0 = M2 $_{L\infty,k}$). These LRT results suggest that there is a small annual variation in length-at-age (particularly on the *k* parameter) that is masked by a slightly larger, but still relatively small spatial variation of L_∞.

Overall, the SEAMAP survey displayed the least spatial and temporal heterogeneity among the four datasets. While this heterogeneity was obviously present (as evidenced by the

better goodness-of-fit of all mixed-effects models than of the homogeneous model shown in Table 2), it was much less distinct than the heterogeneity displayed in the other surveys. The top three most robust models produced for this dataset had much lower standard deviations of random effects compared to the three other datasets, indicating that less of the variance in length data from the southern survey is explained by region or year (Table 4). Also, despite the prominence of spatial over temporal heterogeneity purported by the mixed-effect model results, the spatial variation in length-at-age is least noticeable for SEAMAP among the four surveys (Figure 5). Finally, there was little observable change in parameter estimates produced by Model 4 among either regions or years (Figures 6 and 8).

These inconsistencies are somewhat unexpected for the SEAMAP survey. As the southern survey samples from a larger area than those sampled by the two northern surveys, one would expect spatial variation in length-at-age to be much more prominent. The same goes for temporal variation, as SEAMAP is also tied with NEFSC as the longest-running survey. It may be that spatial and temporal trends in length-at-age are confounded in this dataset due to the high unevenness of sampling effort across both regions and years (Figures 3 and 4).

The survey with the smallest sampling area (ChesMMAP) was the only survey in which temporal length-at-age trends were much more prominent than spatial trends. As in the other three surveys, the lower AIC values of all mixed-effects models (particularly Model 4 which incorporated both region and year as random effects) in comparison to the standard model (M1) suggest a strong influence of both spatial and temporal heterogeneity on length-at-age (Table 2). In contrast to the other surveys, models incorporating temporal heterogeneity were more robust than those incorporating only spatial heterogeneity for ChesMMAP.

Likelihood-ratio tests that treated temporal heterogeneity as the additional component in the full model compared to the null (i.e., θ_A = M4 and θ_0 = M2) exhibited a significant difference in parameters estimated by the two competing models (Table 3). However, the same was true of LRTs that considered region as the extra factor in the full model (i.e., θ_A = M4 and θ_0 = M3), as well as those that considered the second parameter *k* as the extra factor (e.g., θ_A = M2 $_{L\infty,k}$ and θ_0 = M2 $_{L\infty}$). The variation in length-at-age parameters explained by temporal heterogeneity was higher only for the third most robust model for the dataset, which incorporated only temporal heterogeneity (M3; Table 4).

While annual variation in length-at-age appeared to be highest for ChesMMAP among the four surveys (Figures 7 and 8), regional variation and trends were more distinct than temporal heterogeneity within this survey (Figures 5 and 6). As this survey only sampled the Chesapeake Bay, a very small area in relation to the sampling areas of the other three surveys, one would expect spatial variation to be very small or unnoticeable. However, sampling effort for this survey was strongly concentrated in the two southern-most regions (Figure 3). Additionally, one must consider the second most prominent difference in this survey from the others, the fact that the Chesapeake Bay is an estuarine system with environmental conditions which greatly vary among its regions.

In all four surveys, spatial and temporal trends were consistent among the spatially, temporally, and spatially and temporally integrated length-at-age mixed-effects models. However, trends in parameters estimated in the regionally and annually integrated models (M4) were scaled differently than when region and year were considered separately (M2 and M3). For example, when examining parameter estimates produced by the three mixed-effects models for the NEAMAP survey, there appeared to be more variation in L_∞ and *k* among years than regions

in the respective temporally and spatially distinct models (M2 and M3; Figure 9). When we consider L_∞ and k estimates from the spatially and temporally integrated model (M4), however, regional variation remained the same and appeared to be much higher than variation among years. This is due to the scaled random effects of year in the spatially and temporally integrated model, which reveals that annual variation in L_∞ and k is much less than the regional variation present in this dataset. Furthermore, the homogeneous estimates of L_∞ and k, which both appeared to be rough averages of the year-specific estimates produced by the temporal model (M3), were now higher (L_∞) and lower (k) than the heterogeneous estimates for all of the years in the spatial and temporal model (M4). This outcome highlights why the incorporation of both spatial and temporal heterogeneity in length-at-age is critical, as the homogeneous parameter estimates do not describe any of the years sampled in the dataset.

Weight-at-Age

Spatial and temporal heterogeneity also played a significant role in weight-at-age. Mixed-effects models incorporating regional and annual variation fit the data better in all four surveys (Table 7). Spatially and temporally integrated models (M4) were the most robust. In the NEFSC, NEAMAP, and SEAMAP surveys, models which considered the random effects of region and year on two weight parameters had the lowest AIC values, whereas the one-parameter model had the lowest AIC in the ChesMMAP survey (Table 8).

The log weight-at-age curve produced by the homogeneous model (M1) appeared to be a rough average of the regional curves produced by the heterogeneous model (M4) for both of the northern surveys (NEFSC, NEAMAP; Figure 10). While this outcome would initially appear to support the assumption that the standard homogeneous model produced an average estimate of

log weight-at-age that represents the population as a whole, a closer look at the parameters produced by heterogeneous and homogeneous models indicates otherwise. The average W_∞ and t_0 estimates produced by the heterogeneous model (M4) were less than half those produced by the homogeneous model (M1) for the NEAMAP survey, while the average k parameter was more than doubled (Table 10).

We can explore the variation in these parameters by comparing the region-specific parameters W_∞ and k from the heterogeneous model (M4) to those produced by the homogeneous model (M1; Figure 11). In both the NEFSC and NEAMAP surveys, W_∞ changes very little among the five southern regions and then increases in the northern regions. In the NEFSC survey, the W_∞ estimate from Model 1 appears to be an approximate average of the Region 5 and Region 6 estimates from Model 4. This means that the homogeneous estimate is higher than those of each of the five southern regions and lower than those for the two northern regions. Thus, while initially appearing to provide an averaged estimate for the population, the integration of spatial heterogeneity in the mixed-effects model reveals that the homogeneous estimate does not really describe the population in any region of the survey.

This issue is displayed more obviously when looking at the standard log weight-at-age curve (M1) against the spatially heterogeneous (M4) curves in the SEAMAP and ChesMMAP surveys (Figure 10). The average W_∞ estimate produced by the heterogeneous model for the southern survey is more than twice that produced by the homogeneous model (Table 10). The W_∞ estimate from Model 1 is actually lower than the estimates for any of the regions produced by Model 4, and the k estimate is higher (Figure 11). The opposite is seen in the ChesMMAP survey, where homogeneous W_∞ is higher and k is lower than all regional estimates.

The log weight-at-age curve produced by the standard homogeneous model (M1) is much lower than any of the annual curves produced by the spatially and temporally integrated model (M4; Figure 12). By comparing the homogeneous W_∞ estimate to year-specific W_∞ estimates, we see that the "averaged" estimate (M1) is lower than those produced for any of the 12 years sampled by the NEFSC survey (Figure 13). In the NEAMAP survey, however, the W_∞ estimated by Model 1 is higher than those estimated for any of the years in Model 4. The *k* estimates produced by the homogeneous model were lower in both surveys than any produced by the heterogeneous model.

At first glance, the log weight-at-age curve produced by the standard homogeneous model (M1) for the SEAMAP and ChesMMAP surveys appeared to be an average of the annual curves produced by the heterogeneous model (M4; Figure 12). This is similar to what was observed regarding spatial variation in the northern surveys. However, closer inspection of year-specific parameter estimates shows otherwise. The homogeneous-model estimate of W_∞ (M1) is lower than all of the annual estimates produced by the heterogeneous model (M4) for the SEAMAP survey and higher for the ChesMMAP survey (Figure 13). Homogeneous *k* parameters were higher than heterogeneous annual *k* parameters for the southern dataset and lower for the Chesapeake Bay dataset. Thus, the estimates produced by the homogeneous model, which should theoretically be an average of the year-specific estimates, do not describe any of the years sampled by these surveys.

As in the length-at-age models, the two northern surveys (NEFSC and NEAMAP) displayed more spatial rather than temporal variation. In both surveys, spatially incorporated models had lower AIC values than models incorporating only temporal heterogeneity in log weight-at-age (Table 7). Additionally, higher standard deviations of random effects in the three

most robust models for the northern surveys showed that a greater amount of variance in log weight was explained by regional heterogeneity than by annual changes (Table 9).

This is not to say that no temporal heterogeneity was observed in the NEFSC and NEAMAP datasets. Mixed-effects models incorporating spatial, temporal, and both spatial and temporal variation in log weight produced lower AIC values and therefore better goodness-of-fit to the data than the standard homogeneous model (M1) that incorporated no such variation (Table 7). Also, while LRTs that considered region as the extra component in the full over the reduced model (i.e., θ_A = M4, θ_0 = M3) revealed significant differences in parameters estimated between the two, LRTs considering year as the additional component (i.e., θ_A = M4, θ_0 = M2) produced similar results (Table 8). This result suggests that both regional and temporal variation have a strong influence on log weight for these two northern surveys.

Log weight-at-age curves produced by models incorporating both spatial and temporal random effects on weight parameters displayed much more regional variation than either the southern or Chesapeake surveys (Figure 10). Regional trends in parameter estimates of W_∞ and k produced by Model 4 (assuming both spatial and temporal heterogeneity) were much more distinguishable for the NEFSC and NEAMAP surveys (Figure 11). In both surveys, maximum log weight (W_∞) increased proportionally to the decrease in growth rate (k) from south to north.

Annual trends in log weight parameters produced by spatially and temporally heterogeneous models for NEFSC and NEAMAP were much more distinct than those observed in length parameters (Figures 13 and 8). This was also true of the SEAMAP and ChesMMAP surveys. The southern and Chesapeake Bay datasets displayed annual variations in weight-at-age more prominently than regional variation. This is evidenced by the lower AIC statistics produced

by temporally integrated models (i.e., M4 and M3) than those produced by models integrating only spatial heterogeneity (M2; Table 7).

However, differences in the roles of spatial and temporal variation in log weight-at-age were less pronounced for these two surveys than the northern surveys. In mixed-effects models that incorporated both spatial and temporal heterogeneity (M4), less variation in log weight was explained by the random effect of year than by region on the same parameters (Table 9). Conversely, in the mixed-effects models which only incorporated temporal heterogeneity (M3), more variation in log weight was explained by the random effect of year than was explained by either year or region in Model 4.

LRTs from these surveys indicated that parameter estimates were significantly different among full models incorporating the additional effects of both region (i.e., θ_A = M4, θ_0 = M3) and year (i.e., θ_A = M4, θ_0 = M2; Table 8). This result suggests that both spatial and temporal heterogeneity in these datasets influenced log weight-at-age, as in the NEFSC and NEAMAP datasets. Unlike the northern surveys, however, the southern and Chesapeake surveys showed a larger disparity between the one- and two-parameter models. In the SEAMAP survey, LRTs that treated the parameter *k* as the additional component (e.g., θ_A = M2 $_{W\infty,k}$, θ_0 = M2 $_{W\infty}$) found no significant difference between the one- and two-parameter weight models (Table 8). Whereas the same LRTs did reveal a significant difference between these models in the ChesMMAP survey, LRTs which treated region and year as the additional component for the two-parameter models (e.g., θ_A = M4 $_{W\infty,k}$, θ_0 = M2 $_{W\infty,k}$) did not. This difference contrasts the LRTs for the same survey that treated region and year as the additional component for the one-parameter models (e.g., θ_A = M4 $_{W\infty}$, θ_0 = M2 $_{W\infty}$) and reveals a significant difference in parameters estimated from the two models.

As in length-at-age, spatial and temporal trends were consistent among the spatially, temporally, and spatially and temporally integrated log weight-at-age mixed-effects models. Trends in parameters estimated in the regionally and annually integrated models (M4) were again scaled differently than when region and year were considered separately (M2 and M3). For example, when examining parameter estimates produced by the three mixed-effects models for the NEAMAP survey, there appeared to be more variation in W_∞ and k among years than regions in the respective temporally and spatially distinct models (M2 and M3; Figure 14). When we consider W_∞ and k estimates from the spatially and temporally integrated model (M4), however, regional variation remains the same and appears to be much higher than variation among years. This reveals that annual variation in W_∞ and k is much less than the regional variation present in this dataset. Furthermore, the homogeneous estimates of W_∞ and k, which both appeared to be rough averages of the year-specific estimates produced by the temporal model (M3), are now higher (W_∞) and lower (k) than the heterogeneous estimates for all of the years in the spatial and temporal model (M4).

Maturity-at-Age

Spatial and temporal variation displayed strong impacts upon maturity-at-age models. The importance of heterogeneity on Atlantic Weakfish maturity was evidenced by the minimized AIC values produced by mixed-effects models incorporating spatial, temporal, and both spatial and temporal variation (M2, M3, and M4) in comparison to the standard homogeneous model (M1) for both females and males (Table 11). Specifically, models integrating both spatial and temporal variation in maturity-at-age were most robust for both sexes (M4; Table 11).

Female and male maturity-at-age parameters estimated by the standard homogeneous model (M1) were most similar to those estimated by the spatially homogeneous model (M2; Figure 15). The average age at which 50% of the fish are mature (β) was nearly identical for these two models (Table 12; dashed lines in Figure 15). The temporally integrated model (M3) also produced β values similar to those produced by Models 1 and 2, although slightly lower in both females and males. The β value produced by Model 4, which incorporated both spatial and temporal heterogeneity and had the best fit to the data, was higher than those produced by the other three models. This result implies that models incorporating both spatial and temporal variation predict slower maturation for both female and male Weakfish than any of the three other candidate models.

Figure 16 highlights the differences between the most robust maturity models incorporating spatial and temporal heterogeneity (M4) and the least robust homogeneous models (M1) for female and male Weakfish. Female and male maturity displayed more variation among years than regions for the heterogeneous model. Female maturity estimated by the homogeneous model, which theoretically should represent an average among regions and years, was higher than the maturity estimates for the majority of regions and years sampled by the ChesMMAP survey. Male maturity estimated by the homogeneous model was higher than the maturity estimates for all regions and years produced by the heterogeneous model.

Like the length-at-age and log weight-at-age models, maturity-at-age for the ChesMMAP survey displayed stronger temporal than spatial trends. Likelihood ratios tests treating both region (i.e., θ_A = M4, θ_0 = M3) and year (i.e., θ_A = M4, θ_0 = M2) as the additional component in the full model revealed a significant difference between the null and full-model parameters for both female and male Weakfish, suggesting that maturity-at-age in the ChesMMAP dataset has

significant spatial and temporal variation (Table 11). However, a higher percentage of variation in maturity was explained by the random effect of year than region in the three most robust female and male maturity-at-age models (Table 13). Additionally, mixed-effects models that considered only temporal heterogeneity outperformed those that considered only spatial heterogeneity for both sexes (Table 11).

Spatial and temporal trends in maturity-at-age were consistent among the three heterogeneous models. However, these trends were scaled differently in models that considered regional and annual variation separately than in those that integrated both. Female maturity parameters decreased slightly from Region 1 to Region 3, and then increased towards the northern regions of the Chesapeake Bay (Figure 17a, c). When only spatial variation was considered (M2), these changes from region to region were less than those observed in Model 4, which considered both spatial and temporal variation. Temporal trends in female maturity parameters, on the other hand, appeared to be the same when modelled alone (M3) and in conjunction with regional variation (M4; Figure 17b, d). In both models, α peaked in 2004 and 2008, with low values in 2006 and 2009. The parameter βt showed subsequent peaks in 2004 and 2009, with a trough in 2008.

The scale of spatial trends in male maturity also differed among mixed-effects models. When regional variation alone was integrated (M2), male maturity parameters exhibited more drastic changes from region to region (Figure 18a). The general trend was similar to that seen for females, in which parameters decreased from Region 1 to Region 3 and thereafter increased in the northern areas of the Chesapeake Bay. Converse to the female trends, however, these spatial changes in maturity parameters were less distinguished in the model integrating both spatial and temporal variation (M4) than in the model which only integrated spatial variation (M2; Figure

18a, c). Temporal trends seemed to be scaled similarly regardless of model, as in female maturity (Figure 18b, d). In males, α peaked in 2004 and 2007, with low values in 2006 and 2011. As in females, the parameter βt displayed a bimodal trend, with peaks in 2004 and 2010 and a trough in 2006.

2.5 Discussion

In this study, I used mixed-effects models to evaluate the common assumption of homogeneity in life-history models used in fisheries stock assessment. Spatially and temporally integrated mixed-effects models revealed significant trends in length, weight, and maturity of Atlantic Weakfish across regions and years. Heterogeneous mixed-effects models incorporating spatial and temporal variation produced life-history parameter estimates that were better fit to the data than those produced by the standard homogeneous models in all analyses. Furthermore, life-history parameter estimates produced by standard homogeneous models, which theoretically should provide average estimates across all regions and years, most often did not match mean parameter estimates produced by spatially and temporally heterogeneous models. These findings discredit the assumption that the standard homogeneous model produces an average estimate of life history that represents the population as a whole and emphasize the importance of incorporating spatial and temporal heterogeneity into future fishery stock assessments.

In many cases, the homogeneous parameter estimate was much higher or lower than all regional and annual estimates produced by the heterogeneous model. This outcome was observed for length parameters L_∞ and k across both regions and years in the SEAMAP survey (Figures 6 and 8). It was also seen in log weight-at-age parameters across regions in the SEAMAP and ChesMMAP surveys and across years in the NEFSC, NEAMAP, and SEAMAP surveys (Figures

11 and 13). In these cases, the "averaged" growth estimates produced by the standard homogeneous model did not reliably describe any of the spatially or temporally distinct growth estimates produced by the heterogeneous model incorporating both regional and annual heterogeneity.

Spatial trends in growth were consistent among heterogeneous length- and weight-at-age models. In the NEFSC and NEAMAP surveys, growth rate decreased and maximum size increased from south to north (Figures 6 and 11). As these two northern surveys mostly sampled from North Carolina to New York, it is unsurprising that they displayed nearly identical spatial trends. The ChesMMAP survey, which also sampled within this range but only in the Chesapeake Bay, also exhibited a general decrease in growth rate and increase in maximum size from south to north. Spatial variation in this survey was much less conspicuous than in the NEFSC and NEAMAP survey. This result is likely due to the much smaller area sampled by the ChesMMAP survey as well as the fact that the Chesapeake Bay is an estuary and its regions are distinguished more by varying levels of fresh and saltwater mixing than by latitude, as in the other two northern surveys. SEAMAP growth displayed the least spatial variation among the four surveys, despite sampling from an area approximately as large as those sampled by the NEFSC and NEAMAP surveys.

These spatial trends observed in Atlantic Weakfish are consistent with many observations that scientists have already recorded for this species. First, the greatest abundance of Weakfish occurs between New York and North Carolina (Mercer 1985). This area has the optimal environmental conditions for Atlantic Weakfish growth, which helps to explain the much more prominent regional trend of increasing maximum size and decreasing growth rate seen in the northern datasets (i.e., NEFSC, NEAMAP, and ChesMMAP). These trends are consistent with

previous estimations of spatial variation in Atlantic Weakfish growth between Cape Cod, Massachusetts, and Cape Fear, North Carolina (Shepherd and Grimes 1983).

The SEAMAP survey, however, sampled outside of the range of highest Atlantic Weakfish abundance. The decreased abundance of Weakfish in their southern range (North Carolina to Florida) is likely due to the intrinsic and extrinsic factors influencing population dynamics (such as prey availability, variable energetic costs of migration and spawning, temperature, and fishing effort) that differ greatly from northern conditions. These differences in environmental and ecological conditions in the south help to explain the vast contrast in growth parameters observed between Weakfish growth modeled from the northern and southern datasets.

An additional complicating factor in the south that is not present in the north is the distribution overlap with sand seatrout (*Cynoscion arenarius*). This similar species hybridizes with Weakfish in Florida waters where the Atlantic Weakfish distribution extends into the Gulf of Mexico, to which sand seatrout are generally restricted (Tringali et al. 2011). This co-occurrence and hybridization of sand seatrout and Weakfish confuses the identification of both species, which are extremely similar in appearance, especially at young ages. Furthermore, this hybridization may affect expression of life-history traits.

Finally, the seafloor of the southern range of Atlantic Weakfish has a much higher reef coverage than the northern range. This high reef density makes the south a mostly untrawlable habitat, as nets are likely to tear on the high-profile bottom structure as well as damage the reef. Since the SEAMAP survey, like the other surveys used in this study, collected fish by trawling, this causes the sampling effort in this survey to focus mainly on the northern-most region along the coast of North Carolina, where Weakfish are more abundant and fewer reefs are present.

Because of this issue, as well as the aforementioned problems of less favorable environmental conditions and hybridization, southern data are often excluded from demographic analyses of Atlantic Weakfish.

Sources of temporal heterogeneity in Atlantic Weakfish are much more variable. Weather events, fishing pressure, and pollution can change on a daily basis. When such temporal influences build over longer spans of time, they can cause dramatic changes in fish populations from year to year. In addition, these fluxes may cause delayed responses in fish life history. All of these factors collectively seem to cause temporal variations to be generally smaller and more random than spatial variations. This was observed for length- and growth-at-age for all four datasets used in this study (Figures 8 and 13).

Because of the different spatial and temporal factors influencing the different datasets, either regional or temporal heterogeneity was more prominent in each of the four surveys. Growth models from the two northern surveys (NEFSC and NEAMAP) that sampled from large areas of high Atlantic Weakfish abundance were more strongly influenced by regional than annual variation. The SEAMAP survey had more mixed results, with regional variation affecting length-at-age more than annual variation and temporal heterogeneity impacting weight-at-age more than spatial heterogeneity. This discrepancy is likely due to the many factors that complicate sampling effort and influence spatial and temporal heterogeneity for this dataset.

The ChesMMAP survey, which sampled a relatively small area, displayed a stronger sensitivity to temporal variation in maturity as well as growth. The response of maturity-at-age to changes in growth rate has become a frequently studied reaction norm (Morey and Reznick 2000; Day and Rowe 2002; Morita and Fukuwaka 2007). In this study, I found that spatially and

temporally integrated models displayed a bimodal trend in female and male maturity parameter estimates that were reflected in length parameter estimates (βt and L_∞; Figures 17, 18, and 8).

Spatial and temporal trends were consistent among spatially, temporally, and spatially and temporally integrated length-at-age mixed-effects models. However, trends in parameters estimated in the regionally and annually integrated models (M4) were scaled differently than when region and year were considered separately (M2 and M3). The scaled effects of spatial and temporal variation in life history observed in Model 4 (which incorporated both) were more representative of the relative influence of spatial versus temporal variation in each dataset. For example, when comparing mixed-effects models of length- and weight-at-age from the NEAMAP survey, there appears to be more variation in parameters among years than regions in the respective temporally and spatially distinct models (M2 and M3; Figures 9 and 14). When we consider parameter estimates from the spatially and temporally integrated model (M4), however, regional variation remains the same and appears to be much higher than variation among years. This is due to the scaled random effects of year in the spatially and temporally integrated model, which reveals that annual variation in growth parameters is much less than the regional variation present in this dataset.

The varying influence of scaled regional and annual effects among mixed-effect models was also observed in the maturity analyses for both female and male fish sampled in the ChesMMAP survey. When only spatial variation was considered (M2), changes in maturity parameters from region to region were less distinct than those observed in Model 4, which considered both spatial and temporal variation (Figures 17 and 18). Temporal trends in maturity parameters, on the other hand, appeared to be the same when modelled alone (M3) and in conjunction with regional variation (M4).

When comparing the goodness-of-fit of models to life-history data from all four surveys, spatially and temporally incorporated mixed-effects models were more robust than standard homogeneous models in length, weight, and maturity analyses. This generality suggests that the standard approach has more bias than heterogeneous models and that life-history models incorporating spatial and temporal heterogeneity provide a more accurate description of the Atlantic Weakfish population. Of the competing mixed-effects models, those which incorporated both spatial and temporal variation (M4) in growth and maturity tended to be most robust. These models provided two main advantages over other candidate mixed-effects models. First, the combined random effects of region and year explained more variance in life-history data than models that considered spatial and temporal heterogeneity separately. Integrating both regional and annual variation also supplied scaled random effects of space and time that allows the comparison of these different sources of heterogeneity within each model.

In addition to the inclusion of spatial and temporal heterogeneity, the number of growth parameters incorporated in mixed-effects length- and weight-at-age models also affected model performance among the seven candidate models. In a study of growth in northern abalone (*Haliotis kamtschatkana*), Zhang et al. (2009) found that modeling variability in both maximum size and growth rate parameters resulted in better-fitting models, although modeling variation in just maximum size was sufficiently good. Models that allow for variability in just maximum size result in substantially less biased estimates than in growth rate alone (Eveson et al. 2007; Zhang et al. 2009). The results of this study support the assertion by Zhang et al. (2009) that models incorporating variability in both maximum size and growth rate parameters are more robust than one-parameter models. Mixed-effects models that integrated variation in both L_∞ and k for

length-at-age and W_∞ and k for weight-at-age provided better goodness-of-fit than one-parameter models in three of the four surveys.

The differences among growth and maturity estimates resulting from the various candidate models implies differing levels of bias from using one model over another when assessing Atlantic Weakfish. Particularly, the standard homogeneous models can underestimate the uncertainty caused by growth or maturity variation over time or space. Ignoring this variation in management of the fishery may lead to overfishing during periods or in areas of low productivity, or to underfishing in high-productivity situations. Furthermore, overlooking other sources of individual variability in growth and maturity can compound the bias of estimates used in productivity analyses and management strategies. The residual random error of the models presented in this study might be due to sampling selectivity, ageing error, levels of predator-prey populations, or other influential factors.

Mixed-effects models enable us to consider these possible random errors in fisheries analyses by incorporating different suspected sources of individual variability in commonly used fisheries models. The approach presented here can be expanded to evaluate any source of individual variability in any life-history analysis, not only of Atlantic Weakfish, but of any fish species. This does not necessitate, however, that the best-performing model in one analysis will also be the best-performing model in another analysis. Additionally, some effects can be over or underestimated when modeled independently versus together. As evidenced by the results of this study, model performance is highly variable among datasets, even for the same species. The best approach to determine which model is most appropriate for a given case is to compare a set of candidate models for that case and to use Akaike Information Criterion or similar methods to select the best-fitting model from within that set of candidate models. However, this approach

does not work if there are no good models among the candidate models to be discovered by any model-selection methodology. Careful consideration should therefore be made as to which models to include in an analysis. As statistical software continues to improve, it is becoming increasingly easy to incorporate multiple sources of individual variability through the use of multi-model inference with mixed-effects models for fish life-history analyses.

Atlantic Weakfish subpopulations display distinct spatial and temporal trends in life history. Length, weight, and maturity vary from region to region and year to year. However, the standard approach used by many stock assessment modelers does not incorporate or even detect this heterogeneity in life history. The results of this study indicate that standard homogeneous models which assume no spatial or temporal heterogeneity mask regional and annual trends in length, weight, and maturity of Atlantic Weakfish that are much more predictive and insightful of the stock. Furthermore, I found that spatially and temporally integrated mixed-effects models fit life-history data from four fishery-independent surveys much better than standard homogeneous models in all analyses. Ultimately, spatially and temporally integrated life-history models were more informative and robust than standard homogeneous models and are strongly recommended for use in future stock assessments.

2.6 Literature Cited

Akaike, H., 1974. A new look at the statistical model identification. IEEE Transactions on Automatic Control 19: 716-723.

Alós, J., Palmer, M., Alonso-Fernández, A., and Morales-Nin, B. 2010. Individual variability and sex-related differences in the growth of *Diplodus annularis* (Linnaeus, 1758). Fisheries Research 101: 60-69.

Bates, D., Maechler, M., Bolker, B., and Walker, S. 2015. Fitting linear mixed-effects models using lme4. Journal of Statistical Software 67(1): 1-48.

Beacham, T. D. 1983. Growth and maturity of Atlantic cod (*Gadus morhua*) in the southern Gulf of St. Lawrence. Canadian Technical Report of Fisheries and Aquatic Sciences No. 1142, Department of Fisheries and Oceans, Fisheries Research Branch, Pacific Biological Station.

Beverton, R. J. and Holt, S. J. 1957. On the dynamics of exploited fish populations. Fisheries Investigations London Series 2, 533 p.

Bonzek, C. F., Gartland, J., Lange, J. D. Jr., and Latour, R. J. 2009. Northeast Area Monitoring and Assessment Program (NEAMAP) Mid-Atlantic Nearshore Trawl Program Final Report 2005-2009. Atlantic States Marine Fisheries Commission, 341 p.

Bonzek, C. F., Gartland, J., and Latour, R. J. 2011. Data collection and analysis in support of single and multispecies stock assessments in Chesapeake Bay: The Chesapeake Bay Multispecies Monitoring and Assessment Program (ChesMMAP). Virginia Institute of Marine Science, Gloucester Point, Virginia.

Charnov, E. L. 1993. Life History Invariants. Oxford University Press, Oxford.

Eldridge, P. J. 1988. The southeast area monitoring and assessment program (SEAMAP): A state-federal-university program for collection, management, and dissemination of fishery-independent data and information in the southeastern United States. Marine Fisheries Review 50(2):29-39.

Escati-Peñaloza, G., Parma, A. M., and (Lobo) Orensanze, J. M. 2010. Analysis of longitudinal growth increment data using mixed-effects models: individual and spatial variability in a clam. Fisheries Research 105: 91-101.

Eveson, J. P., Polacheck, T., and Laslett, G. M. 2007. Consequences of assuming an incorrect error structure in von Bertalanffy growth models: a simulation study. Canadian Journal of Fisheries and Aquatic Sciences 64: 602-617.

Fitzmaurice, G., Laird, N., and Ware, J. 2004. Applied Longitudinal Analysis. John Wiley & Sons, Hoboken, New Jersey.

Gulland, J. A. 1983. Fish Stock Assessment: A Manual of Basic Methods. John Wiley & Sons, Chichester, UK.

Haddon, M. 2001. Modelling and Quantitative Methods in Fisheries. Chapman &Hall/CRC, Washington, DC, 406 p.

Hart, D. R. and Chute, A. S. 2009. Estimating von Bertalanffy growth parameters from growth increment data using a linear mixed-effects model, with an application to the sea scallop *Placopecten magellanicus*. ICES Journal of Marine Science 66: 2165-2175.

Healy, M. C. 1991. Life history of Chinook salmon (*Oncorhynchus tshawytscha*). *In* Pacific Salmon: Life Histories. *Edited by* C. Groot and L. Margolis. UBC Press, Vancouver, B. C. p. 311-394.

Heath, D. D., Fox, C. W., and Heath, J. W. 1999. Maternal effects on offspring size: variation through early development of Chinook salmon. Evolution 53(5): 1605-1611.

Helser, T. E., and Lai, H. L. 2004. A Bayesian hierarchical meta-analysis of fish growth, with an example for North American largemouth bass, *Micropterus salmoides*. Ecological Modeling 178(3-4): 399-416.

Helser, T. E., Stewart, I. J., and Lai, H. L. 2007. A Bayesian hierarchical meta-analysis of growth for the genus *Sebastes* in the eastern Pacific Ocean. Canadian Journal of Fisheries and Aquatic Sciences 64: 470-485.

Hutchings, J. A., and Myers, R. A. 1994. Timing of cod reproduction: interannual variability and the influence of temperature. Marine Ecology Progress Series 108(5): 21-31.

Isaac, V. J. 1990. The accuracy of some length-based methods for fish population studies. International Centre for Living Aquatic Resources Management, Manila, Philippines, and Kuwait Institute for Scientific Research, Safat, Kuwait. p. 217-238.

Jensen, A. L. 1998. Simulation of relations among fish life history parameters with a bioenergetics-based population model. Canadian Journal of Fisheries and Aquatic Sciences 55(2): 353-357.

Jiao, Y., Rogers-Bennett, L., Taniguchi, I., Butler, J., and Crone, P. 2010. Incorporating temporal variation in the growth of red abalone (*Haliotis rufescens*) using Bayesian growth models. Canadian Journal of Fisheries and Aquatic Sciences 67(4): 730-742.

Jonsson, B., Jonsson, N., and Finstad, A. G. 2012. Effects of temperature and food quality on age and size at maturity in ectotherms: an experimental test with Atlantic salmon. Journal of Animal Ecology 82: 201-210.

Johnston, R. 2012. NEFSC multispecies bottom trawl survey. Ecosystems Survey Branch, NOAA, Woods Hole, Massachusetts: 17 p.

Kimura, D. K. 2008. Extending the von Bertalanffy growth model using explanatory variables. Canadian Journal of Fisheries and Aquatic Sciences 65: 1879-1891.

Krohn, M., Reidy, S., and Kerr, S. 1997. Bioenergetic analysis of the effects of temperature and prey availability on growth and condition of northern cod (*Gadus morhua*). Canadian Journal of Fisheries and Aquatic Sciences 54(S1): 113-121.

Lowerre-Barbieri, S. K., Chittenden, M. E., and Barbieri, L. R. 1996. The multiple spawning pattern of Weakfish in the Chesapeake Bay and Middle Atlantic Bight. Journal of Fish Biology 48: 1139-1163.
McCulloch, C. E., Searle, S. R., and Neuhaus, J. M. 2008. Generalized Linear and Mixed Models, 2nd edition John Wiley & Sons, Hoboken, New Jersey.

McGurk, M. D. 1996. Allometry of marine mortality of Pacific salmon. Fisheries Bulletin 94(1): 77-88.

Mercer, L. P. 1985. Fishery Management Plan for the weakfish, (*Cynoscion regalis*) fishery. Fisheries Management Report No. 7 Atlantic States Marine Fisheries Commission. North Carolina Department of Natural Resources and Community Development, Division of Marine Fisheries Special Scientific Report No. 46, 129 p.

Morey, S. and Reznick, D. 2000. A comparative analysis of plasticity in larval development in three species of spadefoot toads. Ecology 81: 1736-1749.

Morita, K. and Fukuwaka, M. 2007. Why age and size at maturity have changed in Pacific salmon. Marine Ecology Progress Series 335: 289-294.

Nye, J. A. 2002. Plastic reproductive characteristics in Weakfish (*Cynoscion regalis*): fluctuations in response to changes in stock size. Master's thesis, Delaware University, Newark, Delaware.

Paperno, R., Targett, T. E., and Grecay, P. A. 2000. Spatial and temporal variation in recent growth, overall growth, and mortality of juvenile Weakfish (*Cynoscion regalis*) in Delaware Bay. Estuaries 23(1):10-20.

Pilling, G. M., Kirkwood, G. P., Walter, S. G. 2002. An improved method for estimating individual growth variability in fish, and the correlation between von Bertalanffy growth parameters. Canadian Journal of Fisheries and Aquatic Science 59: 424-432.

Pinheiro, J. C. and Bates, D. M. 2000. Mixed-effects models in S and S-Plus. Springer-Verlag, Inc., New York.

Pinheiro, J. C. and Bates, D. M. 2002. Mixed-effects Models in S and S-Plust, second edition. Springer-Verlag, New York.

Punt, A. E., Hobday, D., Gerhard, J., and Troynikov, V. S. 2006. Modelling growth of rock lobsters, *Jasus edwardsii*, off Victoria, Australia using models that allow for individual variation in growth parameters. Fisheries Research 82: 119-130.

Pascoe, S., Bustamante, R., Wilcox, C., and Gibbs, M. 2009. Spatial fisheries management: A framework for multi-objective qualitative assessment. Ocean and Coastal Management 52:130-138.

Quinn, T. J., and Deriso, R. B. 1999. Quantitative Fish Dynamics. Oxford University Press, New York.

Quinn, T. P., Vøllestad, L. A., Peterson, J., and Gallucci, V. 2004. Influences of freshwater and marine growth on the egg size-egg number tradeoff in coho and Chinook salmon. Transactions of the American Fisheries Society 133(1): 55-65.

R Core Team 2014. R: A language and environment for statistical computing. R Foundation for Statistical Computing, Vienna, Austria.

Ricker, W. E. 1975. Computation and Interpretation of Biological Statistics of Fish Populations. Bulletin of Fisheries Research Board Canada No. 191.

Sainsbury, K. J., 1980. Effect of individual variability on the von Bertalanffy growth equation. Canadian Journal of Fisheries and Aquatic Sciences 37: 241-247.

Schaalje, G. B., Shaw, J. L., and Belk, M. C. 2002. Using nonlinear hierarchical models for analyzing annulus-based size-at-age data. Canadian Journal of Fisheries and Aquatic Sciences 59: 1524-1532.

Shepherd, G. and Grimes, C. B. 1983. Geographic and historic variations in growth of Weakfish, *Cynoscion regalis,* in the Middle Atlantic Bight. Fishery Bulletin 81(4):803-813.

Shepherd, G. and Grimes, C. B. 1984. Reproduction of Weakfish, *Cynoscion regalis*, in the New Bight and evidence for geographically specific life history characteristics. Fishery Bulletin 82: 501-511.

Shrump, D. D., Jr., and Chambers, R. C. 2003. An analysis of the frequency and duration of spawning of local Weakfish, *Cynoscion regalis*, based on age and size structure young-of-the-year from the Hudson River, New York. Section VI: 22 p. *In* J. R. Waldman & W. C. Nieder (Editors), Final Reports of the Tibor T. Polgar Fellowship Program, 2002. Hudson River Foundation, New York.

Smith, S. J., Kenchington, E. L., Lundy, M. J., Robert, G., and Roddick, D. 2001. Spatially specific growth rates for sea scallops (*Placopecten magellanicus*). In: Kruse, G. H., Bez, N., Booth, A., Dorn, M., Hillis, S., Lipcius, R., Pelletier, D., Roy, C., Smith, S. J., Witherell, D. (Editors), Spatial Processes and Management of Marine Populations. University of Alaska Sea Grant, Fairbanks, p. 211-231.

Sullivan, P., Buckel, J., and Deroba, J. 2016. Weakfish Benchmark Stock Assessment and Peer Review. Atlantic States Marine Fisheries Commission, Arlington, Virginia; 270 p.

Taylor, M. H. and Villoso, E. P. 1994. Daily ovarian and spawning cycles in Weakfish. Transactions of the American Fisheries Society 123: 9-14.

Thomas, D. L. 1971. An ecological study of the Delaware River in the vicinity of Artificial Island, Part III. The early life history and ecology of six species of drum (Sciaenidae) in the lower Delaware River, a brackish tidal estuary. Ichthyological Associates Bulletin 3: 1-105.

Tringali, M. D., Seyoum, S., Higham, M., and Wallace, E. M. 2011. A dispersal-dependent zone of introgressive hybridization between Weakfish, *Cynoscion regalis*, and sand seatrout, *C. arenarius*, (Sciaenidae) in the Florida Atlantic. Journal of Heredity 102(4): 416-432.

Trippel, E. A. 1995. Age-at-maturity as a stress indicator in fisheries. Bioscience 45(11): 759-771.

Von Bertalanffy, L. 1938. A quantitative theory of organic growth. Human Biology 10(2):181-213.

Weisberg, S. 1993. Using hard-part increment data to estimate age and environmental effects. Canadian Journal of Fisheries and Aquatic Sciences 50(6): 1229-1237.

Weisberg, S., Spangler, G., and Richmond, L. S. 2010. Mixed-effects models for fish growth. Canadian Journal of Fisheries and Aquatic Sciences 67: 269-277.

Wilk, S. J. 1979. Biological and fisheries data on Weakfish, *Cynoscion regalis* (Bloch and Schneider) NOAA Technical Report. U. S. Department of Commerce National Marine Fisheries Service, Highlands, New Jersey.

Zhang, Z., Lessard, J., and Campbell, A. 2009. Use of Bayesian hierarchical models to estimate northern abalone, *Haliotis kamtschatkana*, growth parameters from tag-recapture data. Fisheries Research 95(2-3): 289-295.

2.7 Tables and Figures

Table 1 Areas and years sampled by the four fishery-independent surveys used in this study.

	NEFSC	**NEAMAP**	**SEAMAP**	**ChesMMAP**
Years analyzed	1998-2011	2007-2013	2001-2014	2002-2012
Location	Scotian Shelf, Canada – Cape Lookout National Seashore, NC	Montauk, NY – Cape Hatteras, NC	Cape Hatteras, NC – Cape Canaveral, FL	Chesapeake Bay
Seasonal trawls	February – May; September - October	Spring and Fall	Spring, Summer, and Fall	March - November
Depth range	60'-600'+	60'-120'	N/A	10'-130'
Distance from shore	Offshore	Nearshore	Nearshore	Nearshore

Table 2 Ranking of the seven competing length-at-age models (in descending order) based on minimizing Akaike's Information Criterion for each of the four surveys.

NEFSC	NEAMAP	SEAMAP	ChesMMAP
$M4_{L\infty,k}$	$M4_{L\infty,k}$	$M2_{L\infty}$	$M4_{L\infty,k}$
$M2_{L\infty,k}$	$M2_{L\infty,k}$	$M3_{L\infty}$	$M4_{L\infty}$
$M4_{L\infty}$	$M4_{L\infty}$	$M4_{L\infty,k}$	$M3_{L\infty,k}$
$M2_{L\infty}$	$M2_{L\infty}$	$M2_{L\infty,k}$	$M3_{L\infty}$
$M3_{L\infty}$	$M3_{L\infty,k}$	$M3_{L\infty,k}$	$M2_{L\infty,k}$
$M3_{L\infty,k}$	$M3_{L\infty}$	$M4_{L\infty}$	$M2_{L\infty}$
M1	M1	M1	M1

Table 3 Comparisons of the seven length-at-age models developed for each of the four surveys, including AIC and LRT values: Akaike's Information Criterion (AIC), Akaike differences (Δ_i), Chi-square statistic (χ^2), and *P* –value (*P*).

	AIC		$LRT_{Mx:My}$		
Model	AIC	Δ_i	H_0:H_A	χ^2	P ($>\chi^2$)
NEFSC					
M1	84312	4519			
$M2_{L\infty}$	81312	1520	$M2_{L\infty}$: $M2_{L\infty,k}$	1014.9	<0.0001
$_{L\infty,k}$	80299	507	$M3_{L\infty}$: $M3_{L\infty,k}$	1	1
$M3_{L\infty}$	83722	3930	$M2_{L\infty}$: $M4_{L\infty}$	386.48	<0.0001
$_{L\infty,k}$	84253	4460	$M3_{L\infty}$: $M4_{L\infty}$	2796.4	<0.0001
$M4_{L\infty}$	80928	1135	$M2_{L\infty,k}$: $M4_{L\infty,k}$	510.84	<0.0001
$_{L\infty,k}$	79792	0	$M3_{L\infty,k}$: $M4_{L\infty,k}$	4464.3	<0.0001
NEAMAP					
M1	65367	2320			
$M2_{L\infty}$	63528	481	$M2_{L\infty}$: $M2_{L\infty,k}$	217.93	<0.0001
$_{L\infty,k}$	63312	265	$M3_{L\infty}$: $M3_{L\infty,k}$	33.83	<0.0001
$M3_{L\infty}$	65291	2244	$M2_{L\infty}$: $M4_{L\infty}$	180.4	<0.0001
$_{L\infty,k}$	65259	2212	$M3_{L\infty}$: $M4_{L\infty}$	1943.2	<0.0001
$M4_{L\infty}$	63350	303	$M2_{L\infty,k}$: $M4_{L\infty,k}$	268.83	<0.0001
$_{L\infty,k}$	63047	0	$M3_{L\infty,k}$: $M4_{L\infty,k}$	2215.8	<0.0001
SEAMAP					
M1	177935	193			
$M2_{L\infty}$	177742	0	$M2_{L\infty}$: $M2_{L\infty,k}$	0	1
$_{L\infty,k}$	177755	13	$M3_{L\infty}$: $M3_{L\infty,k}$	33.01	<0.0001
$M3_{L\infty}$	177779	6	$M2_{L\infty}$: $M4_{L\infty}$	0	1
$_{L\infty,k}$	177748	37	$M3_{L\infty}$: $M4_{L\infty}$	0	1
$M4_{L\infty}$	177804	62	$M2_{L\infty,k}$: $M4_{L\infty,k}$	7.08	<0.05
$_{L\infty,k}$	177752	10	$M3_{L\infty,k}$: $M4_{L\infty,k}$	0	1
ChesMMAP					
M1	72813	1629			
$M2_{L\infty}$	72140	956	$M2_{L\infty}$: $M2_{L\infty,k}$	149.77	<0.0001
$_{L\infty,k}$	71992	808	$M3_{L\infty}$: $M3_{L\infty,k}$	111.99	<0.0001
$M3_{L\infty}$	71942	758	$M2_{L\infty}$: $M4_{L\infty}$	682.82	<0.0001
$_{L\infty,k}$	71832	648	$M3_{L\infty}$: $M4_{L\infty}$	485.06	<0.0001
$M4_{L\infty}$	71459	275	$M2_{L\infty,k}$: $M4_{L\infty,k}$	811.44	<0.0001
$_{L\infty,k}$	71184	0	$M3_{L\infty,k}$: $M4_{L\infty,k}$	651.46	<0.0001

Table 4 Random effects produced by the three most robust length-at-age mixed-effects models based on AIC for each survey. Random effects of parameters grouped by either region or year are compared through their standard deviations (SD).

Model	Group	Parameter	SD
NEFSC			
M4 $_{L\infty,k}$	Region	L_∞	53.07
	Region	k	39.67
	Year	L_∞	36.95
	Year	k	28.27
M2 $_{L\infty,k}$	Region	L_∞	63.43
	Region	k	41.46
M4 $_{L\infty}$	Region	L_∞	49.53
	Year	L_∞	39.53
NEAMAP			
M4 $_{L\infty,k}$	Region	L_∞	71.92
	Region	k	0.17
	Year	L_∞	11.16
	Year	k	0.05
M2 $_{L\infty,k}$	Region	L_∞	74.88
	Region	k	0.19
M4 $_{L\infty}$	Region	L_∞	40.52
	Year	L_∞	11.72
SEAMAP			
M2$_{L\infty}$	Region	L_∞	17.47
M3 $_{L\infty}$	Year	L_∞	0.21
M4$_{L\infty, k}$	Region	L_∞	0.31
	Region	k	0
	Year	L_∞	0.01
	Year	k	0
ChesMMAP			
M4 $_{L\infty,k}$	Region	L_∞	70.52
	Region	k	0.11
	Year	L_∞	25.74
	Year	k	0.05
M4 $_{L\infty}$	Region	L_∞	27.76
	Year	L_∞	23.80
M3 $_{L\infty,k}$	Year	L_∞	48.10
	Year	k	0.13

Table 5 Length-at-age parameter mean estimates ± standard error (SE) from the most robust model compared to those from the standard homogeneous model for the four surveys.

Model	L_∞(±SE)	k(±SE)	t_0(±SE)
NEFSC			
a) M4 $_{L\infty,k}$	434.8 (±0.24)	0.55 (±0.01)	-1.1 (±0.01)
b) M1	802.3 (±60.1)	0.11 (±0.01)	-2.2 (±0.07)
NEAMAP			
a) M4 $_{L\infty,k}$	310 (±30.1)	0.74 (±0.08)	-1.06 (±0.04)
b) M1	363.8 (±17.01)	0.34 (±0.04)	-1.67 (±0.09)
SEAMAP			
a) M2 $_{L\infty}$	651.8 (±89.91)	0.10 (±0.02)	-3.16 (±0.15)
b) M1	400 (±19.12)	0.22 (±0.02)	-2.53 (±0.1)
ChesMMAP			
a) M4 $_{L\infty,k}$	390.2 (±31.03)	0.48 (±0.05)	-1.05 (±0.03)
b) M1	412.4 (±11.4)	0.32 (±0.02)	-1.35 (±0.04)

Table 6 Allometric growth estimates (b) and their 95% confidence intervals from the weight-length linear regression.

Survey	b (5%, 95%)
NEFSC	2.997 (2.989, 3.005)
NEAMAP	2.994 (2.976, 3.011)
SEAMAP	3.037 (3.030, 3.045)
ChesMMAP	2.908 (2.895, 2.922)

Table 7 Ranking of the seven competing weight-at-age models (in descending order) based on minimizing Akaike's Information Criterion for each of the four surveys.

NEFSC	NEAMAP	SEAMAP	ChesMMAP
M4 $_{W\infty,k}$	M4 $_{W\infty,k}$	M4 $_{W\infty,k}$	M4$_{W\infty}$
M4 $_{W\infty}$	M2 $_{W\infty,k}$	M4$_{W\infty}$	M3 $_{W\infty,k}$
M2 $_{W\infty}$	M4$_{W\infty}$	M3 $_{W\infty}$	M3 $_{W\infty}$
M2 $_{W\infty,k}$	M2 $_{W\infty}$	M3 $_{W\infty,k}$	M2 $_{W\infty,k}$
M3 $_{W\infty,k}$	M3 $_{W\infty,k}$	M2 $_{W\infty}$	M2 $_{W\infty}$
M3 $_{W\infty}$	M3 $_{W\infty}$	M2 $_{W\infty,k}$	M1
M1	M1	M1	M4 $_{W\infty,k}$

Table 8 Comparisons of the four weight-at-age models developed for each of the four surveys, including AIC and LRT values: Akaike's Information Criterion (AIC), Akaike differences (Δ_i), Chi-square statistic (χ^2), and *P* –value (*P*).

	AIC		$LRT_{Mx:My}$		
Model	AIC	Δ_i	H_0:H_A	χ^2	*P* ($>\chi^2$)
NEFSC					
M1	15743	2425			
M2 W_∞	14348	1030	$M2_{W\infty}$: $M2_{W\infty,k}$	225.29	<0.0001
$W_{\infty,k}$	14631	1313	$M3_{W\infty}$: $M3_{W\infty,k}$	331.93	<0.0001
M3 W_∞	15391	2073	$M2_{W\infty}$: $M4_{W\infty}$	279.3	<0.0001
$W_{\infty,k}$	15061	1743	$M3_{W\infty}$: $M4_{W\infty}$	1322.5	<0.0001
M4 W_∞	14071	753	$M2_{W\infty,k}$: $M4_{W\infty,k}$	1317.4	<0.0001
$W_{\infty,k}$	13318	0	$M3_{W\infty,k}$: $M4_{W\infty,k}$	1747.3	<0.0001
NEAMAP					
M1	13719	1706			
M2 W_∞	12421	409	$M2_{W\infty}$: $M2_{W\infty,k}$	225.29	<0.0001
$W_{\infty,k}$	12198	185	$M3_{W\infty}$: $M3_{W\infty,k}$	4.73	<0.05
M3 W_∞	13632	1620	$M2_{W\infty}$: $M4_{W\infty}$	170.07	<0.0001
$W_{\infty,k}$	13629	1617	$M3_{W\infty}$: $M4_{W\infty}$	1380.9	<0.0001
M4 W_∞	12253	241	$M2_{W\infty,k}$: $M4_{W\infty,k}$	189.38	<0.0001
$W_{\infty,k}$	12013	0	$M3_{W\infty,k}$: $M4_{W\infty,k}$	1620.7	<0.0001
SEAMAP					
M1	32109	1200			
M2 W_∞	31577	668	$M2_{W\infty}$: $M2_{W\infty,k}$	0	1
$W_{\infty,k}$	32093	1184	$M3_{W\infty}$: $M3_{W\infty,k}$	0	1
M3 W_∞	30995	86	$M2_{W\infty}$: $M4_{W\infty}$	635.95	<0.0001
$W_{\infty,k}$	31027	118	$M3_{W\infty}$: $M4_{W\infty}$	53.54	<0.0001
M4 W_∞	30943	34	$M2_{W\infty,k}$: $M4_{W\infty,k}$	1188	<0.0001
$W_{\infty,k}$	30909	0	$M3_{W\infty,k}$: $M4_{W\infty,k}$	122.04	<0.0001
ChesMMAP					
M1	15465	655			
M2 W_∞	15309	499	$M2_{W\infty}$: $M2_{W\infty,k}$	218.49	<0.0001
$W_{\infty,k}$	15092	282	$M3_{W\infty}$: $M3_{W\infty,k}$	119.22	<0.0001
M3 W_∞	14903	93	$M2_{W\infty}$: $M4_{W\infty}$	500.92	<0.0001
$W_{\infty,k}$	14786	24	$M3_{W\infty}$: $M4_{W\infty}$	95.21	<0.0001
M4 W_∞	14810	0	$M2_{W\infty,k}$: $M4_{W\infty,k}$	0	1
$W_{\infty,k}$	15473	663	$M3_{W\infty,k}$: $M4_{W\infty,k}$	0	1

Table 9 Random effects produced by the three most robust weight-at-age mixed-effects models for each survey. Random effects of parameters grouped by either region or year are compared through their standard deviations (SD).

Model	Group	Parameter	SD
NEFSC			
M4 $_{W\infty,k}$	Region	W_∞	0.6909
	Region	k	0.7203
	Year	W_∞	0.7537
	Year	k	1.2841
M4 $_{W\infty}$	Region	W_∞	0.7067
	Year	W_∞	0.6404
M2$_{W\infty}$	Region	W_∞	0.5924
NEAMAP			
M4 $_{W\infty,k}$	Region	W_∞	0.5710
	Region	k	0.5909
	Year	W_∞	0.5673
	Year	k	0.6351
M2$_{W\infty,k}$	Region	W_∞	0.5626
	Region	k	0.6654
M4$_{W\infty}$	Region	W_∞	0.1227
	Year	W_∞	0.0391
SEAMAP			
M4$_{W\infty,k}$	Region	W_∞	1.2505
	Region	k	0
	Year	W_∞	0.3445
	Year	k	1.8715
M4 $_{W\infty}$	Region	W_∞	2.0487
	Year	W_∞	3.8583
M3$_{W\infty}$	Year	W_∞	11.2563
ChesMMAP			
M4 $_{W\infty}$	Region	W_∞	0.5080
	Year	W_∞	0.4002
M3$_{W\infty,k}$	Year	W_∞	0.7514
	Year	k	0.6324
M3$_{W\infty}$	Year	W_∞	0.9707

Table 10 Weight-at-age parameter mean estimates ± standard error (SE) from the most robust model compared to those from the standard homogeneous model for the four surveys.

Model	W_∞(±SE)	k(±SE)	t_0(±SE)
NEFSC			
a) M4 $W_{\infty,k}$	0.838 (±0.032)	0.566 (±0.021)	-1.070 (±0.025)
b) M1	0.819 (±0.086)	0.283 (±0.021)	-1.572 (±0.051)
NEAMAP			
a) M4 $W_{\infty,k}$	0.352 (±0.019)	0.774 (±0.050)	-1.058 (±0.044)
b) M1	0.752 (±0.240)	0.230 (±0.048)	-2.024 (±0.151)
SEAMAP			
a) M4 $W_{\infty,k}$	4.321 (±0.577)	0.069 (±0.004)	-3.498 (±0.057)
b) M1	2.000 (±1.244)	0.095 (±0.029)	-3.555 (±0.245)
ChesMMAP			
a) M4 W_∞	0.367 (±0.025)	0.561 (±0.035)	-0.957 (±0.035)
b) M1	0.509 (±0.053)	0.389 (±0.031)	-1.140 (±0.043)

Table 11 Comparisons of the four maturity-at-age models developed from the ChesMMAP survey, including AIC and LRT values: Akaike's Information Criterion (AIC), Akaike differences (Δ_i), Chi-square statistic (χ^2), and P –value (P).

	AIC		$LRT_{Mx:My}$		
Model	AIC	Δ_i	H_0:H_A	χ^2	P ($>\chi^2$)
Females					
M1	3509	855			
M2	3406	751	M2: M4	757.35	<0.0001
M3	2745	91	M3: M4	96.61	<0.0001
M4	2654	0			
Males					
M1	2358	610			
M2	2315	567	M2: M4	573.22	<0.0001
M3	1781	33	M3: M4	39.22	<0.0001
M4	1748	0			

Table 12 Mean age at 50% maturity (β) for females and males produced by the four different models.

Model	β	
	Females	Males
M1	1.17	1.9
M2	1.16	1.9
M3	1.13	1.89
M4	1.37	2.19

Table 13 Random effects produced by the maturity-at-age mixed-effects models. Random effects of parameters grouped by either region or year are compared through their standard deviations (SD).

Model	Group	Parameter	SD
Females			
M2	Region	α	0.15
		βt	0.36
M3	Year	α	0.63
		βt	1.25
M4	Region	α	0.37
		βt	0.26
	Year	α	0.64
		βt	1.29
Males			
M2	Region	α	0.42
		βt	0.14
M3	Year	α	0.81
		βt	0.73
M4	Region	α	0.35
		βt	0.19
	Year	α	0.80
		βt	0.74

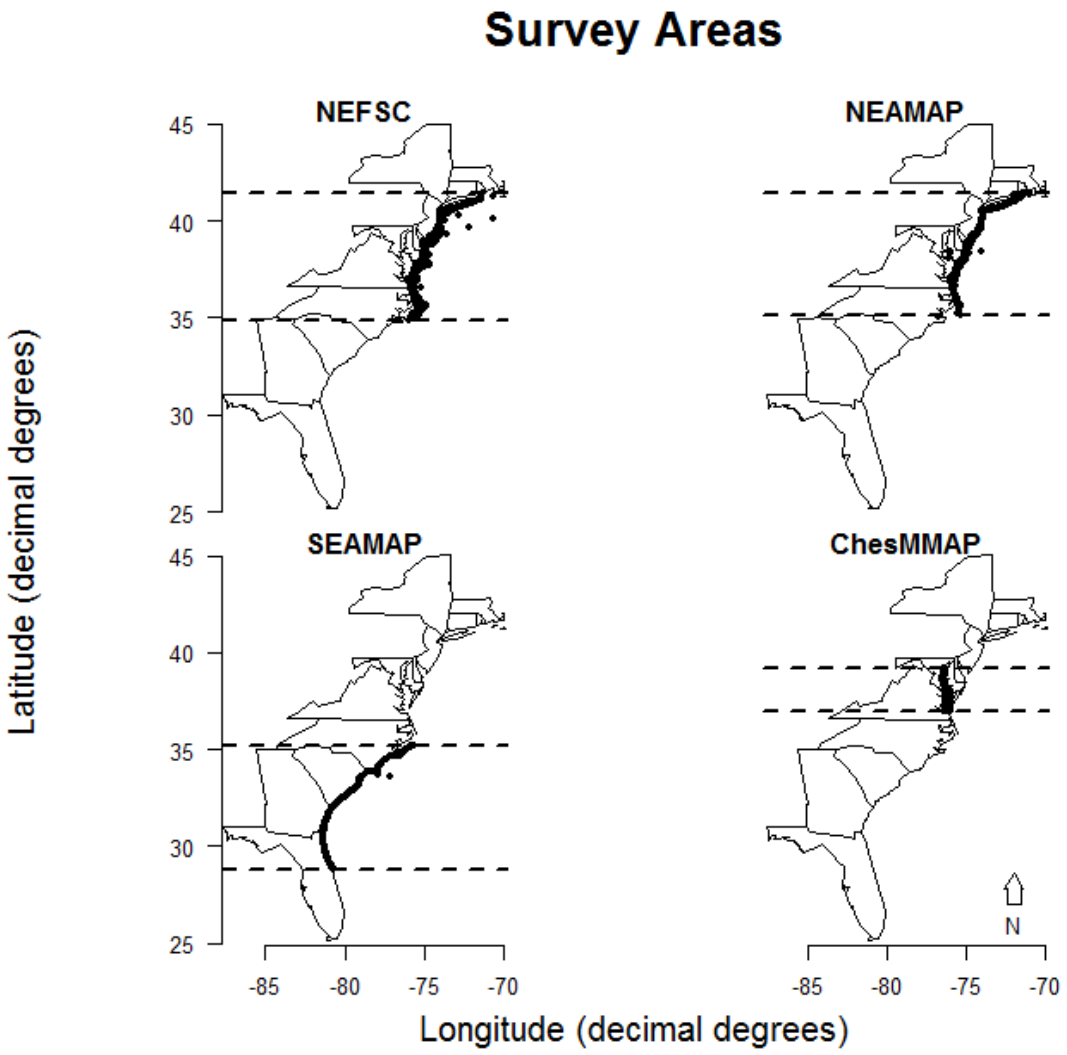

Figure 1 Stations surveyed by the four fishery-independent surveys used in this study.

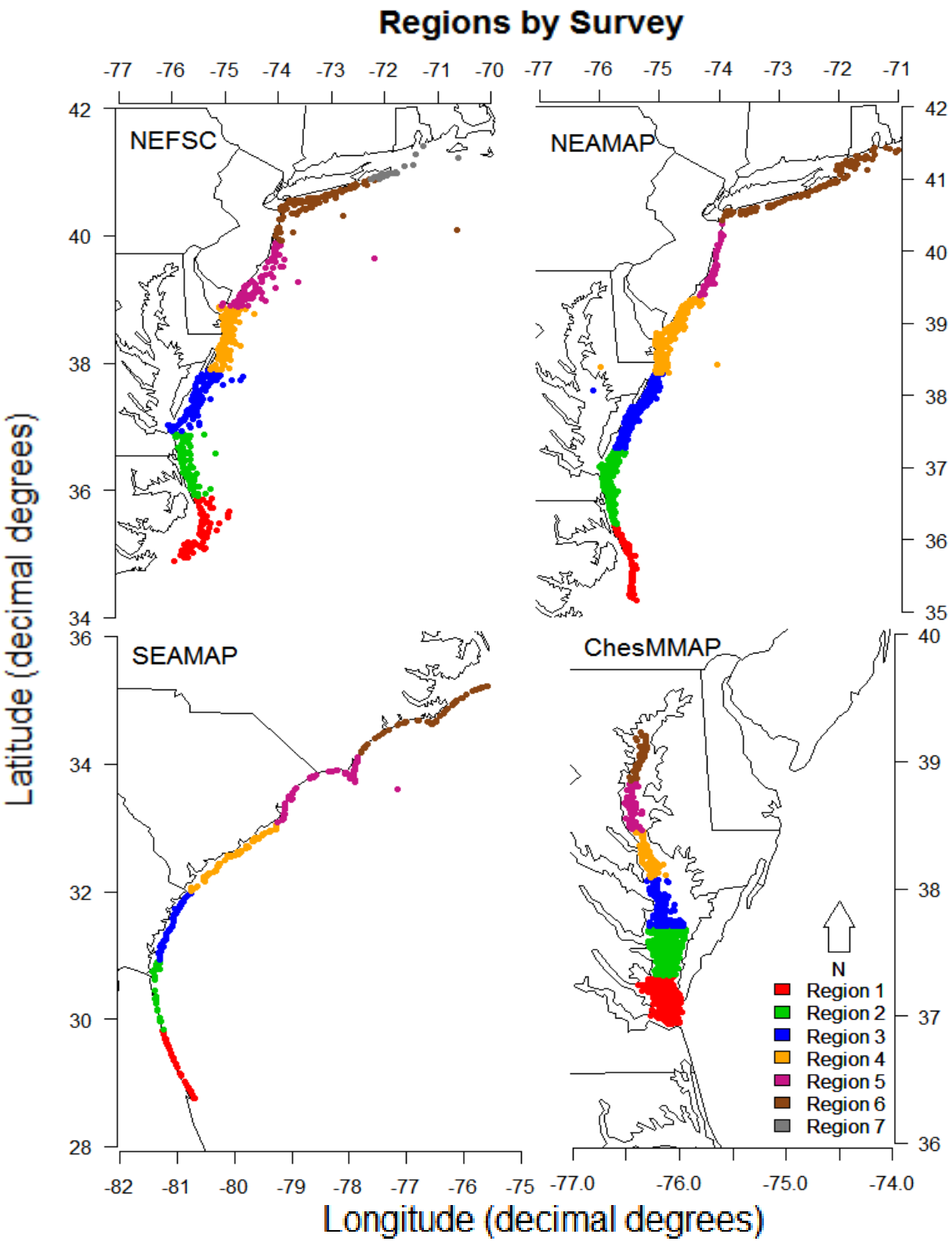

Figure 2 Regions defined for each of the four surveys used in this study.

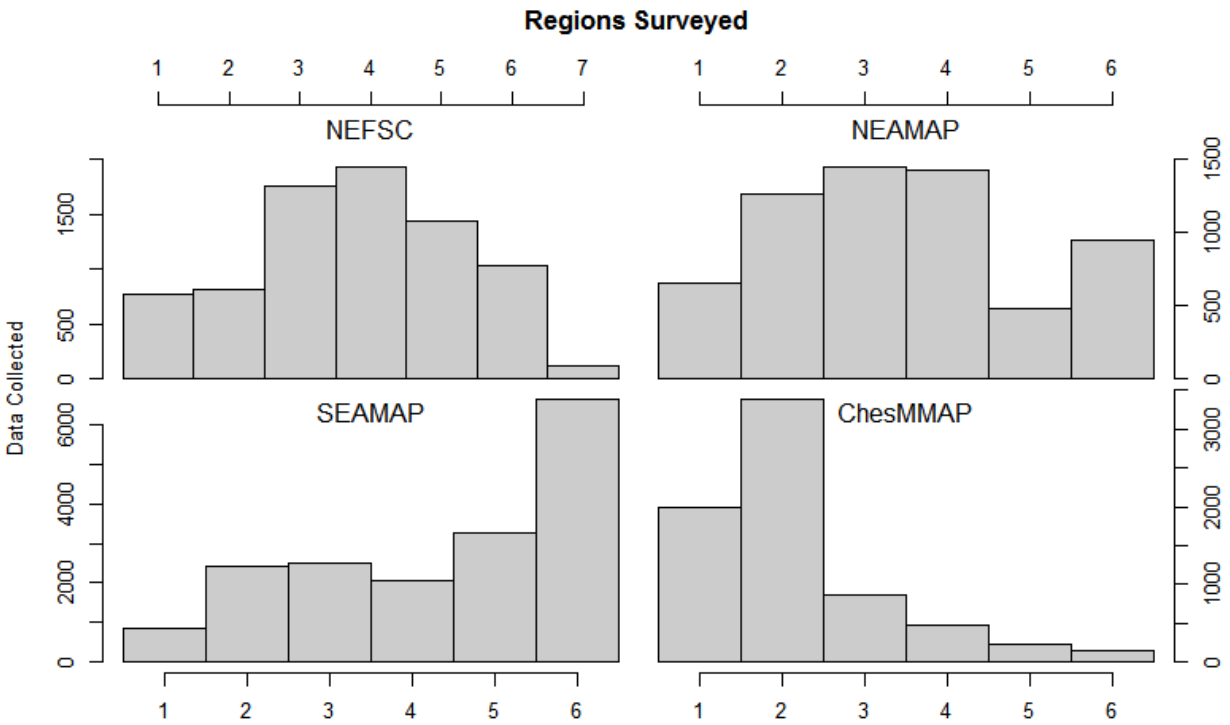

Figure 3 Data distributions of the regions surveyed from each of the four datasets.

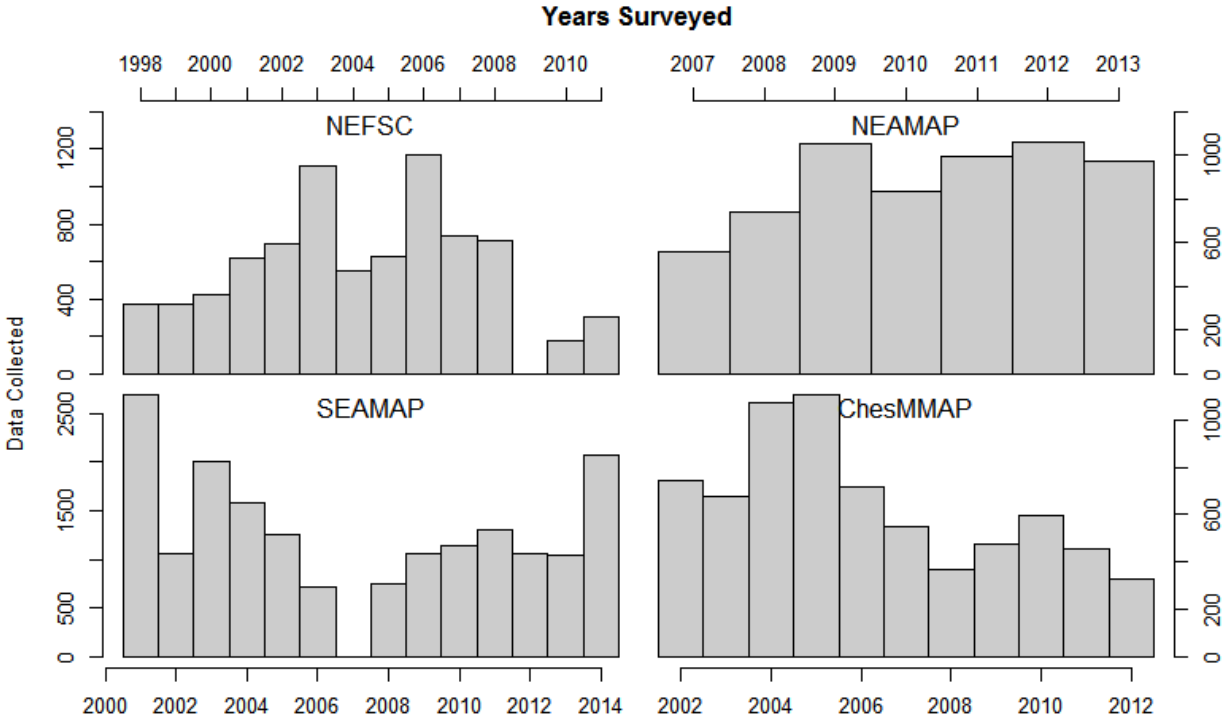

Figure 4 Data distributions of the years surveyed from each of the four datasets.

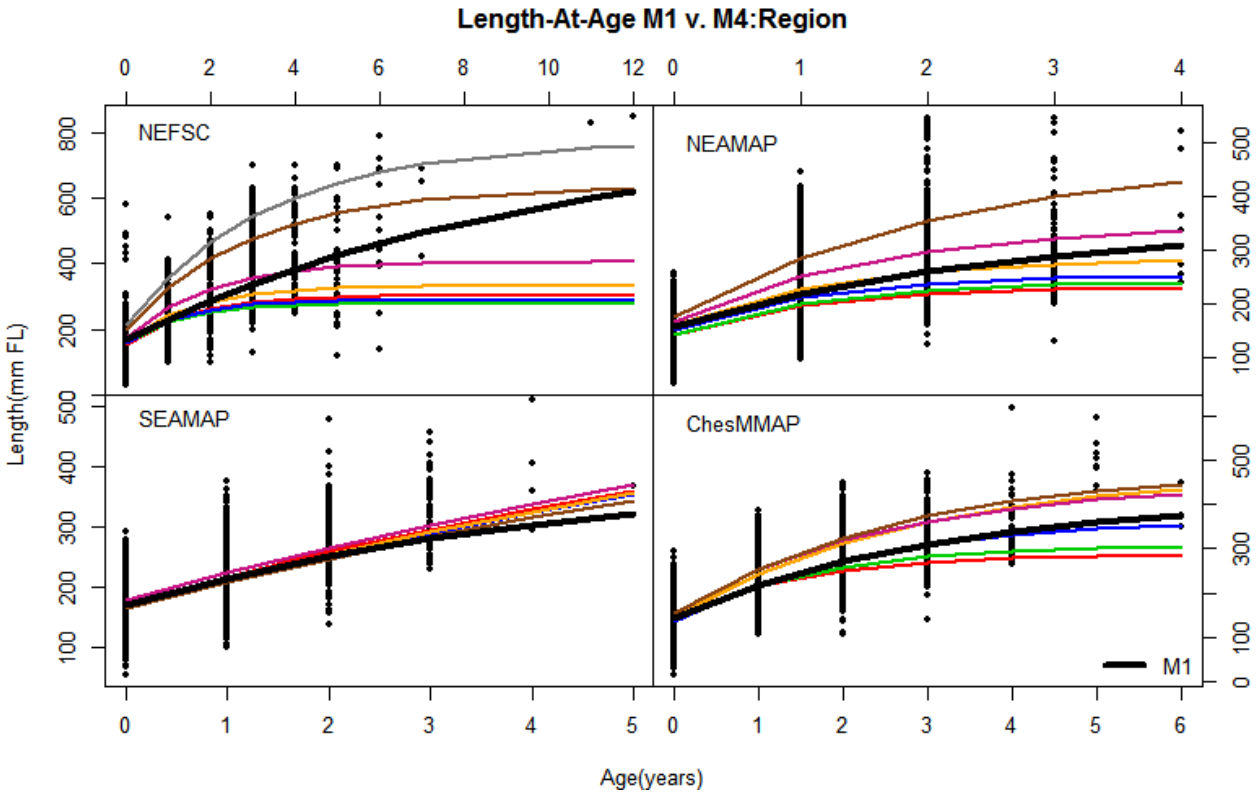

Figure 5 Spatial variation of length-at-age curves produced by M4 (assuming both spatial and temporal heterogeneity) plotted against the non-heterogeneous curve produced by M1. Colored lines represent curves fitted to different regions in each dataset, and the thick black line is the standard curve fitted by M1.

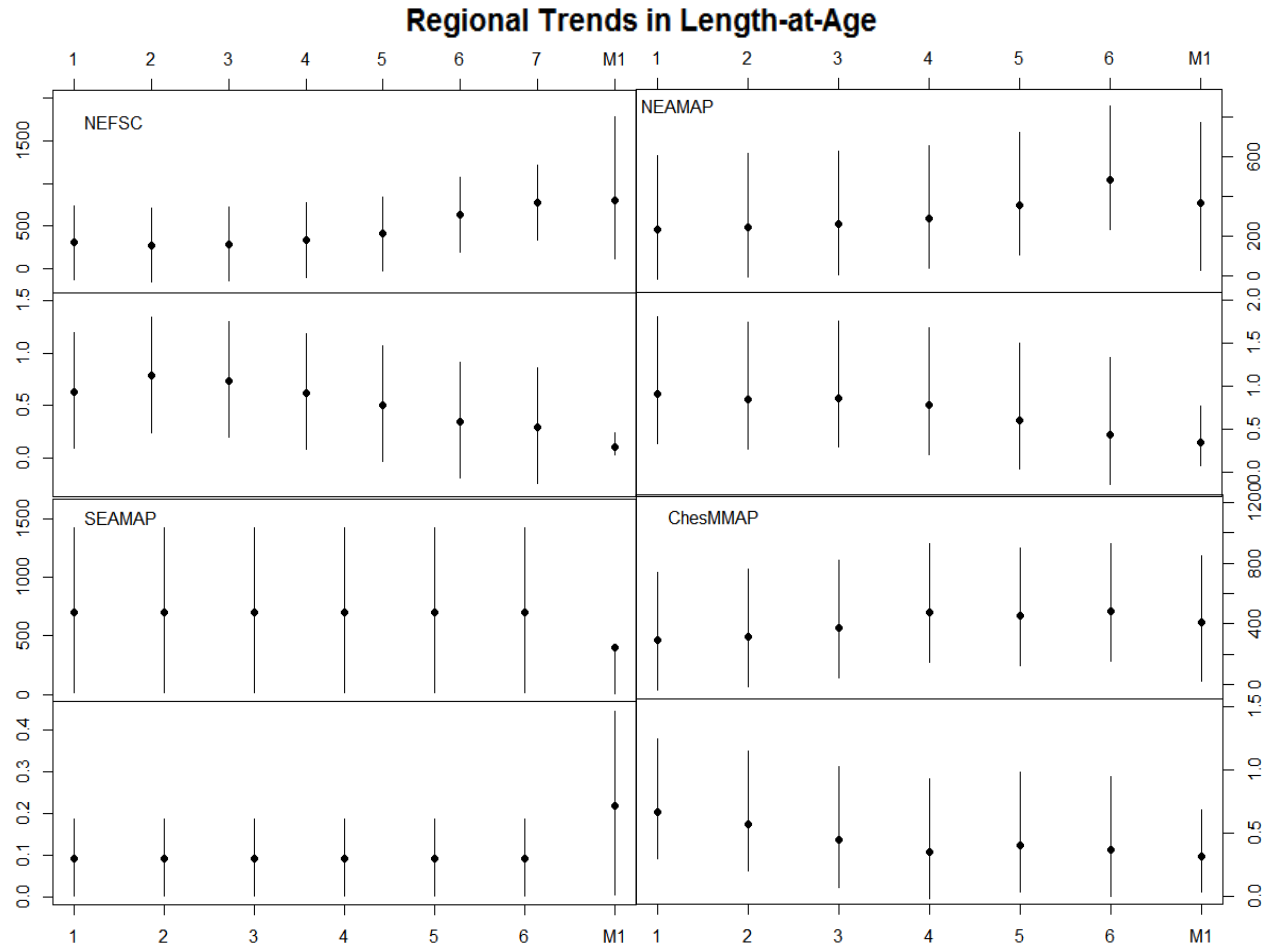

Figure 6 Spatial trends of combined fixed and random effects of L_∞ (top) and k (bottom) for each survey. Spatial estimates were produced by length-at-age mixed-effects model M4 which incorporates both spatial and temporal heterogeneity and compared to the averaged estimate produced by the homogeneous model M1. Error bars represent the 95% confidence intervals of the parameter estimates.

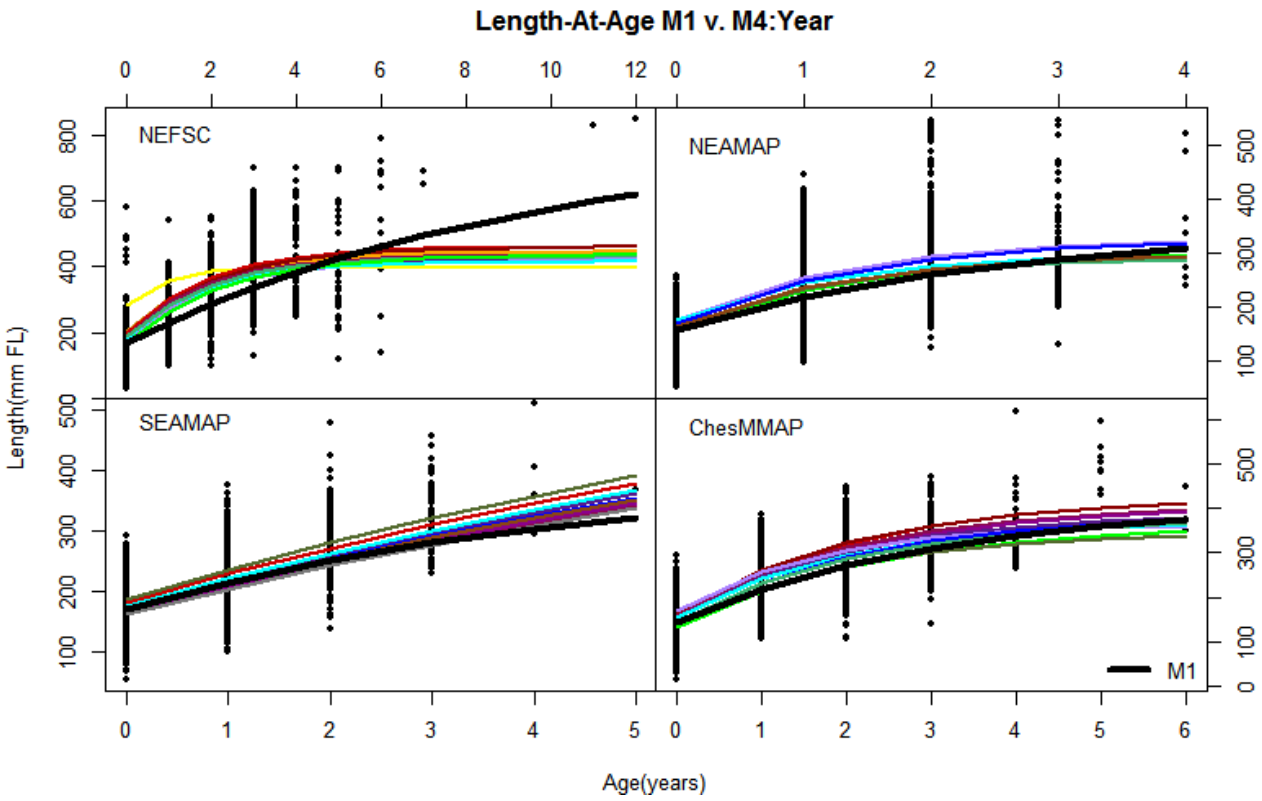

Figure 7 Temporal variation of length-at-age curves produced by M4 (colored lines) against the non-heterogeneous curve produced by M1 (thick black line).

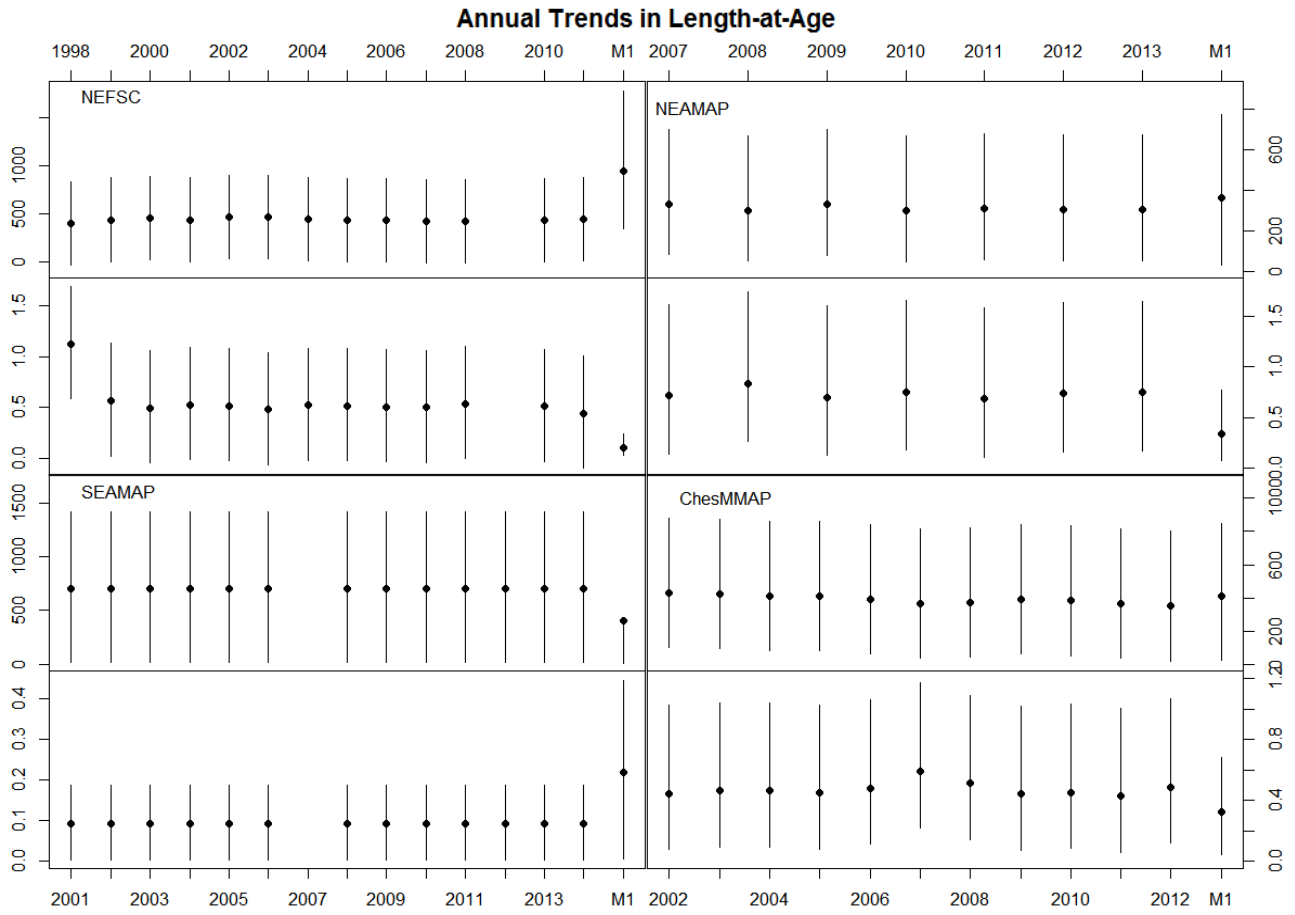

Figure 8 Temporal trends of combined fixed and random effects of L_∞ (top) and k (bottom) for each survey. Temporal estimates were produced by length-at-age mixed-effects model M4 which incorporates both spatial and temporal heterogeneity and compared to the averaged estimate produced by the homogeneous model M1. Error bars represent the 95% confidence intervals of the parameter estimates.

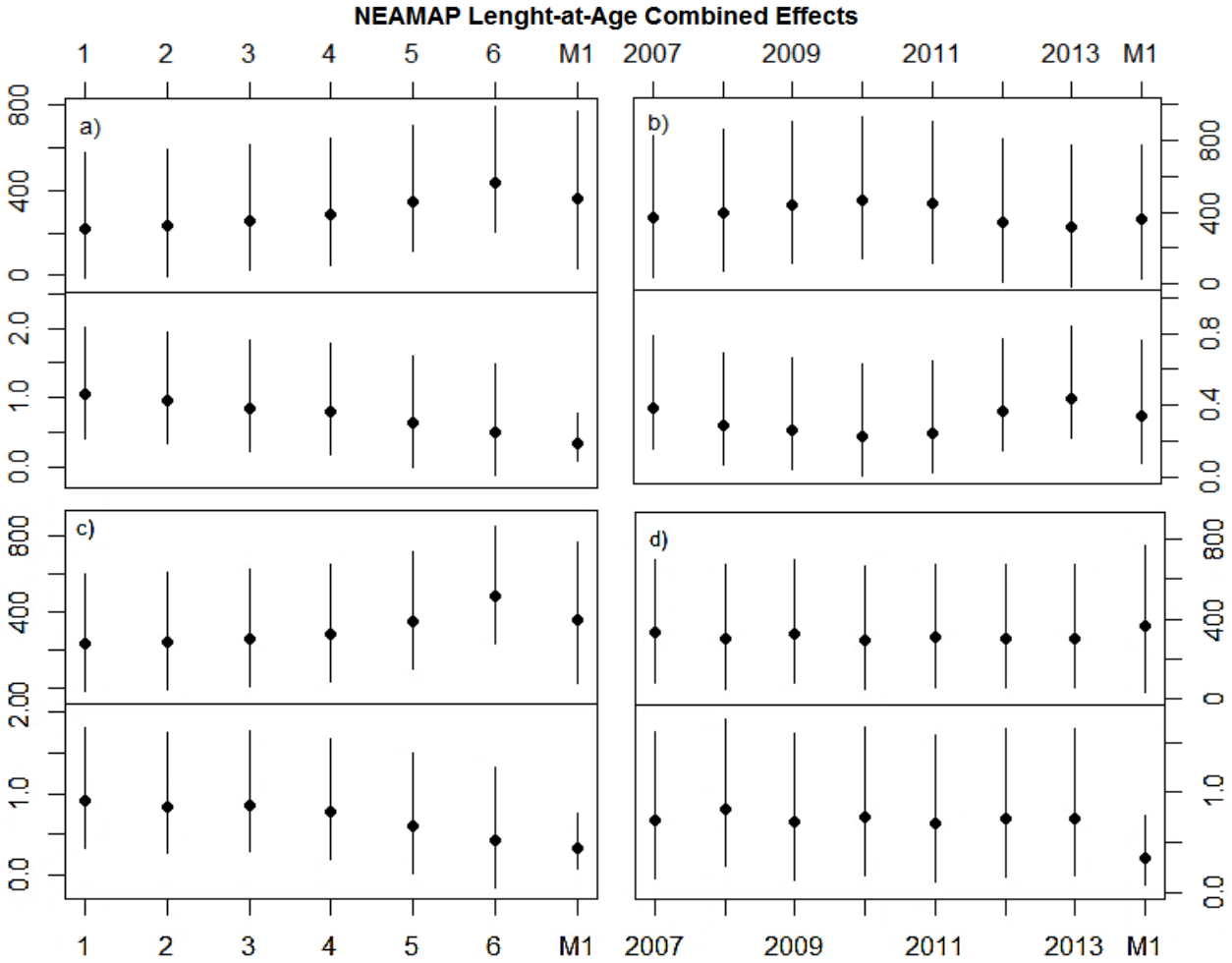

Figure 9 Combined fixed and random effects and their 95% confidence intervals of parameters L_∞ (top) and k (bottom) from each of the three NEAMAP length-at-age mixed-effects models: a) M2 grouped by region, b) M3 grouped by year, c) M4 grouped by region, and d) M4 grouped by year.

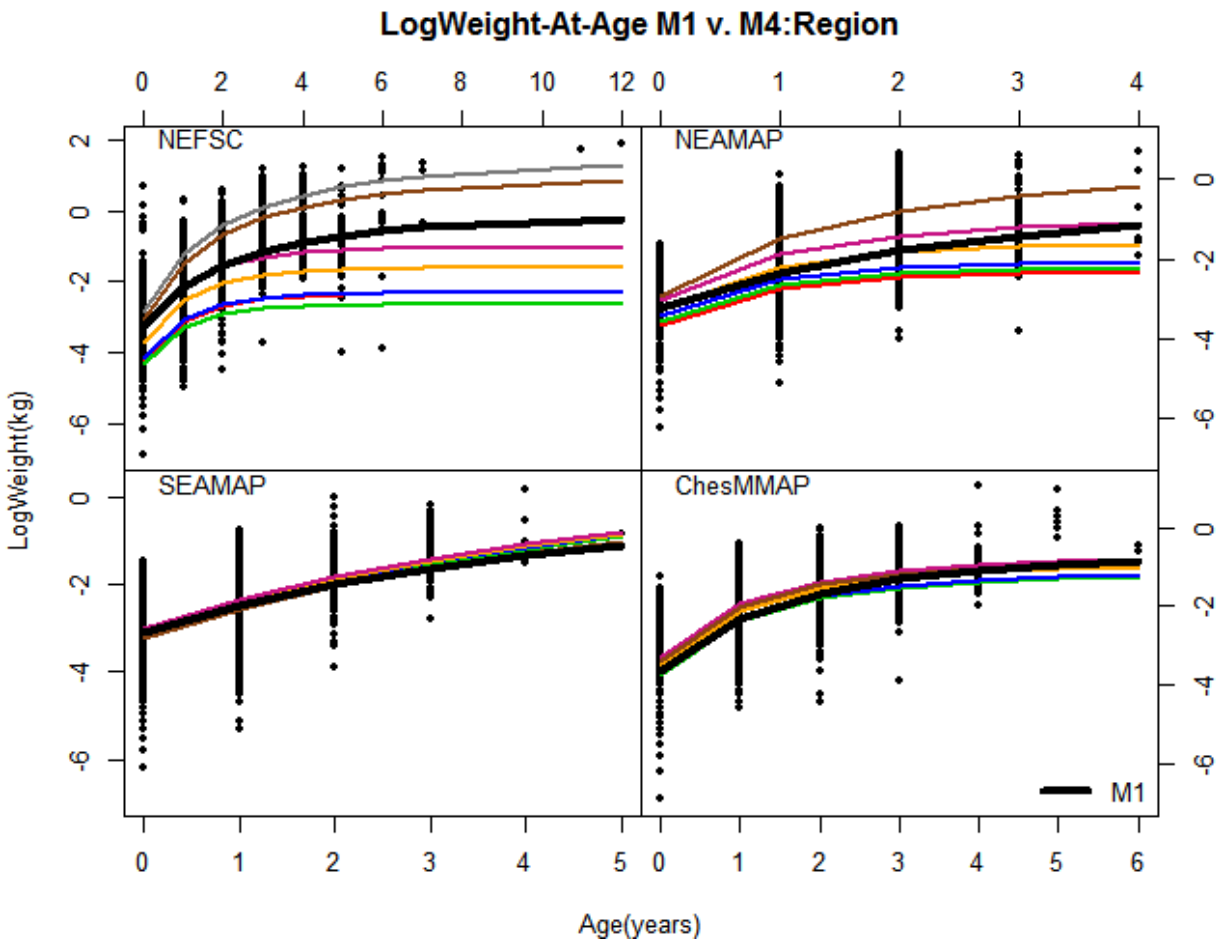

Figure 10 Spatial variation of weight-at-age curves produced by M4 plotted against the non-heterogeneous curve produced by M1. Colored lines represent curves fitted to different regions in each dataset, and the thick black line is the standard curve fitted by M1.

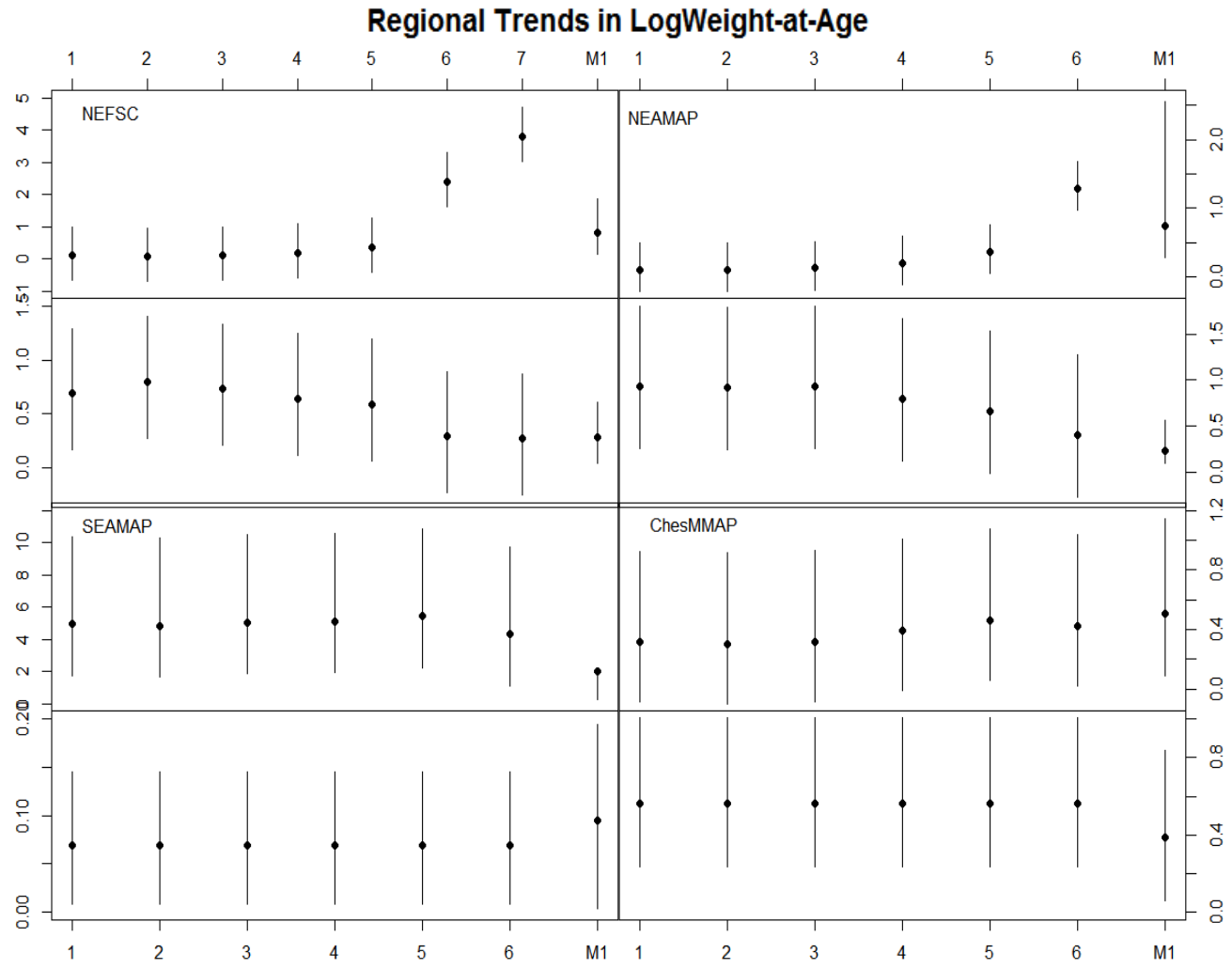

Figure 11 Spatial trends of combined fixed and random effects of W_∞ (top) and k (bottom) for each survey. Spatial estimates were produced by log weight-at-age mixed-effects model M4 which incorporates both spatial and temporal heterogeneity and compared to the averaged estimate produced by the homogeneous model M1. Error bars represent the 95% confidence intervals of the parameter estimates.

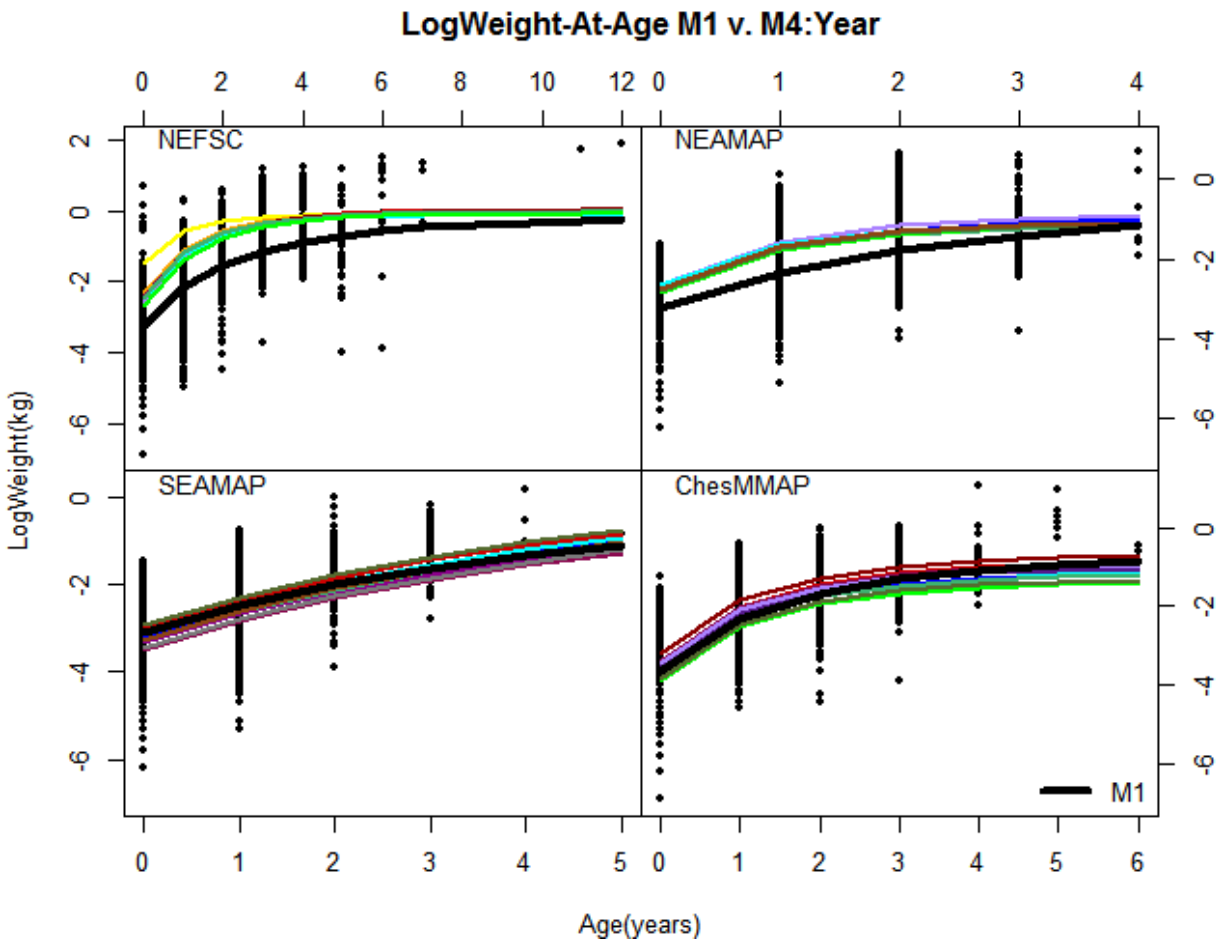

Figure 12 Temporal variation of weight-at-age curves produced by M4 (colored lines) against the non-heterogeneous curve produced by M1 (thick black line).

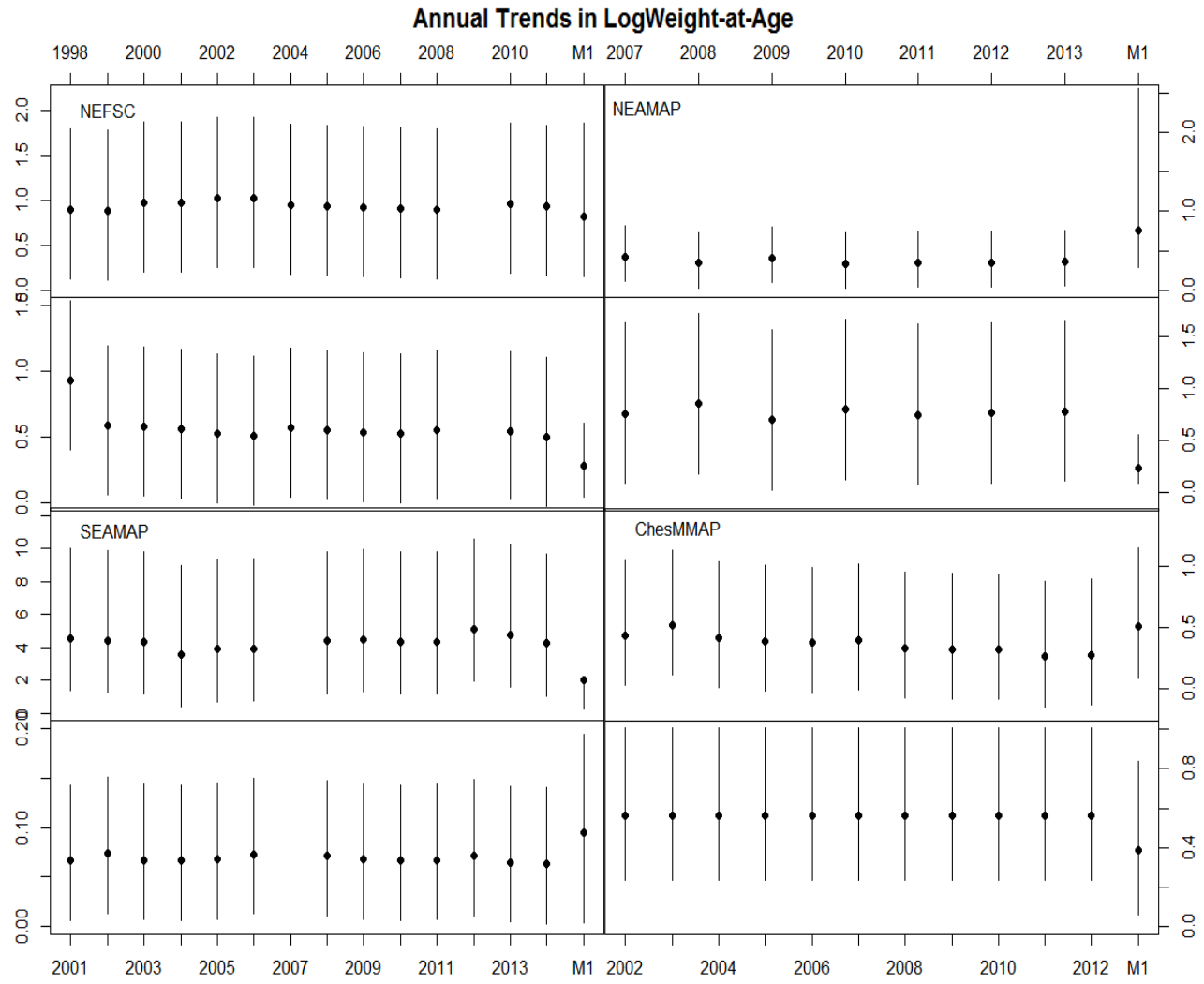

Figure 13 Temporal trends of combined fixed and random effects of W_∞ (top) and k (bottom) for each survey. Temporal estimates were produced by log weight-at-age mixed-effects model M4 which incorporates both spatial and temporal heterogeneity and compared to the averaged estimate produced by the homogeneous model M1. Error bars represent the 95% confidence intervals of the parameter estimates.

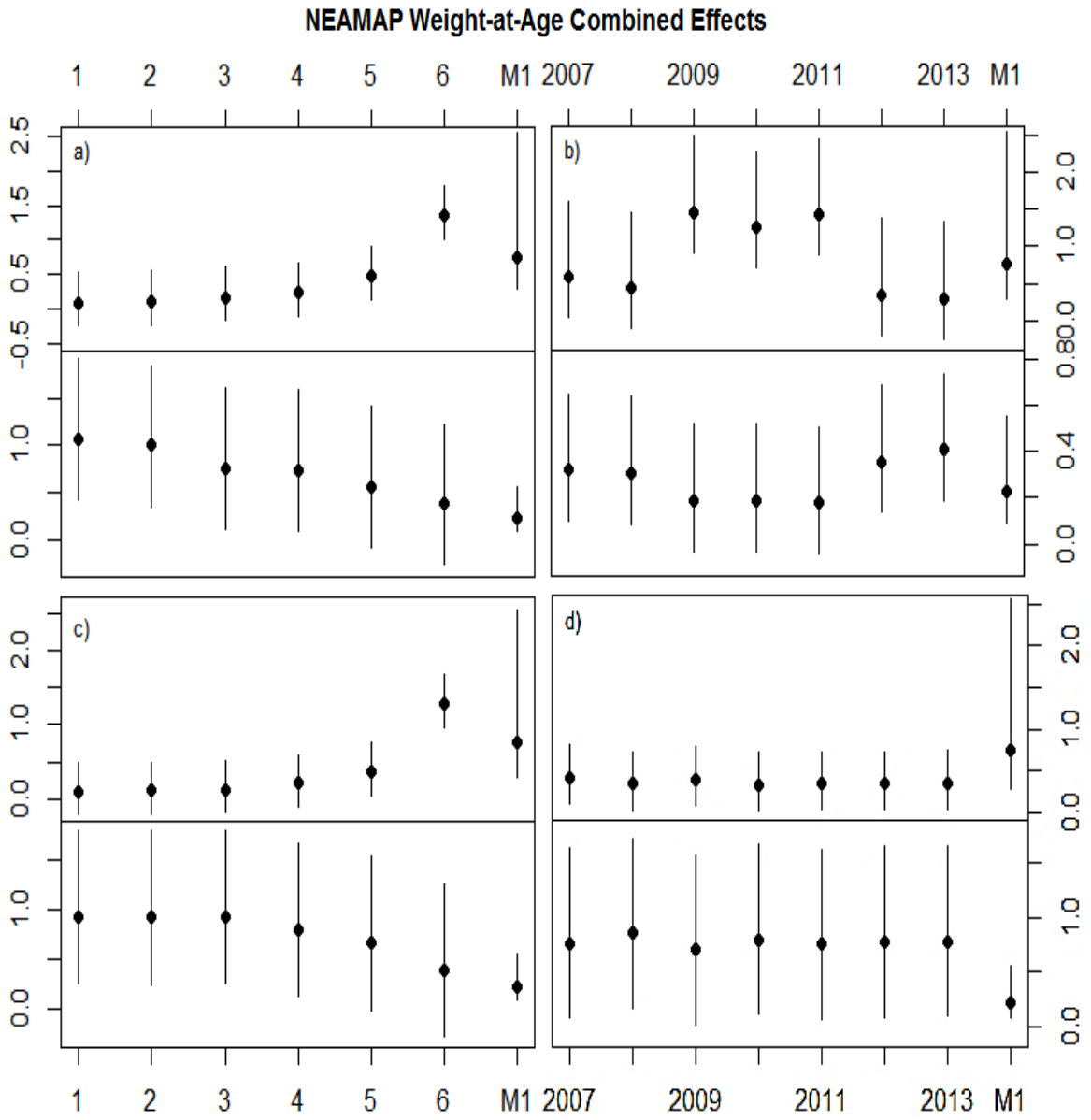

Figure 14 Combined fixed and random effects and their 95% confidence intervals of parameters W_∞ (top) and k (bottom) from each of the three NEAMAP log weight-at-age mixed-effects models: a) M2 grouped by region, b) M3 grouped by year, c) M4 grouped by region, and d) M4 grouped by year.

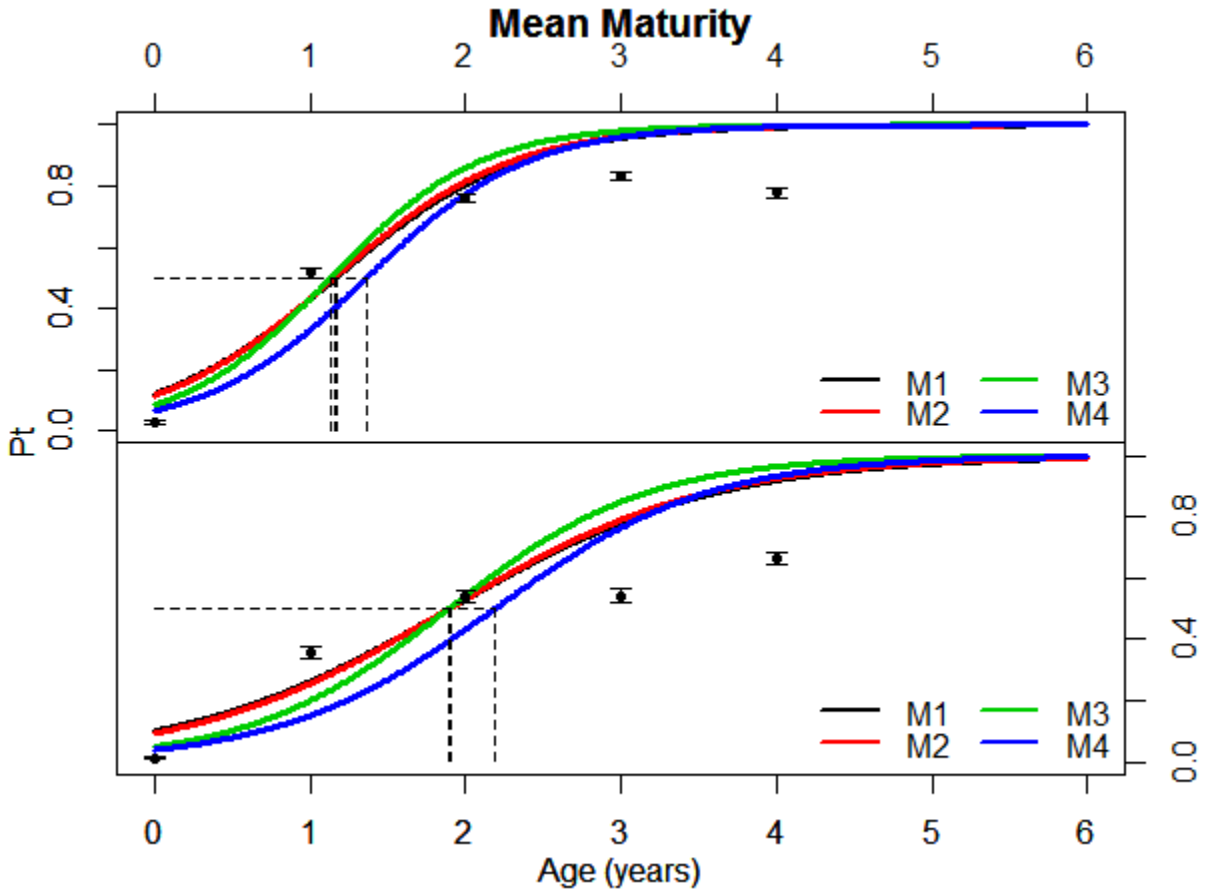

Figure 15 Mean female (top) and male (bottom) maturity-at-age relationships produced by the four candidate models. Model estimates (colored lines) are compared to proportion of mature fish (*Pt*) recorded for each sex in the ChesMMAP dataset. Error bars represent 95% confidence intervals of *Pt* at each age. Dashed lines show the age at which 50% of the fish are mature (β in Table 12) for each model curve.

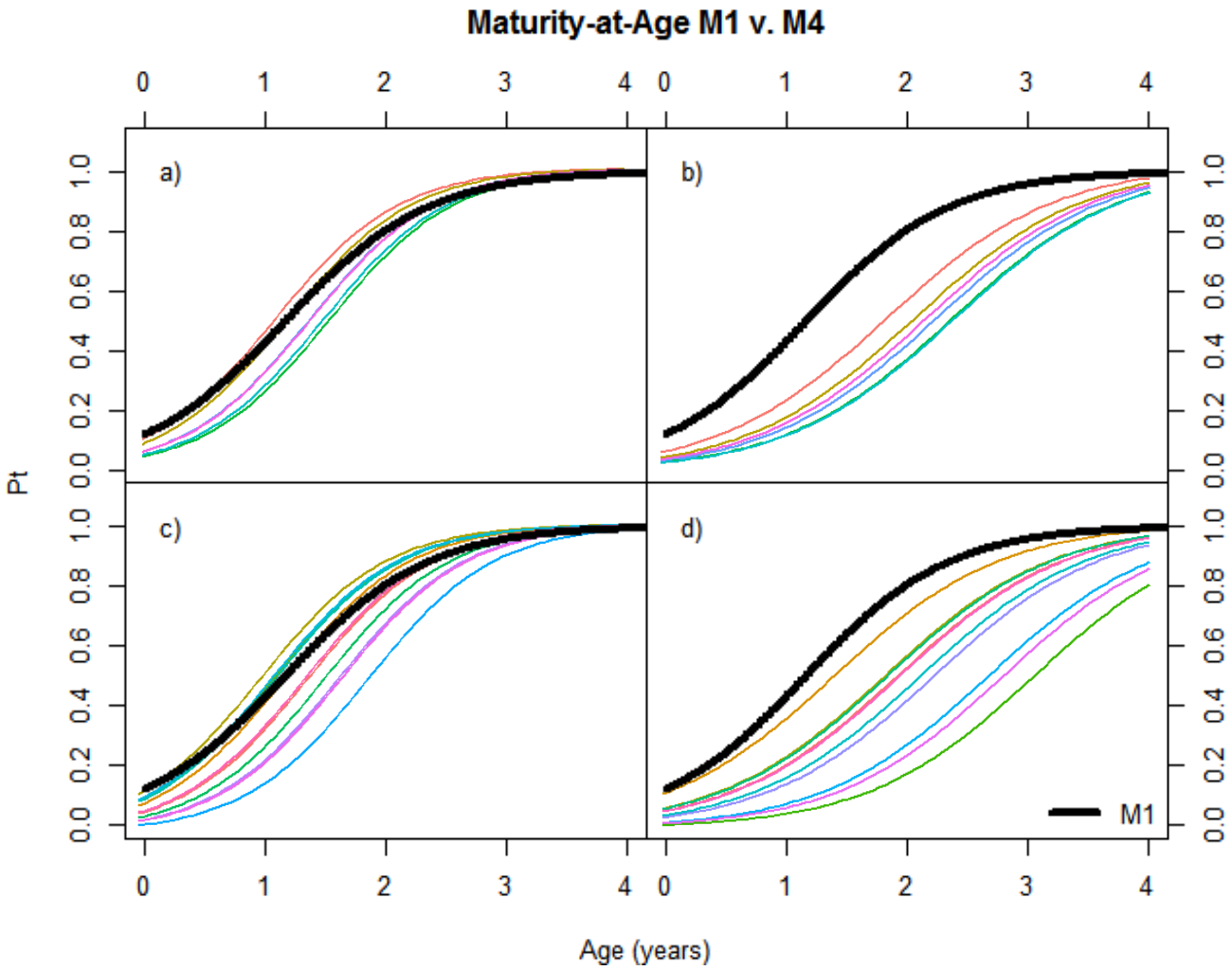

Figure 16 Spatial and temporal heterogeneity in maturity-at-age curves produced by M4 (colored lines) plotted against the standard homogeneous curve fitted by M1 (thick black line): a) regional variation in female maturity, b) regional variation in male maturity, c) annual variation in female maturity, and d) annual variation in male maturity.

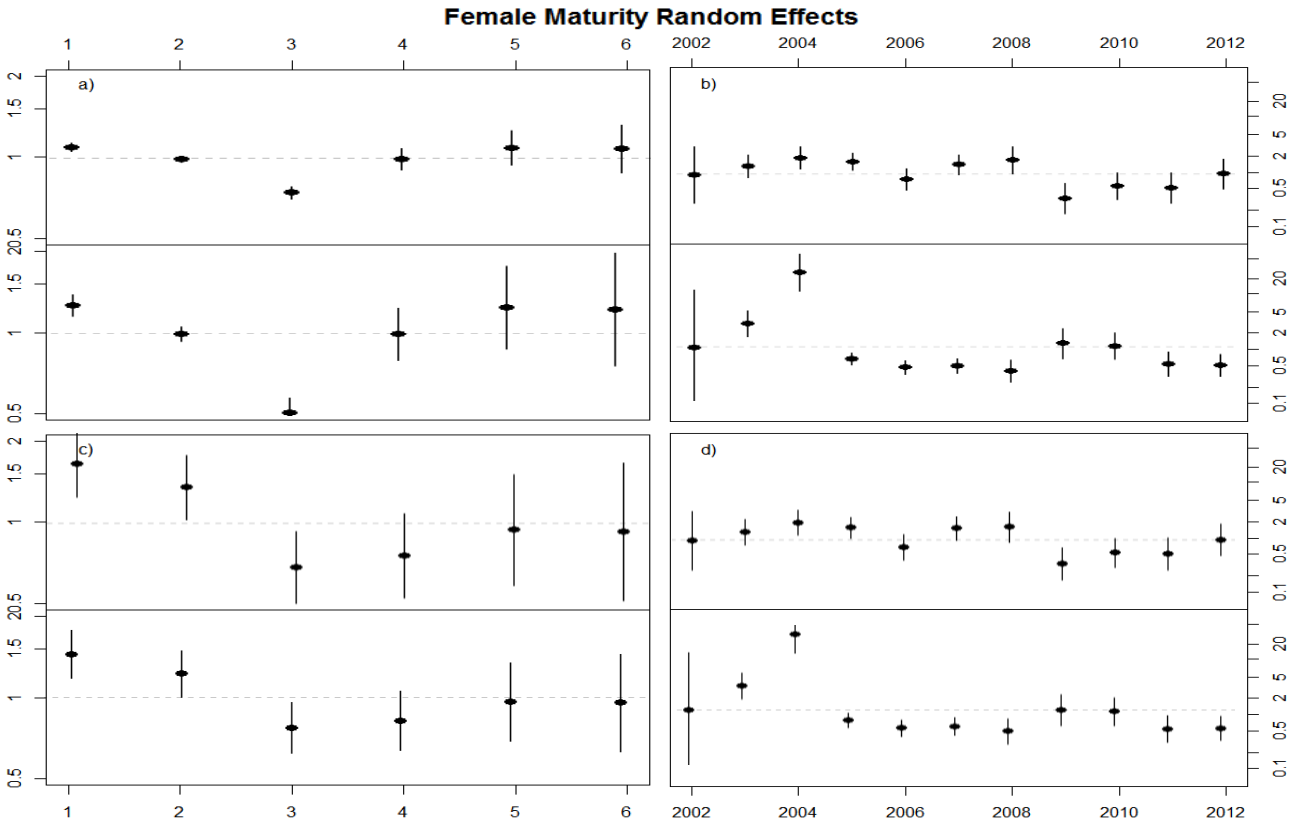

Figure 17 Random effects of female maturity-at-age parameters α (top) and βt (bottom) produced by the three mixed-effects models; a) M2 grouped by region, b) M3 grouped by year, c) M4 grouped by region, and d) M4 grouped by year. Gray dashed line at 1 is shown for reference.

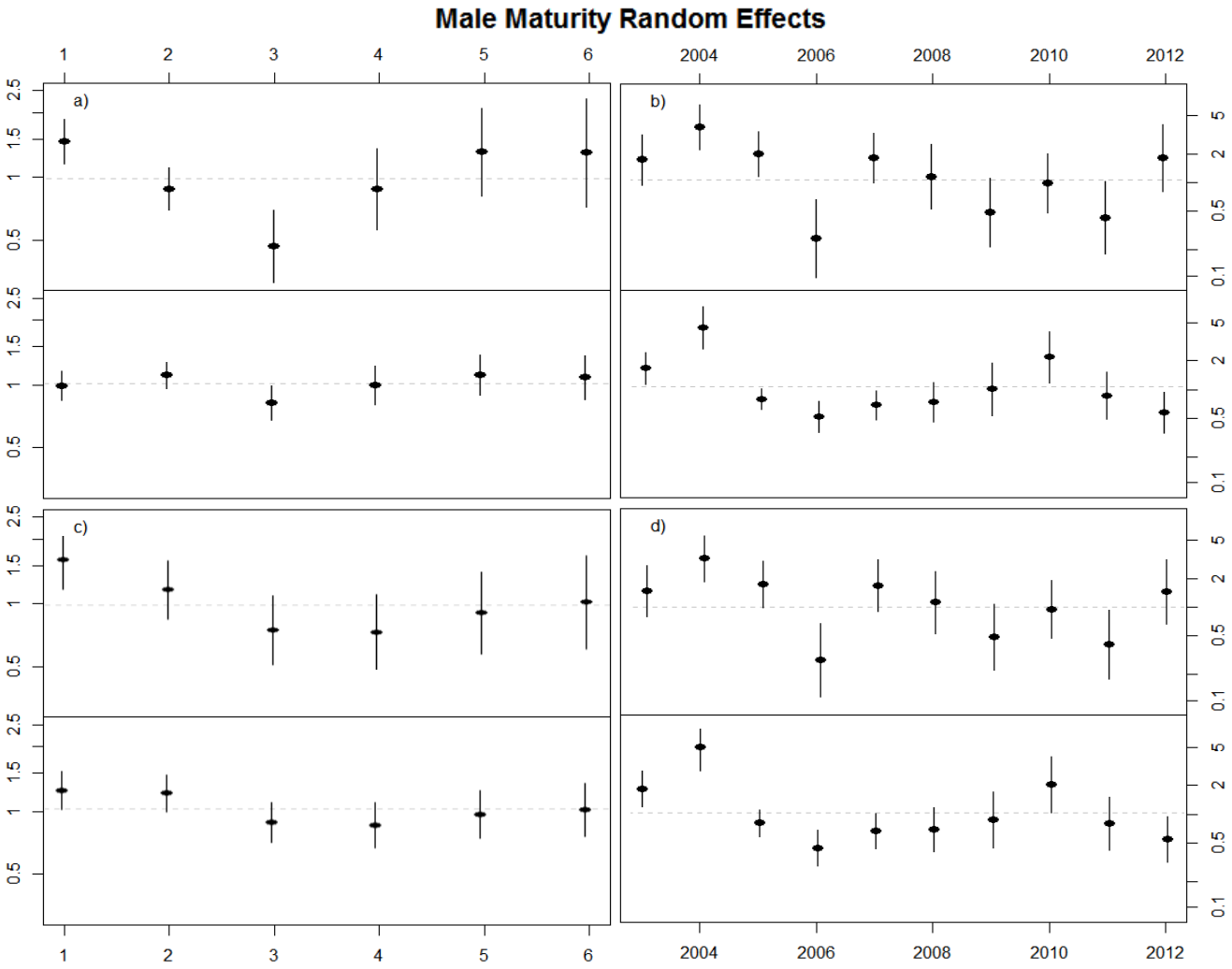

Figure 18 Random effects of male maturity-at-age parameters α (top) and βt (bottom) produced by the three mixed-effects models; a) M2 grouped by region, b) M3 grouped by year, c) M4 grouped by region, and d) M4 grouped by year. Gray dashed line at 1 is shown for reference.

CHAPTER THREE: Sensitivity of yield and spawning stock biomass per-recruit to spatial and temporal variations in life history of Atlantic Weakfish (*Cynoscion regalis*)

3.1 Abstract

Per-recruit models measure productivity and provide biological reference points, but rely heavily upon life-history characteristics such as growth that are inherently heterogeneous across space and time. This heterogeneity is often overlooked, and life-history parameters used in productivity models are generally "averaged" across space and time. Thus, the biological reference points determined in these productivity models are not representative of spatial or temporal trends in fish populations. Ignoring these variations in per-recruit models can distort stock assessment results and reduce the effectiveness of management strategies. This study examined the sensitivity of yield and spawning stock biomass per-recruit to spatially and temporally integrated weight using Atlantic Weakfish (*Cynoscion regalis*) as an example. Both spatial and temporal variation in weight parameters exhibited strong influences on yield and spawning stock biomass per-recruit. Associated biological reference points were highly sensitive to spatial and temporally heterogeneity. In several cases, reference points used as management targets were so significantly different that ignoring spatial and temporal heterogeneity in Atlantic Weakfish life history would likely cause overfishing or underfishing of Weakfish in certain regions and years.

Keywords: Yield per-recruit, spawning stock biomass per-recruit, sensitivity analysis, spatial heterogeneity, temporal heterogeneity, Atlantic Weakfish

3.2 Introduction

Per-recruit models are frequently used to evaluate the status of a fishery. Yield per-recruit (YPR) and spawning stock biomass per-recruit (SPR) models evaluate how changes in fishing mortality or size limits will impact the yield or spawning stock biomass of a cohort of fish recruits (Beverton and Holt 1957; Quinn and Deriso 1999). Per-recruit models rely on life-history parameters such as weight and maturity to derive biological reference points (BRPs), which are commonly applied as management targets or thresholds.

Most fishery population models assume that life-history characteristics do not exhibit spatial or temporal heterogeneity. Therefore, per-recruit models that are dependent on these life-history characteristics also are assumed to be uniform across space and time. However, these assumptions are often wrong. Ignoring the inherent spatial and temporal variations in fish populations can distort the results of stock assessment models (Ralston and O'Farrell 2008; Okamura et al. 2014; Truesdell et al. 2016, Chapter Two). In turn, ignoring heterogeneity can reduce the effectiveness of management strategies based on stock assessments and potentially have negative consequences for the target fish populations. To properly evaluate the effects of spatial and temporal management on heterogeneous populations, appropriately structured models must be developed to describe the population dynamics of a given stock species (Punt et al. 2000).

Several recent studies have examined the sensitivity of productivity models to spatially and temporally heterogeneous fishing effort. One of the earliest of these studies included a spatially-referenced SPR model that included variation in the fishing effort for the Sparid fish *Pterogymnus laniarius* among different locations on the Agulhas Bank in South Africa (Booth 2000). This study found that SPR is sensitive to spatial variation in fishing mortality and

suggested that fishing grounds that are heavily fished impact the stock more than those that are lightly fished, creating a bias towards heavily fished areas in the standard use of "averaged" fishing mortality. A subsequent study by Hart (2001) provided further support for Booth's (2000) conclusion by developing an individual-based YPR model to account for variation in fishing mortality of the Atlantic sea scallop (*Placopecten magel/anicus*). Further research found that per-recruit models are also sensitive to heterogeneous fishing effort due to locations, seasons, depths, and bias (Ralston and O'Farrell 2008; Okamura et al. 2014; Lin et al. 2015; Cadigan and Wang 2016; Truesdell et al. 2016)

As fishery-based parameters depend almost exclusively on anthropogenic interactions, heterogeneity in these parameters is relatively easy to measure. More difficult to pinpoint are variations in life-history parameters. Heterogeneity of fish life-history attributes is largely due to less predictable variations in environmental conditions. Changes in factors such as water temperature, nutrient levels, and biological interactions can cause local, seasonal, or annual shifts in per-recruit life-history parameters, including natural mortality, growth, and maturity. This study used spatially and temporally integrated weight estimates modeled in the previous chapter to explore the sensitivity of YPR and SPR models to heterogeneous life-history parameters using Atlantic Weakfish (*Cynoscion regalis*) as an example.

Atlantic Weakfish occur along the North American Atlantic coast from Nova Scotia to Florida (Mercer 1985). This is a very large geographical area in which environmental conditions vary significantly. Thus, it is not surprising that previous studies have found significant spatial variation in Weakfish life-history attributes (Shepherd and Grimes 1983; Paperno et al. 2000; Chapter Two). The greatest abundance of Weakfish lies between New York and North Carolina (Mercer 1985).

Less is known about Weakfish subpopulations south of North Carolina, where the species is less abundant. This is largely due to inconsistencies in sampling effort in this region due to the high density of untrawlable habitat and hybridization with similar species. The seafloor of the southern range of Atlantic Weakfish has a much higher reef coverage in comparison to the northern range. This high reef density makes the south a mostly untrawlable habitat, as nets are likely to tear on the high-profile bottom structure as well as damage the reef. An additional complicating factor in the south not present in the north is the distributional overlap with sand seatrout (*Cynoscion arenarius*). This species has been found to hybridize with Weakfish in Florida waters where the respective distributions merge, which is generally restricted to the Gulf of Mexico (Tringali et al. 2011). This co-occurrence and hybridization of sand seatrout and Weakfish confuses the identification of both species, which are extremely similar in appearance, especially at young ages. These inherent differences in Atlantic Weakfish between their northern and southern ranges were considered in this study to explore the spatial variation in per-recruit.

As part of their northern and inshore spring migration, Atlantic Weakfish are commonly found in Chesapeake Bay from around April through November each year (Pearson 1941; Massmann et al. 1958; Wilk 1979). They use this estuarine habitat as feeding and spawning grounds, and support one of the region's most important fisheries (Rothschild et al. 1981). Much evidence has been provided to suggest that subpopulations of Atlantic Weakfish in the Chesapeake Bay (as well as throughout the rest of their large distribution) display significant temporal variations in life history (Shepherd and Grimes 1983; Lowerre-Barbieri et al. 1996; Paperno et al. 2000; Chapter Two). Given its small geographical area and high abundance of Atlantic Weakfish, Chesapeake Bay was used as a case study to examine the temporal variation of Weakfish yield and spawning stock biomass per-recruit in this study.

Due to their dependency on life-history estimates, trends in productivity models should reflect those observed in life-history models. Thus, yield and spawning stock biomass per-recruit analyzed in this chapter are expected to display trends that are similar and proportional to the spatial and temporal trends found in weight-at-age modelled using mixed-effects methods in Chapter Two of this thesis. Furthermore, I expect that biological reference points commonly used in Atlantic Weakfish stock assessments exhibit a strong sensitivity to spatial and temporal variations in region and year. As BRPs are used as management thresholds in fisheries stocks, the results of this analysis will pose implications regarding the possible influence of spatial and temporal variation on management effectiveness.

3.3 Methodology

3.3a Data Source

Data were taken from three fishery-independent surveys that sampled various regions and years. These surveys were the Northeast Area Monitoring and Assessment Program (NEAMAP), the Southeast Area Monitoring and Assessment Program for the South Atlantic (SEAMAP-SA or SEAMAP), and the Chesapeake Bay Multispecies Monitoring and Assessment Program (ChesMMAP). Collectively, these surveys sampled from the approximate equivalent of the entire Atlantic Weakfish geographic distribution and have been collecting data for 33 years.

The NEAMAP bottom trawl survey has been operating in the spring and fall of each year since 2007 (Bonzek et al. 2009). This survey sampled fishes and invertebrates from Montauk, NY to Cape Hatteras, NC. The SEAMAP-SA shallow-water trawl survey has sampled the South Atlantic Bight from Cape Hatteras, NC to Cape Canaveral, FL during the spring, summer, and fall since 1983 (Eldridge 1988). For the purpose of this study, these two surveys were each

divided into six regions by latitude in 1° increments. The NEAMAP survey was chosen to represent the northern distribution of Atlantic Weakfish, while the SEAMAP survey was chosen to represent the southern distribution (Figure 1).

The ChesMMAP large-mesh bottom-trawl survey has been sampling the Chesapeake Bay since 2002 (Bonzek et al. 2011). The survey runs every March through November and targets late juvenile and adult fishes. Data collected between 2002 and 2012 were used in this study to observe the impact of temporal variation in life-history attributes on productivity of Atlantic Weakfish.

3.3b Per-recruit Models

In order to examine the impact of spatially and temporally heterogeneous life-history parameters on Atlantic Weakfish productivity, spatially and temporally integrated per-recruit models were compared to base models assuming uniform spatial and temporal parameters. Atlantic Weakfish productivity was estimated using yield per-recruit (YPR) and spawning stock biomass per-recruit (SPR).

Yield Per-recruit

Spatially and temporally integrated yield per-recruit were calculated as seen in Chen (1997). In terms of weight:

$$YPR = \sum_{t=t_R}^{t_\lambda} W_{t\delta} \frac{FS_t}{FS_t + M}(1 - e^{-FS_t - M})(\exp \sum_{j=t_R}^{t-1} -FS_j - M) ; \qquad (1)$$

where t_R is the age at first capture, t_λ is some maximum age, W_t is the average weight estimate at each age incorporating spatial or temporal effect δ, F is the given fishing mortality, S_t is the

selectivity at each age, and *M* is the natural mortality. For the purposes of this study, *F* was simulated in 0.002 increments from 0 to 4. Natural mortality, *M*, was taken from the most recent Atlantic Weakfish stock assessment and assumed to be constant at 0.43 (Sullivan et al. 2016). Selectivity of Weakfish into the commercial fishery also was taken from the stock assessment results (Table 2). Weight-at-age was modeled as described in Section 3.3c below.

Spawning Stock Biomass Per-recruit

Spatially and temporally integrated spawning stock biomass per-recruit was estimated using a model adopted from Goodyear's (1989) model for potential fecundity per-recruit. This model was calculated as:

$$SPR = \sum_{t=t_R}^{t_\lambda} m_{t\delta} W_{t\delta} (\exp \sum_{j=t_R}^{t-1} -S_j F - M)_{;} \quad (2)$$

where t_λ is the number of ages in the unfished population, t_R is the minimum age of recruitment, and S_j is the density-independent annual probability of survival for females age t while they were age j. The values of F, M, S_j and W_t used in this model were the same as those used in the YPR model, and maturity at age was the same as that used in the most recent stock assessment for Atlantic Weakfish (Sullivan et al. 2016; Table 2).

3.3c Spatially and Temporally Heterogeneous Parameters

Weight was treated as a variable parameter in the per-recruit models above in order to examine the effects of spatial and temporal variation in life history of Atlantic Weakfish. All weight-at-age relationships were modeled in Chapter Two of this thesis. Von Bertalanffy weight was calculated from age and weight data for 12 total regions between the NEAMAP and

SEAMAP surveys and 11 years sampled by the ChesMMAP survey. Nonlinear mixed-effects models were used to incorporate random effects caused by variation among regions and years. A base model assuming no spatial or temporal variation was calculated using nonlinear least squares regression. The respective weight parameters used in the following scenarios are shown in Table 1.

3.3d Per-recruit Model Scenarios

Three scenarios were applied to the per-recruit models in order to observe the influence of spatially and temporally heterogeneous and homogeneous life-history parameters (Table 2). Scenario 1 serves as the base case and assumes no spatial or temporal variation in weight. This scenario was repeated for all datasets. In Scenario 2, spatially integrated life-history parameters were used in the calculation of YPR and SPR using the NEAMAP and SEAMAP datasets. Scenario 3 applied temporally integrated life-history parameters to the per-recruit models for data from the ChesMMAP survey.

The effects of spatial and temporal heterogeneity in life-history parameters were measured by comparing Scenarios 2 and 3 to Scenario 1. The sensitivity of YPR and SPR models to the spatially and temporally integrated life-history parameters was estimated through Relative Change (RC). Relative Change was defined as

$$\frac{PR_{Scenario_i|F=x}}{PR_{Scenario_1|F=x}} \times 100\% \quad ; \qquad (3)$$

where PR is either YPR or SPR, and Scenario *i* represents Scenarios 2 or 3. YPR and SPR are calculated for set values of fishing mortality F_x. Relative change for the two scenarios assuming heterogeneity of life-history parameters was calculated for $F_{0.001}$, $F_{1.0}$, $F_{2.0}$, and $F_{3.0}$.

Further comparison of the three scenarios was made by looking at their respective biological reference points (BRPs). These reference points are commonly used by stock assessment scientists to set management limits or goals. For each of the four YPR scenarios, three BRPs were calculated: F_{MSY}, and $F_{0.1}$. F_{MSY} represents the fishing mortality at which the maximum sustainable YPR occurs. This reference point is often used to define the threshold past which overfishing occurs. A more conservative reference point to use for this threshold is $F_{0.1}$. This is the fishing mortality at which the rate of change of YPR is equal to 10% of the rate of change of YPR when fishing mortality is equal to zero.

For each of the three SPR scenarios, one BRP was calculated. This was $F_{SSB40\%}$, or the fishing mortality at which spawning stock biomass is 40% of the maximum, which always occurs at F equals zero. This is the overharvesting threshold suggested for Atlantic Weakfish by the Atlantic States Marine Fisheries Commission in their most recent stock assessment (Sullivan et al. 2016). All models and analyses were performed using R statistical software (R Core Team 2014).

3.4 Results

The incorporation of spatially and temporally integrated weight-at-age had a major influence on predicted yield and spawning stock biomass per-recruit. Spatial variation in both YPR and SPR was larger and more distinct in the northern survey than in the southern survey (Figure 2). Region-specific estimates of YPR and SPR derived from spatially heterogeneous weight parameters for the NEAMAP dataset increased from south to north. This trend mirrors that observed in region-specific estimates of maximum weight parameter (W_{∞}; Table 3). Region-specific estimates displayed much less variation in the SEAMAP dataset. As in the northern

survey, spatial trends in YPR and SPR matched those seen in region-specific estimates of the maximum weight. Unlike the NEAMAP survey, per-recruit in the SEAMAP survey displayed no south-to-north trends.

The standard homogeneous modeling approach assuming neither spatial nor temporal variation (S1) produced YPR and SPR curves that were shaped differently than those produced by the spatially heterogeneous estimates (S3) for both the NEAMAP and SEAMAP surveys (Figure 2). In the northern survey, homogeneous maximum YPR and SPR appeared to be near the median of the region-specific per-recruit estimates. However, the slopes of the homogeneous per-recruit curves are slightly higher than the median of the region-specific per-recruit curves. These differences in maximum and slope are explained by examining the associated weight-at-age maximum and rate parameters (Table 3). In this survey, the maximum weight (W_∞) estimated from the standard homogeneous weight-at-age model used in Scenario 1 was higher than W_∞ found for the five southern regions sampled by NEAMAP and lower than the W_∞ found for the northernmost region (S2). However, the growth rate parameter (k) produced by the homogeneous model is lower than any of those produced by the spatially integrated weight-at-age model. The combination of the effects of these maximum and rate parameters on per-recruit are what caused spatially heterogeneous YPR and SPR model curves to have a different shape than the homogeneous model curves.

Per-recruit curves estimated using the standard homogeneous model approach (S1) were lower than most of the region-specific curves estimated from spatially heterogeneous weight parameters (S2) for the SEAMAP survey (Figure 2). In this dataset, the maximum weight (W_∞) parameter estimated using the standard homogeneous model approach was much lower than any heterogeneous estimates of W_∞ produced by spatially incorporated weight-at-age models (Table

3). In fact, the W_∞ value used in Scenario 1 was less than half that of the lowest region-specific W_∞ value used in Scenario 2. Growth-rate parameter (k), on the other hand, was higher for Scenario One than for any of the spatially incorporated k estimates.

Despite the more prominent spatial variation displayed by YPR and SPR models from the NEAMAP survey, per-recruit yield from the SEAMAP survey was more sensitive to regional changes in weight-at-age. Relative change between spatially heterogeneous (S2) estimates of YPR and SPR and homogeneous estimates (S1) were higher for nearly all southern regions (Tables 4 and 5). This was due to the greater disparity between weight estimates produced by the standard homogeneous and spatially integrated weight-at-age models for this survey. However, spatial trends in relative change are more distinct among the NEAMAP survey. In both YPR and SPR, average relative change increases from south to north.

Per-recruit yield was even more sensitive to temporal variation in the ChesMMAP survey. Relative changes between temporally heterogeneous (S3) and homogeneous (S1) estimates of YPR and SPR were generally higher than those produced by the spatially heterogeneous (S2) estimates in either the NEAMAP or SEAMAP surveys (Tables 4 and 5). Additionally, distinct temporal trends were found in per-recruit estimates derived from temporally heterogeneous weight parameters. Average relative change decreased from 2002 to 2012, with a spike in both YPR and SPR in 2008.

The YPR and SPR model curves estimated from homogeneous weight-at-age models (S1) for the Chesapeake Bay appeared to fall relatively close to the median year-specific per-recruit curves estimated from temporally heterogeneous weight-at-age (S3; Figure 3). This outcome mirrors the relationship observed between homogeneous weight estimates and temporally integrated weight estimates (Table 3).

Biological reference points derived from YPR and SPR were highly sensitive to both spatial and temporal heterogeneity. The fishing mortality at which the maximum sustainable yield per-recruit (F_{MSY}) occurred was most sensitive to temporal variation in life history (Figure 5). Values of F_{MSY} in the ChesMMAP survey ranged from 1.46 in 2008 to 4.0 in 2003, 2006, 2007, and 2012 (Table 6). YPR at these fishing mortalities (YPR_{MSY}) displayed less temporal variation, although YPR_{MSY} for 2012 was approximately half the average value for all years and the homogeneous $YPR_{MSY.}$

Values of F_{MSY} were less sensitive to spatial variation in life history (Figure 4). In the SEAMAP survey, F_{MSY} was equal across all regions described by the spatially heterogeneous weight parameters and roughly half the homogeneous value of F_{MSY} (Table 6). $YPR_{MSY,}$ on the other hand, was lower than the majority of region-specific YPR_{MSY} values estimated from spatially heterogeneous weight parameters. The homogeneous YPR_{MSY} value produced for the NEAMAP dataset displayed slight regional variation that was approximately normally distributed around the homogeneous $YPR_{MSY.}$ This YPR_{MSY} was slightly more sensitive to spatial variation than in the southern survey, with possible outliers in Regions 5 and 6.

The fishing mortality at which the rate of change of YPR is equal to 10% of the initial rate of change ($F_{0.1}$) was also most sensitive to temporal heterogeneity in weight-at-age (Figure 5). For the ChesMMAP survey, $F_{0.1}$ varied between 0.591 in 2008 and 1.12 in 2012. The standard $F_{0.1}$ produced from homogeneous weight parameters fell somewhere near the median of the temporally heterogeneous parameters. $YPR_{0.1}$ displayed less temporal variation, and the standard homogeneous value appeared to be roughly equal to the temporal mean.

Values of $F_{0.1}$ were less sensitive to spatial variation in weight (Figure 4). As in F_{MSY}, $F_{0.1}$ was equal across all regions sampled by the SEAMAP survey (Table 6). Unlike F_{MSY}, the

homogeneous $F_{0.1}$ was very close to the spatially heterogeneous $F_{0.1}$ in this dataset. Homogeneous $YPR_{0.1}$ was lower than five of the six region-specific $YPR_{0.1}$ estimated from spatially heterogeneous weight from the southern survey. NEAMAP $F_{0.1}$ was much more sensitive to spatial variation than F_{MSY}, and homogeneous $F_{0.1}$ was lower than all but one value of the spatially heterogeneous $F_{0.1}$. Spatial variation in $YPR_{0.1}$ was even more prominent than in $F_{0.1}$ (Figure 4). Homogeneous $YPR_{0.1}$ appeared to be near the spatial mean $YPR_{0.1}$ in the northern survey.

The fishing mortality at which spawning stock biomass is 40% of the maximum ($F_{SSB40\%}$) was most sensitive to temporal heterogeneity in weight-at-age (Figure 5). $F_{SSB40\%}$ varied between 0.993 in 2008 and 2.309 in 2012 for years sampled in the ChesMMAP survey (Table 6). The temporal mean of $F_{SSB40\%}$ was roughly equal to the homogeneous $F_{SSB40\%}$. Spawning stock biomass at these fishing mortalities ($SSB_{40\%}$) exhibited less sensitivity to temporal variation than $F_{SSB40\%}$. The temporal mean $SSB_{40\%}$ was also approximately equal to the homogeneous $SSB_{40\%}$.

Values of $F_{SSB40\%}$ were nearly as sensitive to spatial variation in weight parameters from the NEAMAP survey (Figure 4). $SSB_{40\%}$ appeared to be more sensitive to spatially integrated weight parameters than in the ChesMMAP survey. In the northern survey, both $F_{SSB40\%}$ and $SSB_{40\%}$ from the homogeneous model were lower than the spatially heterogeneous values. $F_{SSB40\%}$ displayed the least spatial variation for the SEAMAP survey, and spatially heterogeneous $F_{SSB40\%}$ values were lower than the homogeneous $F_{SSB40\%}$. $SSB_{40\%}$ in the northern survey was slightly more sensitive to spatial variation, and spatially heterogeneous $SSB_{40\%}$ values were higher than the homogeneous $SSB_{40\%}$.

3.5 Discussion

Life history of fishes is seldom, if ever, evenly distributed throughout space and time, yet this is a common assumption in many models used in fisheries stock assessment. This assumption is carried over to productivity models that are dependent on life-history parameter estimates. In this study, I found that spatial and temporal variability in weight estimates can dramatically alter yield and spawning stock biomass per-recruit. Biological reference points derived from these per-recruit models were also strongly sensitive to the incorporation of regionally and annually heterogeneous weight estimates.

Spatially and temporally integrated weight has the potential to increase or decrease yield and spawning stock biomass per-recruit compared to the homogeneous case. Homogeneous YPR and SPR were much lower than the spatial means. Relative changes between mean spatially heterogeneous and homogeneous YPR and SPR estimates were greater than 100% for all values of *F* in both the northern and southern surveys analyzed in Scenario 2. The homogeneous estimates of per-recruit were much closer to the mean temporal estimates observed for the Chesapeake Bay survey analyzed in Scenario 3. Relative changes between mean temporally heterogeneous and homogeneous YPR and SPR were between 85% and 99% for all values of *F*.

The impacts of spatially varying growth can change the interpretation of the relationship between fishing mortality and YPR or SPR. While homogeneous per-recruit curves appear to fall within the spatially distinct estimates, average relative changes between the two were greater than 100% for three of the six regions sampled in the NEAMAP survey. In the SEAMAP survey, spatially heterogeneous per-recruit varied by more than 100% for all *F* values in five of the six regions. Average relative change between temporally heterogeneous and homogeneous per-

recruit estimates were less than 100% for only five of the 11 years sampled by the ChesMMAP survey.

Variability in life-history parameters can drastically change the biological reference points derived from yield and spawning stock biomass per-recruit. F_{MSY} in the homogeneous scenario was nearly half the spatially distinct values of five of the six northern regions. In the south, however, the homogeneous F_{MSY} was twice the spatial mean. Temporal variation in F_{MSY} was much higher than regional variation, although homogeneous F_{MSY} was closer to the annual mean. $F_{0.1}$ and $F_{SSB40\%}$ were both less sensitive to spatial and temporal variation in weight. Homogeneous $F_{0.1}$ and $F_{SSB40\%}$ estimates were similar to both spatial and temporal means in all three datasets.

While these BRPs were clearly influenced by variations in life-history parameters, it should be noted that the life-history parameters themselves were subject to error and uncertainty. Some of the maximum weight parameters (W_{∞}) used in the yield and spawning stock biomass per-recruit models were too low to be biologically realistic, while their corresponding growth rate parameters (k) were too high (Table 3). These unrealistic parameter estimates could be the result of model uncertainty or an uneven sampling distribution among regions or years (Chapter Two). The inclusion of these unrealistic parameters in this analysis may have led to an exaggeration of the sensitivity of BRPs to variation in weight parameters. However, variation in BRPs was still observed even among regions and years which had weight parameter estimates that were much more realistic. Thus, while the true variation in BRPs may be less dramatic than what was observed in this study, there is still evidence that BRPs are sensitive to any variation in life-history parameters.

Several previous studies support our findings that per-recruit models are strongly sensitive to spatial and temporal variations in life-history parameters. Most recently, Cadigan and Wang (2016) found that biological reference points are sensitive to local perturbations to productivity processes and increase when growth rates increase. Truesdell et al. (2016) examined the impact of depth-integrated growth on YPR of the U.S. Atlantic sea scallop fishery. The resulting BRPs were found to be significantly higher in deeper-water than in shallow-water sites. In addition, spatial and temporal changes in other life-history parameters, such as natural mortality, have been found to have significant impacts on per-recruit models (McShane and Naylor 1995; Bunnell and Miller 2005; Leaf et al. 2008; Lin et al. 2015).

Fisheries management strategies employ biological reference points to determine overfishing thresholds. Stock assessment scientists use these BRPs to evaluate the status of fish stocks and decide whether current management practices are sufficiently effective to prevent future overfishing. The high sensitivity of BRPs to spatial and temporal variations in weight estimates found in this study suggest a strong need for further research into the spatial and temporal management of Atlantic Weakfish.

Scale is the first issue which should be addressed in spatial and temporal management measures. Sensitivity analyses such as those performed in this study can be used to determine appropriate spatial and temporal units of management. In this chapter, I chose to use two spatially distinct surveys to examine the effect of spatial variation in weight on Weakfish productivity. The NEAMAP survey samples from the distribution of Atlantic Weakfish north of Cape Hatteras, NC, where they are most abundant. I selected the SEAMAP survey for comparison because it samples from the range of the Atlantic Weakfish distribution south of

Cape Hatteras, NC, and because life-history parameter trends in this dataset are different from those in the northern survey (Chapter Two).

The differences in BRPs between these two spatially distinct regions (north and south) imply that they should be managed separately. Spatial means were higher for all BRPs calculated for the NEAMAP survey than those from the SEAMAP survey. The fishing mortality at which spawning stock biomass is 40% of the maximum ($F_{SSB40\%}$), which always occurs at F equals zero is the overharvesting threshold suggested for Atlantic Weakfish by the Atlantic States Marine Fisheries Commission in their most recent stock assessment (Sullivan et al. 2016).

The spatial mean of spawning stock biomass is 40% of the maximum ($SSB_{40\%}$) was approximately 0.2 for both surveys. However, the $F_{SSB40\%}$ at which this occured was 1.69 in the NEAMAP survey and 0.98 in the SEAMAP survey. If managers assumed that the $F_{SSB40\%}$ from the NEAMAP survey, where Atlantic Weakfish are more abundant, also described the southern Weakfish stock, targeting an $F_{SSB40\%}$ of 1.69 would allow fishing effort in the southern region disproportional to the true spawning stock biomass per-recruit relationship to F. This bias in productivity modelling due to poor spatial scaling could cause Atlantic Weakfish in the southern region to be fished past their true $F_{SSB40\%}$, eventually leading to a decline in southern subpopulations.

Similar biases in Atlantic Weakfish productivity also could result from ignoring temporal variation in life history. $F_{SSB40\%}$ estimated for the Chesapeake Bay was 1.21 for the homogeneous case assuming no annual variation. In comparison, the temporal mean $F_{SSB40\%}$ was 1.40. While this difference is less than those observed among the spatial mean estimates from the NEAMAP and SEAMAP surveys, the variation among specific years is higher. $F_{SSB40\%}$ ranged from 0.99 in 2008 to 2.31 in 2012. $SSB_{40\%}$ decreased significantly between these years, which supports the

claim that Atlantic Weakfish spawning stock biomass has been declining rapidly in recent years that was made in the most recent stock assessment for the species (Sullivan et al. 2016).

In addition to spatial and temporal scale, careful consideration should also be given to which life-history parameter estimates are used to set management thresholds. Beverton and Holt (1957) found that the maximum weight parameter W_∞ did not affect the shape of the YPR curve. Lin et al. (2015) further stated that the BRPs F_{MSY} and $F_{0.1}$ were also uninfluenced by W_∞. These relationships were supported by the results of the present study. Yield per-recruit in the SEAMAP survey was derived from spatially heterogeneous estimates of W_∞ but not k. These spatially heterogeneous maximum weight parameters produced reference points F_{MSY}, $F_{0.1}$, and $F_{SSB40\%}$ that were identical among the six southern regions.

In the ChesMMAP survey, YPR was derived from temporally heterogeneous estimates of both W_∞ and k. Two of the years sampled in the Chesapeake Bay survey had roughly equal W_∞ estimates and different k estimates. The growth rate parameter k in 2003 was 0.6, while in 2009 it was only 0.4. Resultant F_{MSY}, $F_{0.1}$, and $F_{SSB40\%}$ estimates were all higher in 2003 than in the later year. This is consistent with the results of Lin et al. (2015) and Cadigan and Wang (2016). In these studies, as well as the present Chapter, per-recruit BRPs increased as growth rates increased.

Optimal management strategies would target thresholds derived from maximum weight and growth rate parameters incorporating variation across appropriate spatial and temporal scales. Appropriate scales of spatial and temporal management units can be determined by comparing productivity trends among regions and years defined by significant variations in life-history parameters. In the present study, such an analysis revealed a high sensitivity of yield per-recruit, spawning stock biomass per-recruit, and associated biological reference points to spatial

and temporal variations in weight parameter estimates (from Chapter Two) for Atlantic Weakfish. The results of this thesis indicate that management of this species could reduce the amount of modelling bias by targeting biological reference points which incorporate both temporal and spatial variation separately for the northern and southern ranges of the Weakfish distribution defined in relation to Cape Hatteras, NC.

3.6 Literature Cited

Beverton, R. J. and Holt, S. J. 1957. On the dynamics of exploited fish populations. Fisheries Investigations London Series 2, 533 p.

Bonzek, C. F., Gartland, J., Lange, J. D. Jr., and Latour, R. J. 2009. Northeast Area Monitoring and Assessment Program (NEAMAP) Mid-Atlantic Nearshore Trawl Program Final Report 2005-2009. Atlantic States Marine Fisheries Commission, 341 p.

Bonzek, C. F., Gartland, J., and Latour, R. J. 2011. Data collection and analysis in support of single and multispecies stock assessments in Chesapeake Bay: The Chesapeake Bay Multispecies Monitoring and Assessment Program (ChesMMAP). Virginia Institute of Marine Science, Gloucester Point, Virginia.

Booth, A. J. 2000. Incorporating the spatial component of fisheries data into stock assessment models. ICES Journal of Marine Science 57:858-865.

Bunnell, D. B., and Miller, T. J. 2005. An individual-based modeling approach to spawning-potential per-recruit models: an application to blue crab (*Callinectes sapidus*) in Chesapeake Bay. Canadian Journal of Fisheries and Aquatic Sciences 62: 2560-2572.

Caddy, J. F. 1975. Spatial model for an exploited shellfish population, and its application to Georges Bank scallop fishery. Journal of the Fisheries Research Board of Canada 32: 1305-1328.

Caddy, J. F. 1999. Fisheries management in the twenty-first century: will new paradigms apply? Reviews in Fish Biology and Fisheries 9: 1-43.

Cadigan, N. G., and Wang, S. 2016. Local sensitivity of per-recruit fishing mortality reference points. Journal of Biological Dynamics 10(1): 525-545.

Chen, Y. 1997. A comparison study of age- and length-structured yield-per-recruit models. Aquatic Living Resources 10: 271-280.

Cope, J. M., and Punt, A. E. 2011. Reconciling stock assessment and management scales under conditions of spatially-varying catch histories. Fisheries Research 107: 22-38.

Eldridge, P. J. 1988. The southeast area monitoring and assessment program (SEAMAP): A state-federal-university program for collection, management, and dissemination of fishery-independent data and information in the southeastern United States. Marine Fisheries Review 50(2):29-39.

Goodyear, C. P. 1989 Spawning stock biomass per-recruitment: the biological basis for a fisheries management tool. Collective Volume of Scientific Papers ICCAT 32 (2):487-497.

Hart, D. R. 2001. Individual-based yield-per-recruit analysis with an application to the Atlantic sea scallop, *Placopecten magellanicus*. Canadian Journal of Fisheries and Aquatic Sciences 58: 2351-2358.

Leaf, R. T., Rogers-Bennet, L., and Jiao, Y. 2008. Exploring the use of a size-based egg-per-recruit model for the red abalone fishery in California. North American Journal of Fisheries Management 28: 1638-1647.

Lin, Y. J., Sun, C. L., Chang, Y. J., and Tzeng, W. N. 2015. Sensitivity of yield-per-recruit and spawning-biomass-per-recruit models to bias and imprecision in life history parameters: an example based on life history parameters of Japanese eel (*Anguilla japonica*). Fishery Bulletin 113(3): 302-311.

Lowerre-Barbieri, S. K., Chittenden, M. E., and Barbieri, L. R. 1996. The multiple spawning pattern of Weakfish in the Chesapeake Bay and Middle Atlantic Bight. Journal of Fish Biology 48: 1139-1163.

Massmann, W. H., Whitcomb, J. P., and Pacheco, A. L. 1958. Distribution and abundance of Gray Weakfish in the York River system, Virginia. Transactions of the North American Wildlife Conference 23: 361-369.

McShane, P. E., and Naylor, J. R. 1995. Small-scale spatial variation in growth, size at maturity, and yield- and egg-per-recruit relations in the New Zealand abalone *Haliotis iris*. New Zealand Journal of Marine and Freshwater Research 29: 603-612.

Mercer, L. P. 1985. Fishery Management Plan for the weakfish, (*Cynoscion regalis*) fishery. Fisheries Management Report No. 7 Atlantic States Marine Fisheries Commission. North Carolina Department of Natural Resources and Community Development, Division of Marine Fisheries Special Scientific Report No. 46, 129 p.

Okamura, H., McAllister, M. K., Ichinokawa, M., Yamanaka, L., and Holt, K. 2014. Evaluation of the sensitivity of biological reference points to the spatio-temporal distribution of fishing effort when seasonal migrations are sex-specific. Fisheries Research 158: 116-123.

Orensanz, J. M., and Jamieson, G. S. 1998. The assessment and management of spatially structured stocks: an overview of the North Pacific Symposium on invertebrate stock assessment and management. *In* Proceedings of the North Pacific Symposium on Invertebrate Stock Assessment and Management. (ed. by G. S. Jamieson and A. Campbell). Canadian Special Publication of Fisheries and Aquatic Sciences 125: 441-459.

Paperno, R., Targett, T. E., and Grecay, P. A. 2000. Spatial and temporal variation in recent growth, overall growth, and mortality of juvenile Weakfish (*Cynoscion regalis*) in Delaware Bay. Estuaries 23(1):10-20.

Pearson, J. C. 1941. The young of some marine fishes taken in lower Chesapeake Bay, Virginia with special reference to the Gray Sea Trout *Cynoscion regalis* (Block & Schneider). U.S. Fish and Wildlife Service Fishery Bulletin 50: 79-102.

Punt, A. E., Pribac, F., Walker, T. I., Taylor, B. L., and Prince, J. D. 2000. Stock assessment of School Shark, *Galeorhinus galeus*, based on a spatially explicit population dynamics model. Marine and Freshwater Research 51: 205-220.

Quinn, T. J., and Deriso, R. B. 1999. Quantitative Fish Dynamics. Oxford University Press, New York.

R Core Team 2014. R: A language and environment for statistical computing. R Foundation for Statistical Computing, Vienna, Austria.

Ralston, S., and O'Farrell, M. R. 2008. Spatial variation in fishing intensity and its effect on yield. Canadian Journal of Fisheries and Aquatic Sciences 65: 588-599.

Rothschild, B. J., Jones, P. W., and Wilson, J. S. 1981. Trends in Chesapeake Bay Fisheries. Transactions of the 46th Annual Meeting of the North American Wildlife and Natural Resources Conference 1981: 284-298.

Shepherd, G. and Grimes, C. B. 1983. Geographic and historic variations in growth of Weakfish, *Cynoscion regalis*, in the Middle Atlantic Bight. Fishery Bulletin 81(4):803-813.

Sullivan, P., Buckel, J., and Deroba, J. 2016. Weakfish Benchmark Stock Assessment and Peer Review. Atlantic States Marine Fisheries Commission, Arlington, Virginia; 270 p.

Truesdell, S. B., Hart, D. R., and Chen, Y. 2016. Effects of spatial heterogeneity in growth and fishing effort on yield-per-recruit models: an application to the U.S. Atlantic sea scallop fishery. ICES Journal of Marine Science 73(4): 1062-1073.

Wilk, S. J. 1979. Biological and fisheries data on Weakfish, *Cynoscion regalis* (Bloch and Schneider) NOAA Technical Report. U. S. Department of Commerce National Marine Fisheries Service, Highlands, New Jersey.

3.7 Tables and Figures

Table 1 Types of life-history attributes used in the three scenarios applied to the per-recruit analyses and the surveys used in each scenario.

	W_∞	Survey(s)
S1	uniform	All
S2	spatially integrated	NEAMAP/SEAMAP
S3	temporally integrated	ChesMMAP

Table 2 Selectivity (S_t) at age t, maturity-at-age (m_t), and natural mortality (M) from the most recent stock assessment of Atlantic Weakfish (Sullivan et al. 2016).

Age (years)	S_t	m_t	M
1	0.22	0.9	0.43
2	0.58	1	0.43
3	1	1	0.43
4	1	1	0.43
5	1	1	0.43
6	1	1	0.43

Table 3 Life-history parameters used in each scenario to calculate yield and spawning stock biomass per-recruit, as calculated in Chapter Two. W_∞, k, t_0, and b are the average maximum weight (kg), growth rate parameter toward the maximum, hypothetical age at weight zero, and allometric growth parameters in the von Bertalanffy weight-at-age equation respectively. W_∞ and k vary by region in Scenario 2 and by year in Scenario 3.

Scenario	Region/Year	W_∞	k	t_0	b
S1	NEAMAP	0.75	0.2	-2.0	2.99
S2	NM1	0.09	1.0	-1.1	2.99
	NM2	0.11	1.0	-1.1	2.99
	NM3	0.17	0.8	-1.1	2.99
	NM4	0.24	0.7	-1.1	2.99
	NM5	0.47	0.6	-1.1	2.99
	NM6	1.35	0.4	-1.1	2.99
S1	SEAMAP	2.00	0.10	-3.6	3.04
S2	SM1	5.42	0.07	-3.5	3.04
	SM2	5.10	0.07	-3.5	3.04
	SM3	5.58	0.07	-3.5	3.04
	SM4	5.81	0.07	-3.5	3.04
	SM5	5.98	0.07	-3.5	3.04
	SM6	4.58	0.07	-3.5	3.04
S1	ChesMMAP	0.51	0.4	-1.1	2.91
S3	2002	0.63	0.4	-1.0	2.91
	2003	0.43	0.6	-1.0	2.91
	2004	0.40	0.5	-1.0	2.91
	2005	0.33	0.6	-1.0	2.91
	2006	0.24	0.7	-1.0	2.91
	2007	0.19	0.9	-1.0	2.91
	2008	0.67	0.4	-1.0	2.91
	2009	0.44	0.4	-1.0	2.91
	2010	0.30	0.5	-1.0	2.91
	2011	0.26	0.5	-1.0	2.91
	2012	0.09	1.0	-1.0	2.91

Table 4 Relative changes in yield per-recruit estimates from the two heterogeneous scenarios over Scenario 1, given *F* values of 0.001, 1, 2, and 3. Averages are calculated from the four selected *F* values for each scenario. All relative changes are given as a percentage of YPR in the heterogeneous scenario as they relate to Scenario 1.

		F				Region/Year
Scenario	Region/Year	0.001	1	2	3	Averages
Spatial Mean	NEAMAP	100	113	119	121	
S2	1	34	46	53	57	48
	2	41	54	62	66	56
	3	57	72	79	83	73
	4	77	96	105	109	97
	5	131	150	157	160	150
	6	260	261	256	252	257
Spatial Mean	SEAMAP	119	113	110	109	
S3	1	119	113	110	109	113
	2	112	106	104	102	106
	3	123	116	113	112	116
	4	128	121	118	117	121
	5	132	124	121	120	124
	6	101	95	93	92	95
Temporal Mean	ChesMMAP	86	92	95	97	
S3	2002	131	131	130	130	131
	2003	116	129	136	139	130
	2004	101	109	113	114	109
	2005	88	97	101	103	97
	2006	70	82	88	91	83
	2007	63	78	87	92	80
	2008	112	105	101	99	104
	2009	92	93	93	93	93
	2010	74	79	81	82	79
	2011	62	65	66	66	65
	2012	33	44	51	55	46

Table 5 Relative changes in spawning stock biomass per-recruit estimates from the two heterogeneous scenarios over Scenario 1, given *F* values of 0.001, 1, 2, and 3. Averages are calculated from the four selected *F* values for each scenario. All relative changes are given as a percentage of SPR in the heterogeneous scenario as they relate to Scenario 1.

		F				Region/Year
Scenario	Region/Year	0.001	1	2	3	Averages
Spatial Mean	NEAMAP	105	117	121	123	
S2	1	40	52	59	63	54
	2	47	61	68	72	62
	3	64	78	84	87	78
	4	85	103	110	115	103
	5	138	154	160	162	154
	6	257	253	247	241	250
Spatial Mean	SEAMAP	117	111	108	107	
S2	1	117	111	108	107	111
	2	110	104	102	101	104
	3	120	114	112	110	114
	4	125	119	116	115	119
	5	129	122	120	118	122
	6	99	94	92	91	94
Temporal Mean	ChesMMAP	88	95	98	99	
S3	2002	130	130	130	128	130
	2003	122	135	140	144	135
	2004	104	112	115	116	112
	2005	92	100	104	106	101
	2006	75	87	93	96	88
	2007	70	86	95	101	88
	2008	108	101	98	95	101
	2009	93	93	93	92	93
	2010	76	80	82	83	80
	2011	63	65	66	67	65
	2012	39	51	58	63	53

Table 6 Biological reference points derived from each of the three scenarios. F_x represents the fishing mortality of each respective biological reference point. YPR_x is the yield per-recruit at each BRP and SSB_x is the spawning stock biomass per-recruit.

Scenario	Region/Year	F_{MSY}	YPR_{MSY}	$F_{0.1}$	$YPR_{0.1}$	$F_{SSB40\%}$	$SSB_{40\%}$
S1	NEAMAP	2.67	0.086	0.623	0.075	1.095	0.202
S2	Spatial Mean	3.63	0.107	0.884	0.088	1.69	0.213
	1	4.0	0.051	1.08	0.039	2.207	0.081
	2	4.0	0.059	1.05	0.045	2.107	0.095
	3	4.0	0.073	0.903	0.058	1.717	0.129
	4	4.0	0.096	0.885	0.076	1.669	0.172
	5	4.0	0.139	0.763	0.116	1.379	0.278
	6	1.76	0.221	0.621	0.196	1.061	0.520
S1	SEAMAP	4.0	0.072	0.607	0.061	1.08	0.169
S2	Spatial Mean	2.6	0.078	0.563	0.069	0.98	0.197
	1	2.6	0.078	0.563	0.069	0.98	0.198
	2	2.6	0.074	0.563	0.065	0.98	0.186
	3	2.6	0.080	0.563	0.071	0.98	0.203
	4	2.6	0.084	0.563	0.074	0.98	0.212
	5	2.6	0.086	0.563	0.076	0.98	0.218
	6	2.6	0.066	0.563	0.058	0.98	0.167
S1	ChesMMAP	2.11	0.093	0.647	0.081	1.121	0.212
S3	Temporal Mean	3.10	0.090	0.766	0.076	1.396	0.187
	2002	1.98	0.121	0.647	0.106	1.115	0.275
	2003	4.0	0.129	0.763	0.108	1.373	0.258
	2004	3.17	0.105	0.723	0.090	1.281	0.221
	2005	3.89	0.095	0.747	0.080	1.335	0.194
	2006	4.0	0.085	0.829	0.069	1.527	0.159
	2007	4.0	0.087	0.949	0.068	1.825	0.149
	2008	1.46	0.094	0.591	0.085	0.993	0.230
	2009	2.04	0.086	0.653	0.076	1.129	0.196
	2010	2.97	0.076	0.713	0.065	1.259	0.160
	2011	2.57	0.061	0.691	0.053	1.211	0.133
	2012	4.0	0.053	1.12	0.040	2.309	0.082

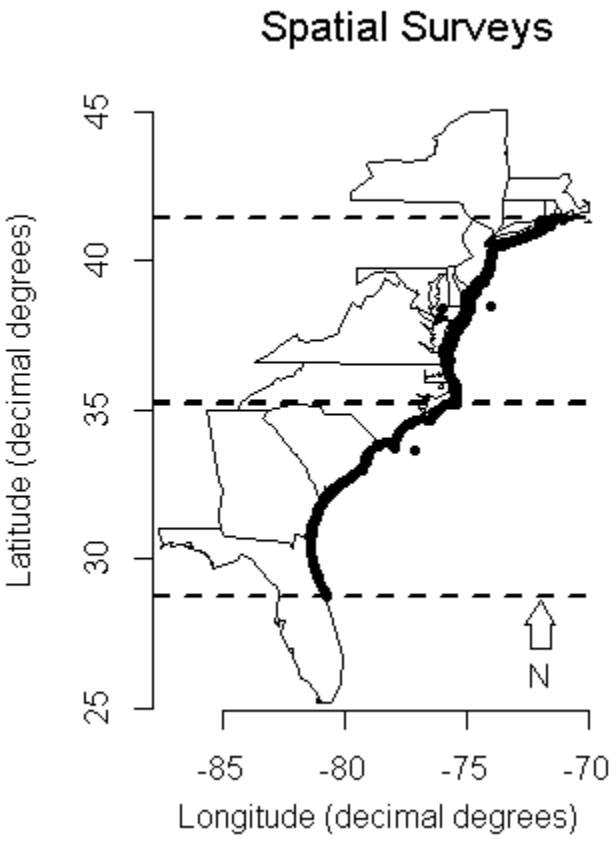

Figure 1 Map of the two surveys used in the spatial analysis of per-recruit. The northern bounded region represents the NEAMAP survey stations. The southern region shows the SEAMAP survey stations.

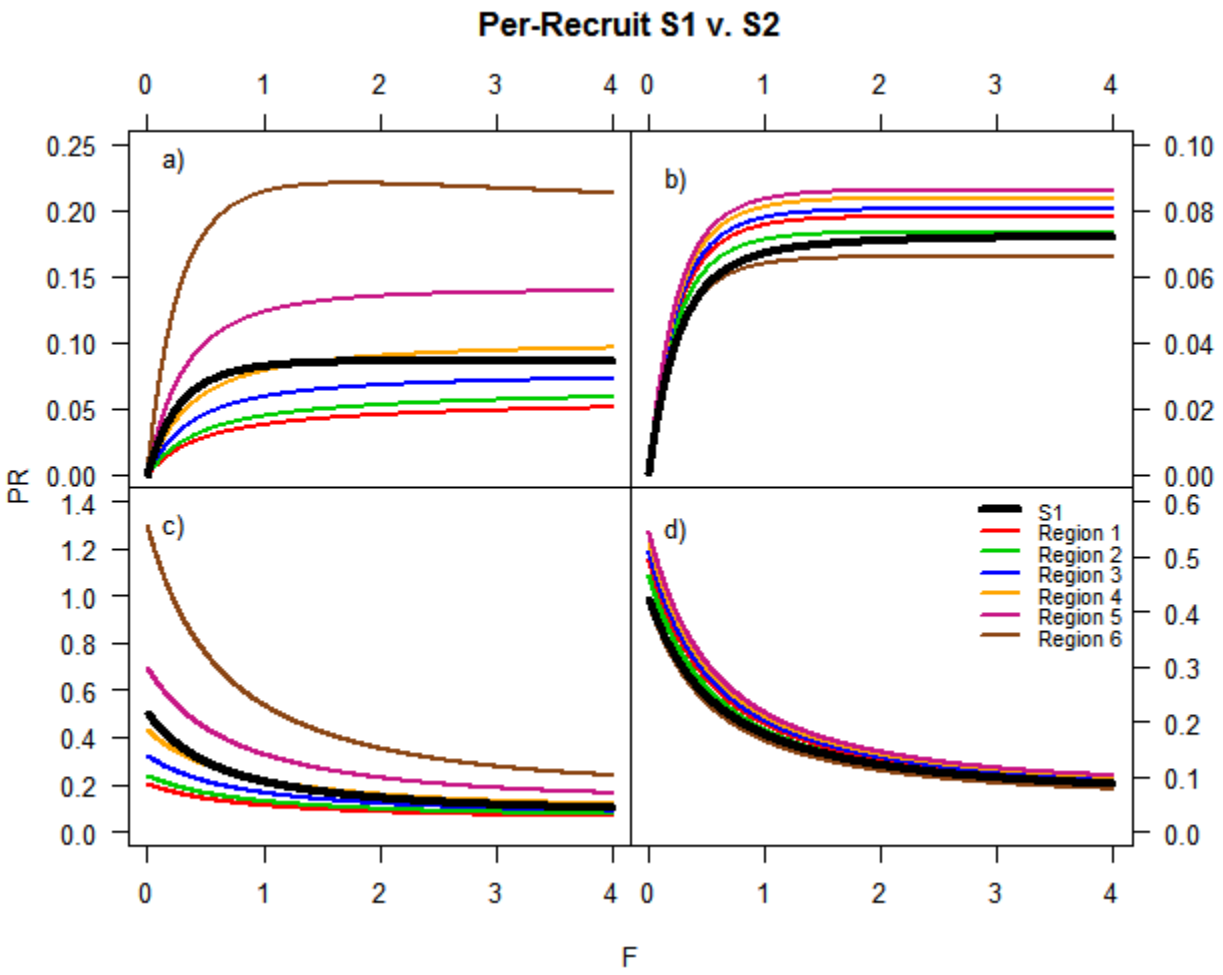

Figure 2 Spatial per-recruit estimates produced by S2 (colored lines) plotted against homogeneous S1 per-recruit (thick black line) for the NEAMAP and SEAMAP surveys; a) NEAMAP yield per-recruit, b) SEAMAP yield-per-recruit, c) NEAMAP spawning stock biomass per-recruit, and d) SEAMAP spawning stock biomass per-recruit.

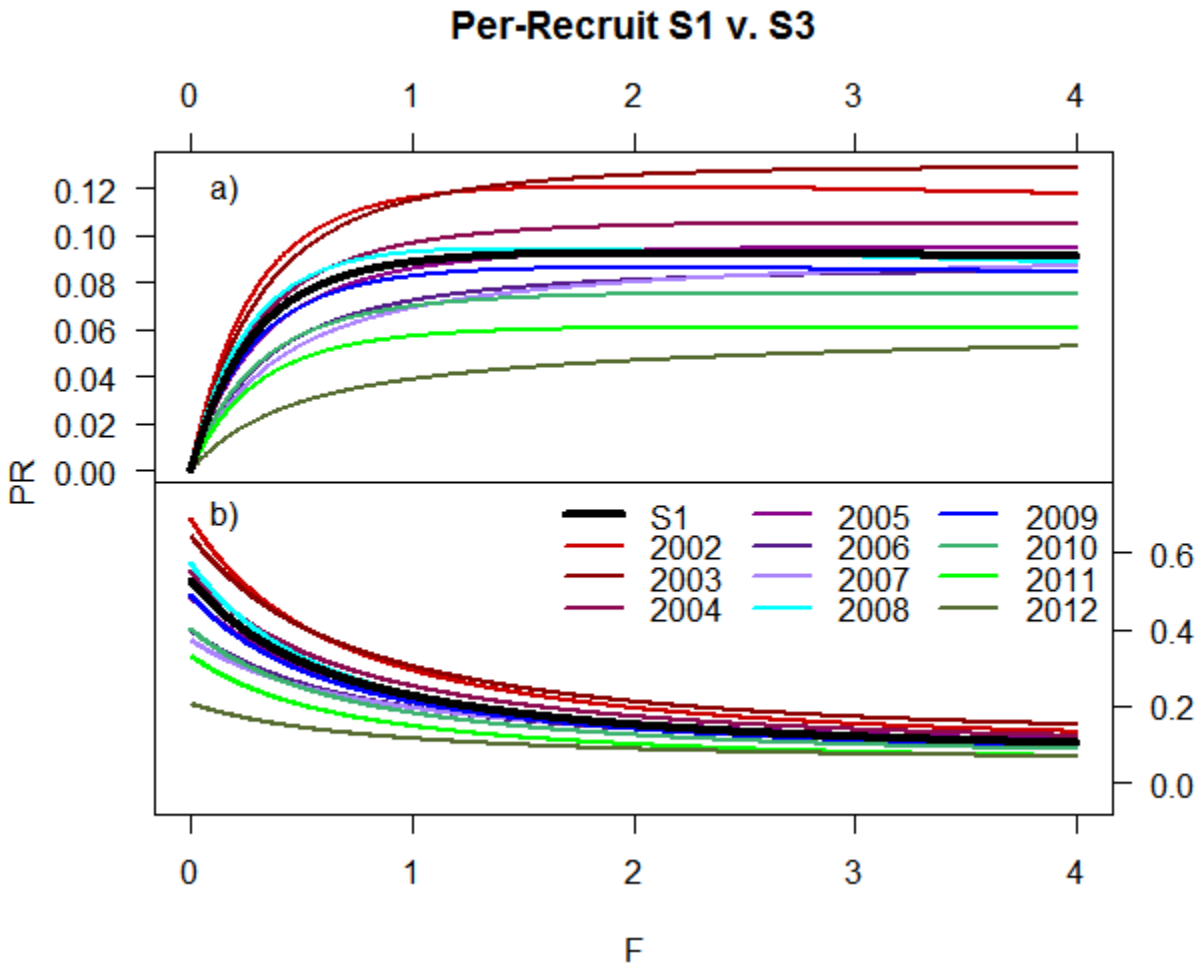

Figure 3 Temporal per-recruit estimates produced by S3 (colored lines) plotted against homogeneous S1 per-recruit (thick black line) for the ChesMMAP survey; a) ChesMMAP yield per-recruit, and b) ChesMMAP spawning stock biomass per-recruit.

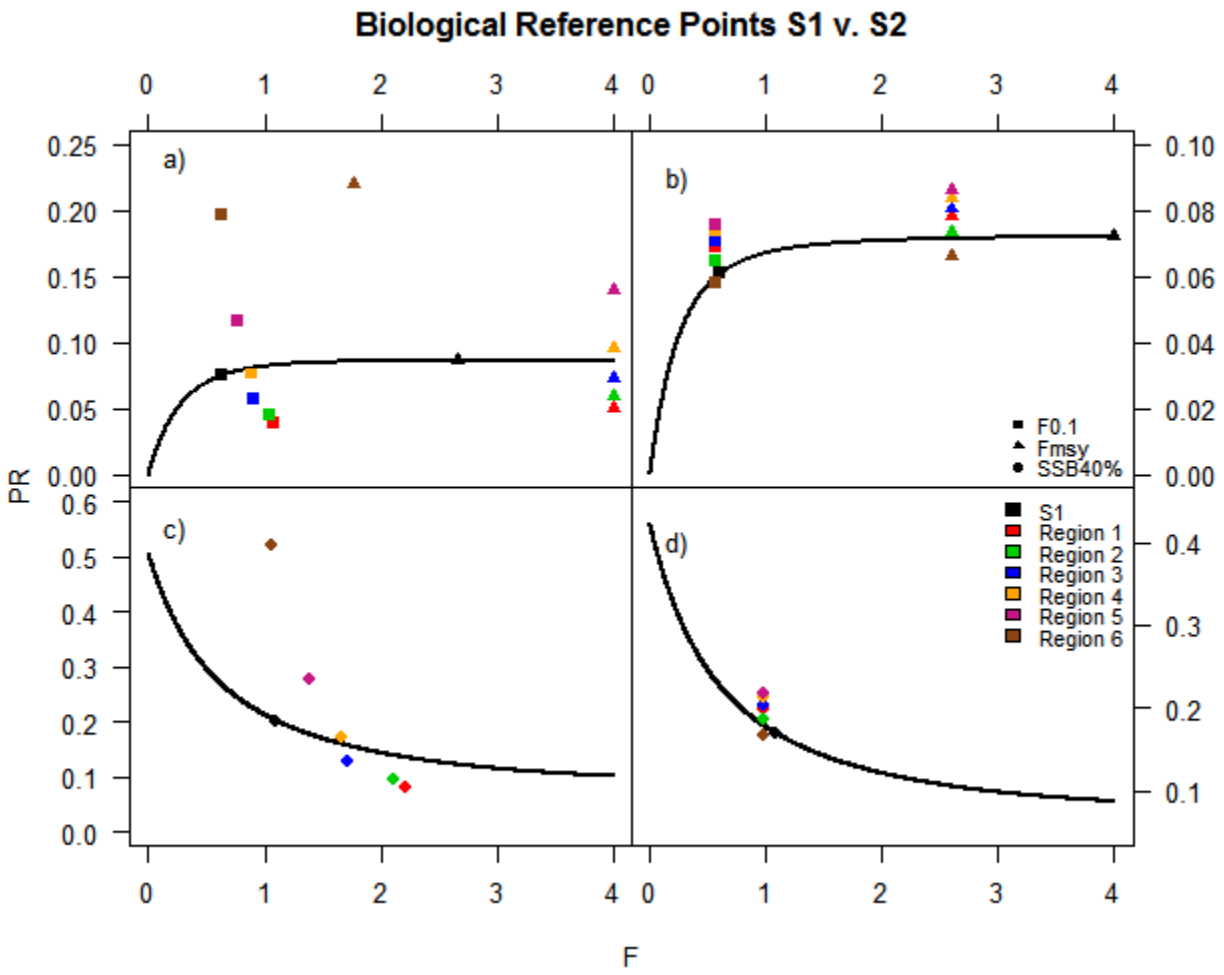

Figure 4 Biological reference points derived from spatial per-recruit estimates (S2, colored points) compared to BRPs derived from homogeneous per-recruit estimates (S1, black points and lines) for the NEAMAP and SEAMAP surveys; a) F_{MSY} and $F_{0.1}$ from NEAMAP yield per-recruit, b) F_{MSY} and $F_{0.1}$ from SEAMAP yield per-recruit, c) $SSB_{40\%}$ from NEAMAP spawning stock biomass per-recruit, and d) $SSB_{40\%}$ from SEAMAP spawning stock biomass per-recruit.

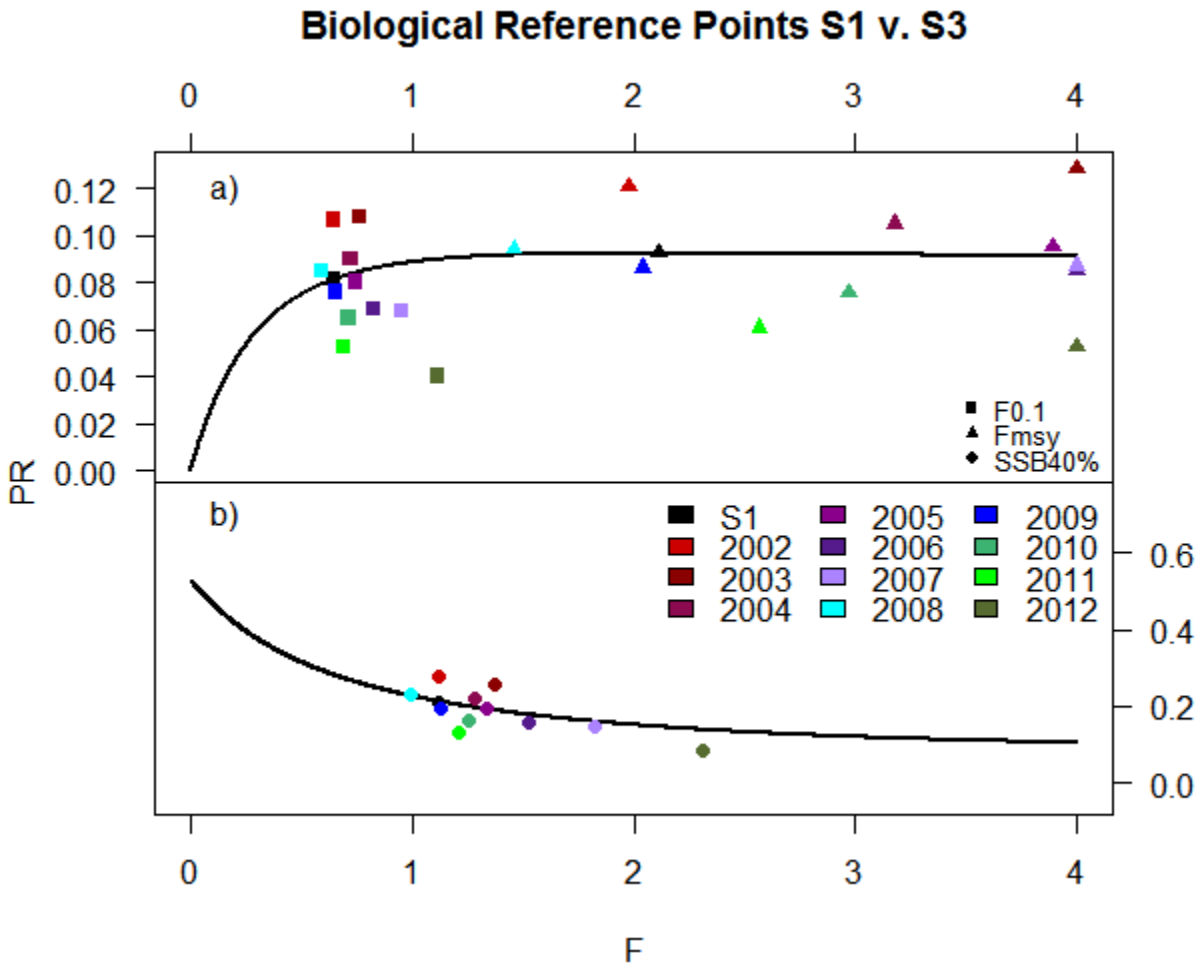

Figure 5 Biological reference points derived from temporal per-recruit estimates (S3, colored points) compared to BRPs derived from homogeneous per-recruit estimates (S1, black points and lines) for the ChesMMAP survey; a) F_{MSY} and $F_{0.1}$ from yield per-recruit, and b) $SSB_{40\%}$ from spawning stock biomass per-recruit.